The mechanism of HIV-1 Tat-induced changes in NMDA receptor function

A DISSERTATION
SUBMITTED TO THE FACULTY OF
THE UNIVERSITY OF MINNESOTA
BY

KELLY ALLEN KROGH

IN PARTIAL FULFILLMENT OF THE REQUIREMENTS
FOR THE DEGREE OF
DOCTOR OF PHILOSOPHY

STANLEY A. THAYER, ADVISOR

AUGUST 2014

Dedication

To my Mom and Dad: Thank you for all the years of love and support, for leading by example, and for teaching me the importance of working hard. I get my tenacity, dedication, and work ethic from both of you.

To my lovely wife, Kelly: Thank you for all the love and support, for always believing in me, and for being my rock in turbulent waters.

Acknowledgements

I did not make it this far in my academic career without the help of many people, and I would like to thank each of them for their part in helping me along the way. First, I would like to thank my graduate mentor, Dr. Stan Thayer. Since joining your lab, you've helped me to improve in every aspect of my approach to science. Despite obvious shortcomings in my scientific writing and experimental design when I joined the lab, you're patience, guidance, and instruction helped me to develop these scientific skills. Furthermore, you've helped to refine my approach to scientific presentation by teaching me slow down, to use precise language, to be conversational, and to sell the science using my natural enthusiasm for the subject matter. Most importantly, you've changed the way I think about science. I now approach scientific questions with clear and testable hypotheses. And if the outcome of an experiment is likely to change the way I think about a scientific project, then that is the experiment that should be conducted first to prevent from building a 'house of cards'. No one person has had more of an impact on my scientific training than you. Thank you.

I would also like to thank the members of my graduate thesis committee: Dr. Jonathan Marchant, Dr. Colin Campbell, and Dr. Paul Mermelstein. Thank you for your patience, for taking time out of your busy schedules to read and critique my preliminary exam, doctoral dissertation, and for your guidance over the past years. I selected each of you for my graduate committee because I knew you'd be challenging, thorough, fair, and would have high expectations for me. I'm a better scientist because you were a rigorous committee. Thank you for your commitment to my development.

I would like to thank the members of the PharmacoNeuroImmunology (PNI) training program for providing many opportunities to improve my scientific skills. Particularly, I want to thank Dr. Sabita Roy, Dr. Tom Molitor, and Yorie Smart. Thank you for allowing me the opportunity to speak at the PNI retreat, to present at PNI symposia, for the support to attend the SNIP and SfN conferences and grant writing workshops, and for providing an excellent education in the PNI sponsored classes and seminars. PNI is a great group of people. Thank you for allowing me to be part of it.

I would also like to thank my fellow collaborators. In particular, I'd like to thank Dr. Nicole Wydeven, Dr. Kevin Wickman, Dr. Xudong Feng, Dr. Li Na Wei, Jon Chan, Dr. Jonathan Marchant, Jonathan Popko, Dr. Yan Li, and Dr. Colin Campbell. Thank you for all your help and for the opportunities to collaborate.

I'd also like to thank the faculty and staff of the Department of Pharmacology at The University of Minnesota. Whether you taught me in the classroom, helped organize a departmental event, or ensured that my paperwork was in order, I appreciate all that you've done for me. Thank you.

Thank you to all of the educators who've taught me along the way. Specifically, I'd like to thank Dr. Craige Wrenn, Mr. Pat Garvey, Dr. Ron Torry, Dr. Klaus Bartschat, Dr. Andrew Brittingham, Mrs. Leslie Mamoorian, and the entire faculty and staff at Drake University. Your time and effort in my development is greatly appreciated.

Lastly, I want to thank my friends and family for all the love, support, and encouragement over the years. I'm fortunate to have you in my life. Thank you.

Summary of Publications

1. **Krogh KA,** Lyddon EA, Thayer SA, (2014) HIV-1 Tat activates a RhoA/ROCK signaling pathway to reduce NMDA-evoked calcium increases in hippocampal neurons via an actin-dependent mechanism (***submitted***)

2. Feng X-D, **Krogh KA,** Wu C-Y, Lin Y-W, Tsai H-C, Thayer SA, and Wei L-N. (2014) Receptor-interacting protein 140 attenuates endoplasmic reticulum stress in neurons and protects against cell death. ***Nat. Commun.*** 5:4487 doi: 10.1039/ncomms5487

3. **Krogh KA,** Wydeven N, Wickman K, Thayer SA (2014) HIV-1 protein Tat produces biphasic changes in NMDA-evoked increases in intracellular Ca^{2+} concentration via activation of Src kinase and nitric oxide signaling pathways. ***J Neurochem***. 10.1111/jnc.12724. ***Selected for editorial highlight*** (details below).

    a. Review of **Krogh et al., 2014**: Popescu GK, (2014) Dynamic plasticity of NMDA receptor-mediated calcium entry in neurons exposed to HIV-tat. ***J Neurochem***. 10.1111/jnc.12737

4. Li Y, Popko J, **Krogh KA,** Thayer SA, (2013) Epileptiform stimulus increases Homer 1a expression to modulate synapse number and activity in hippocampal cultures. ***J Neurophysiol***. 109(6): 1494-504

5. Li Y, **Krogh KA,** Thayer SA, (2012) Epileptic stimulus increases Homer 1a expression to modulate endocannabinoid signaling in hippocampal neurons ***Neuropharmacology*** 63(6): 1140-9

Abstract

Worldwide, more than 35 million people are currently infected with the human immunodeficiency virus (HIV). Approximately half of HIV-infected patients in the U.S. experience cognitive impairment despite effective control of viral load with combination anti-retroviral therapy (cART). The neurological complications that stem from an HIV infection are known as HIV-associated neurocognitive disorders (HAND). HAND ranges in severity from subtle difficulties with day-to-day tasks to severe functional impairment requiring assistance to survive. Although cART has improved patient survival by effectively managing viral load, it is ineffective at treating the majority of HAND. Consequently, the prevalence of HAND remains persistently high.

The symptoms of HAND correlate with neuronal damage, such as synapse loss and dendritic beading. Such synaptodendritic damage results from HIV-infected cells within the central nervous system (CNS) shedding neurotoxic agents, such as the HIV-1 protein transactivator of transcription (Tat). Tat potentiates N-methyl D-aspartate (NMDA) receptor function allowing excessive Ca^{2+} influx leading to neurotoxicity. In this dissertation, two studies are outlined investigating the mechanisms of NMDA receptor (NMDAR) dysfunction following exposure to Tat. The graphical abstract summarizes these studies.

First, the effect of Tat on NMDAR function was investigated. This study showed that Tat caused a time-dependent, *biphasic* change in NMDAR function. Initially, Tat *potentiated* NMDAR function via the low-density lipoprotein receptor-related protein (LRP) and activation of Src tyrosine kinase. Subsequently, NMDAR function *adapted* by

gradually returning to basal levels following 24 h exposure to Tat and eventually falling below control responses by 48 h. Adaptation resulted from activation of a nitric oxide synthase (NOS), soluble guanylate cyclase (sGC), cGMP-dependent protein kinase (PKG) signaling pathway.

Next, effectors downstream of PKG responsible for adaptation of NMDAR function were identified. Tat activated a signaling pathway including the small GTPase RhoA and Rho-associated protein kinase (ROCK). RhoA/ROCK activation caused remodeling of the actin cytoskeleton resulting in reduced NMDAR function.

Taken together, these studies indicate that Tat causes a *biphasic* change in NMDAR function. *Potentiation* of NMDAR function is mediated by LRP-dependent activation of Src kinase; *adaptation* of NMDAR function occurs after activation of a NOS/sGC/PKG signaling pathway leading to RhoA/ROCK-mediated remodeling of the actin cytoskeleton. Adaptation of NMDAR function may be a neuroprotective mechanism to reduce excess Ca^{2+} influx and prevent neurotoxicity. These studies provide molecular and temporal detail of the dynamic changes in NMDAR function following exposure to Tat and offer insight into potential therapeutic targets for the treatment of HAND.

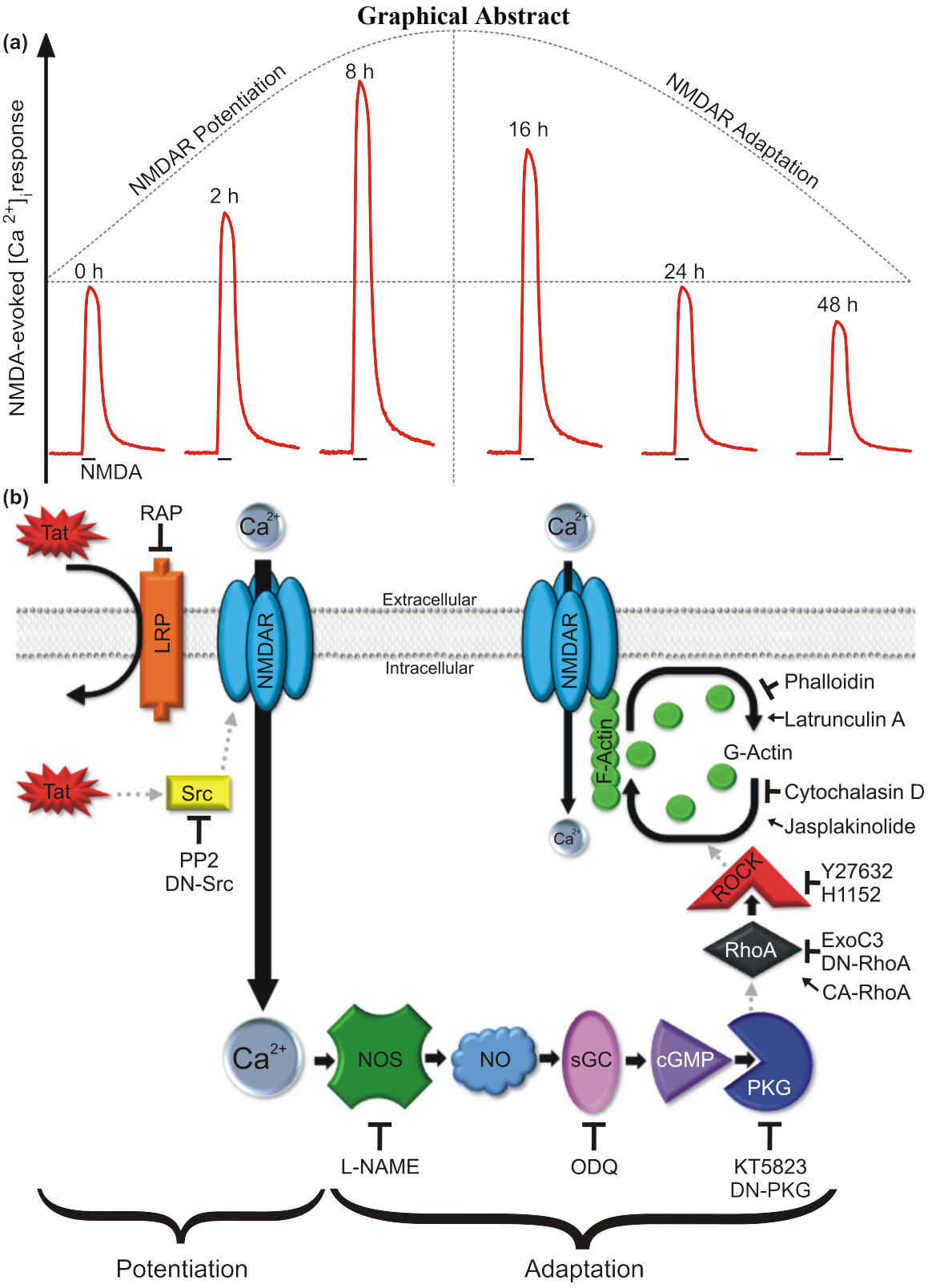
Graphical Abstract
(a)
NMDA-evoked [Ca 2+]i response
NMDAR Potentiation
NMDAR Adaptation
0 h
2 h
8 h
16 h
24 h
48 h
NMDA
(b)
Tat
RAP
LRP
Ca2+
NMDAR
Extracellular
Intracellular
Phalloidin
Latrunculin A
G-Actin
F-Actin
Cytochalasin D
Jasplakinolide
Src
PP2
DN-Src
ROCK
Y27632
H1152
RhoA
ExoC3
DN-RhoA
CA-RhoA
NOS
NO
sGC
cGMP
PKG
L-NAME
ODQ
KT5823
DN-PKG
Potentiation
Adaptation

Graphical abstract.
a, Stylized traces (▬) illustrate NMDA-evoked Ca^{2+} influx following treatment with Tat for the time indicated above the trace. Tat-induced potentiation begins following 2 h exposure and peaks by 8 h. Subsequently, NMDA-evoked Ca^{2+} responses begin to adapt by gradually returning to basal levels by 24 h and dropping below control responses by 48 h. **b,** Proposed mechanism of Tat-induced biphasic change in NMDAR function. Tat interacts with the LRP leading to Src kinase-mediated potentiation of NMDAR function that then adapts after activation of a NOS/cGMP/PKG signaling pathway resulting in RhoA/ROCK-mediated remodeling of the actin cytoskeleton and reduction of NMDAR function. Solid and dashed arrows represent direct and potentially indirect connections, respectively.

List of Figures

Abbreviations

AIDS, Acquired immunodeficiency syndrome

ALS, amyotrophic lateral sclerosis

ANI, asymptomatic neurocognitive impairment

ANOVA, analysis of variance

AP-2, adaptor protein complex 2

BBB, blood-brain barrier

BSA, bovine serum albumin

Ca^{2+}, calcium

$[Ca^{2+}]_i$, intracellular Ca^{2+} concentration

CA, constitutively active

CAMKII, calmodulin-dependent protein kinase II

cART, combination antiretroviral therapy

CCR5, chemokine (C-C motif) receptor 5

CD4, cluster of differentiation 4, cluster of designation 4

cDNA, complementary deoxyribonucleic acid

cGMP, cyclic guanosine monophosphate

CNS, central nervous system

CO_2, carbon dioxide

CPE, CNS penetration effectiveness

CREB, cyclic adenosine monophosphate response element binding protein

CSF, cerebrospinal fluid

CXCR4, chemokine (C-X-C motif) receptor 4

DMEM, Dulbecco's modified eagle medium

DN, dominant negative

DNA, deoxyribonucleic acid

DTT, dithiothreitol

EGTA, ethylene glycol tetraacetic acid

ERK, extracellular signal-regulated kinase

F-actin, filamentous actin

Fura-2-AM, fura-2-acetoxymethylester

GABA, gamma-amino butyric acid

G-actin, globular actin

GECI, genetically-encoded Ca^{2+} indicator

GFP, green fluorescent protein

Glu, glutamate

gp41, envelope glycoprotein 41

gp120, envelope glycoprotein 120

HAD, HIV-associated dementia

HAND, HIV-associated neurocognitive disorders

HEK293, human embryonic kidney 293 cells

HEPES, hydroxyethyl piperazine ethanesulfonic acid

HHSS, HEPES Hanks salt solution

HI, heat-inactivated

HIV-1, human immunodeficiency virus type 1

HIV-2, human immunodeficiency virus type 2

HS, horse serum

IL-1β, interleukin-1 beta

L-NAME, L-NG-nitroarginine methyl ester

LRP, low density lipoprotein receptor-related protein

MEK1, map kinase kinase 1

Mg^{2+}, magnesium

MND, mild neurocognitive disorder

mRNA, messenger RNA

MS, multiple sclerosis

NMDA, N-methyl-D-aspartate

NMDAR, NMDA receptor

NO, nitric oxide

NOS, nitric oxide synthase

nNOS, neuronal nitric oxide synthase

NHS-PEG4, N-hydroxysulfosuccinimide-polyethylene glycol 4

OI, opportunistic infection

PBS, phosphate-buffered saline

PMSF, phenylmethanesulfonyl fluoride

PKG, cyclic GMP-dependent protein kinase, protein kinase G

PSD95, postsynaptic density protein 95

RAP, receptor-associated protein

RFP, red fluorescent protein

ROCK, rho-associated protein kinase

ROS, reactive oxygen species

RNA, ribonucleic acid

SDS, sodium dodecyl sulfate

SEM, standard error of the mean

SFK, src family kinase

sGC, soluble guanylate cyclase

TAR, trans-activation response region

Tat, transactivator of transcription

Tyr, tyrosine

VASP, vasodilator-associated phosphoprotein

$Zn2^{+}$, zinc

Chapter One:

Introduction

I. HIV pathogenesis and virology

Human immunodeficiency virus (HIV) is the causal agent of acquired immunodeficiency syndrome (AIDS) (Barre-Sinoussi et al., 1983; Gallo et al., 1984; Popovic et al., 1984; Sarngadharan et al., 1984; Schupbach et al., 1984) and is one of the deadliest diseases in history. HIV has infected more than 70 million people resulting in more than 35 million AIDS-related deaths (WHO Global Health Observatory, 2014). Today, approximately 35 million people are infected with HIV (UNAIDS, 2013) and despite improved prevention programs and pharmacotherapy, the pandemic is far from over.

The transmission of HIV occurs by exchange of bodily fluids commonly occurring via sexual intercourse with a host (U.S. Dept. of Health and Human Services, 2014c). Flu-like symptoms such as fever, fatigue, and rash begin within days to weeks of infection with HIV and persist for up to 10 weeks (Kahn and Walker, 1998). Symptoms of acute HIV infection rarely lead to an accurate diagnosis, as patients are usually unaware of the exposure. However, HIV can be detected as within 2 weeks of infection (Cohen et al., 2010). Eventually, the acute symptoms subside as the disease progresses to clinical latency, which can persist an average of 10 years, although the rate of progression varies dramatically between individuals (U.S. Dept. of Health and Human Services, 2014b). During clinical latency and without treatment, HIV depletes the immune system of CD4-positive lymphocytes to below 200 cells/mm^3 resulting in progression of the disease from HIV to AIDS (U.S. Dept. of Health and Human Services, 2014b). Typically, people with AIDS die within three years without antiretroviral therapy (U.S. Dept. of

Health and Human Services, 2014b). Compromised immune function renders the patient increasingly vulnerable to opportunistic infections (OI) such as *pneumocystis carinii* pneumonia, tuberculosis, toxoplasmosis, *cryptococcus neoformans*, and progressive multifocal leukoencephalopathy (Kaplan et al., 2000; Sepkowitz, 2002). The average life expectancy of a person with AIDS with an OI is one year (Walensky et al., 2006; U.S. Dept. of Health and Human Services, 2014b). Such severe immunosuppression impairs nearly all organ systems including the central nervous system (CNS) (Chu and Selwyn, 2011).

HIV-1 belongs to the family *Retroviridae*, subfamily *Lentivirinae*, and genus *Lentivirus* (Votteler, 2008). Each virion of HIV-1 contains two ribonucleic acid (RNA) strands approximately 9.7 kilobases in length (Votteler, 2008). Each RNA strand encodes nine viral genes including gag, env, pol, vpu, vif, vpr, nef, rev, and tat. These genes encode proteins that fall in into structural (gag, env), catalytic (pol), accessory (vpu, vif, vpr, nef), or regulatory (rev, tat) classes (Votteler, 2008). Additionally, each virion contains three essential enzymes necessary for viral replication, including reverse transcriptase (Chandra et al., 1986), integrase (Stevenson et al., 1990), protease (Schneider and Kent, 1988), and two viral RNA strands (Feinberg et al., 1986). The nucleocapsid of HIV, composed of the core capsid protein p24 (Gelderblom et al., 1987), encases the viral contents (Wills and Craven, 1991; Dorfman et al., 1994). The viral envelope, composed of a lipid bilayer formed during budding from the membrane of the infected host cell, surrounds the nucleocapsid. Embedded within the viral envelope are the surface proteins gp120 (Barin et al., 1985) and gp41 (Veronese et al., 1985).

HIV is an obligate intracellular parasite requiring human cells for replication. Viral tropism is determined by the cell surface protein gp120 (Chan et al., 1997; Berger et al.), which is essential for viral infection of the host cells. Infection with HIV occurs when gp120 binds to CD4 receptors (Dalgleish et al., 1984; Kwong et al., 1998) and either co-receptor CXCR4 (Feng et al., 1996; Lapham et al., 1996) or CCR5 (Wu et al., 1996). Subsequently, gp41 undergoes a conformational change resulting in the insertion of the N-terminal hydrophobic fusion-peptide into the membrane of host cell (Furuta et al., 1998). Next, gp41 collapses into a trimer-of-hairpins that pulls the virus closer to the cell until the two eventually fuse (Gonzalez-Scarano et al., 1987; Root et al., 2001). Fusion enables the viral contents to spill into the cytoplasm of the host cell where the process of viral replication can begin. Viral RNA generates viral DNA by reverse transcription (Preston et al., 1988; Roberts et al., 1988). Viral DNA is transported into the nucleus of the host cell and integrated into the host cell genome by the viral enzyme, integrase (Bukrinsky et al., 1992). Integrated HIV is a provirus. Proviral DNA is transcribed into HIV RNA as part of normal cellular genomic activity. HIV RNA transcripts are translated into immature viral polypeptides; protease assists in the maturation of immature polypeptides into their functional forms via proteolysis (Greene and Peterlin, 2002). Following replication of all necessary viral components, they are packaged into the nucleocapsid, which buds from the host cell membrane to form a new viral particle in search of other cells to infect (Greene and Peterlin, 2002).

Two types of HIV are known to exist: HIV-1 and HIV-2, although HIV-1 accounts for the majority of infections worldwide (McCutchan, 2006). HIV-1 and -2

differ in the zoonotic origin with HIV-1 most closely resembling simian immunodeficiency virus from chimpanzees (Huet et al., 1990) whereas HIV-2 appears to have originated in the sooty mangabey (Hirsch et al., 1989). HIV-1 is more virulent, results in higher viral loads, and has a greater rate of disease progression relative to HIV-2 (Marlink et al., 1994). HIV-1 is divided into three groups: Main (M), Outlier (O), and Non-M, Non-O (N) (McCutchan, 2006). The M-group constitutes the majority of infections worldwide whereas the O- and N-group are rare and mostly confined to the African country of Cameroon (McCutchan, 2006). The M-group is subdivided into nine clades; A through K, with clades B and C being the most common global subtypes (McCutchan, 2006). Interestingly, the induction of neuropathogenesis is clade-dependent with clade B being more neurotoxic than clade C (Rao et al., 2008).

II. Treatment of HIV

HIV infection has no known cure, however the efficacy of pharmacotherapy has improved dramatically in the past 30 years (Heaton et al., 2011). Consequently, HIV has been transformed from a fatal infection to a manageable condition due to combination antiretroviral therapy (cART). The use of cART as standard therapy began 1996 and has remained the recommended treatment for HIV infection ever since (U.S. Dept. of Health and Human Services, 2014a). Therapeutic regimens consist of combinations of at least three antiretroviral drugs including viral fusion inhibitors, nucleoside reverse transcriptase inhibitors, non-nucleoside reverse transcriptase inhibitors, protease inhibitors, and integrase inhibitors (U.S. Dept. of Health and Human Services, 2014a).

Drugs within these respective classes target distinct steps in the viral replication cycle and have been instrumental for the treatment and management of HIV. Combination therapy improves patient outcomes by reducing peripheral viral load and decreasing opportunistic infections thereby increasing patient survival (Kaplan et al., 2000; Hogg, 2008).

While current-generation cART effectively reduces peripheral viral load and prolongs the lifespan of the patient, viral reservoirs persist within the central nervous system (CNS) (Lambotte et al., 2003). These latent viral reservoirs persist in the brain due to insufficient drug distribution to the CNS, inadequate treatment, decreased effectiveness of cART, and other factors that contribute to the persistently high prevalence of HIV-associated neurocognitive disorders (HAND) (Valcour et al., 2011).

III. HIV-associated neurocognitive disorders

HIV enters the CNS as early as 2 weeks following the initial infection (Resnick et al., 1988; Davis et al., 1992; An et al., 1999). Multiple pathways have been proposed for how HIV enters the CNS. The "Trojan Horse" hypothesis suggests that HIV enters the CNS undetected by hiding inside monocytes or CD4+ T-cells, which routinely traffic into the CNS (Peluso et al., 1985; Nath, 1999). Alternatively, HIV crosses the endothelial cells of the blood-brain barrier (BBB) by transcytosis to enter the CNS (Bomsel, 1997; Banks et al., 2004). Once inside the CNS, HIV causes neurotoxicity leading to HAND (Clifford and Ances, 2013). HAND affects approximately half of the HIV-infected patients in the U.S. and it is likely that the prevalence is higher in regions of the world

where cART is uncommon. Thus, up to half of the 35 million patients infected with HIV are at risk of developing HAND (Cysique et al., 2004; Tozzi et al., 2005; Heaton et al., 2011). Symptoms of HAND are categorized based on the severity of impairment and range from subtle impairment in day-to-day tasks to severe functional impairment (Heaton et al., 2004; Antinori et al., 2007). The prevalence of asymptomatic neurocognitive impairment (ANI), mild neurocognitive disorder (MND), and HIV-associated dementia (HAD) vary depending on the stage of HIV disease, but constitute approximately 20%, 20%, and 8% of the HIV-infected population in the U.S.A, respectively (Antinori et al., 2007). Patients with ANI have subtle impairment in at least two ability domains with no impairment in day-to-day functioning (Antinori et al., 2007). Patients with MND have modest impairment in at least two ability domains and have mild cognitive decline resulting in impaired day-to-day functioning (Antinori et al., 2007). Patients suffering from HAD exhibit marked impairment in cognitive function with significant difficulty performing day-to-day tasks (Antinori et al., 2007). The pre-cART prevalence of HAD was 4%, 12%, and 17% for the respective CDC stages of HIV disease A, B, and C (Heaton et al., 2011). However, in the cART era, the prevalence of HAD is approximately 8% across all disease stages (Heaton et al., 2011). Unfortunately, the prevalence of all other forms of HAND remains persistently high despite effective control of viral load with cART (Heaton et al., 2010).

The persistence of HAND is thought to arise, at least in part, from latent viral reservoirs within the CNS that are not entirely accessible to current-generation cART (Valcour et al., 2011). Anti-retroviral therapies with higher CNS penetration

effectiveness (CPE) scores significantly improve cognitive function in patients with HAND relative to HAND patients receiving drugs with lower CPE scores (Cysique et al., 2009). These data indicate that reducing or eradicating viral reservoirs using therapies with improved CNS penetrance may reduce the prevalence of HIV-associated cognitive impairment. In recent years, adjunctive therapies to treat HIV-associated cognitive impairment have gained significant interest. Some of these drugs include the anti-epileptic, valproic acid (Schifitto et al., 2006), the monoamine oxidase inhibitor, selegiline (Sacktor et al., 2000; Evans et al., 2007; Schifitto et al., 2007a), the glycogen synthase kinase 3-beta inhibitor, lithium (Letendre et al., 2006; Schifitto et al., 2009), the calcium channel blocker, nimodipine (Navia et al., 1998), and the NMDAR antagonist, memantine (Schifitto et al., 2007b; Zhao et al., 2010). A meta-analysis investigated the efficacy of 10 promising adjunctive therapies in treating cognitive impairment in HAND patients and determined that these drugs are ineffective at treating or preventing HAND (Uthman and Abdulmalik, 2008). These data highlight the importance of improving the distribution of cART to the CNS and enhancing our understanding of the pathophysiological mechanisms that cause HAND so that targeted CNS therapies can be developed.

Another reason for the persistence of HAND is due to prolonged lifespans of patients resulting from successful cART regimens. Aging HIV+ patients are especially susceptible to cognitive decline (Valcour et al., 2004). By 2015, over half of the HIV+ population of the United States will be over the age of 50 placing them at increased risk for the development of HAND (Adekeye et al., 2012). Thus, while the HIV+ population

continues to grow and age, very few options are available to treat or prevent the HIV-associated cognitive decline they are likely to develop. In order to develop new therapies or use existing treatments against HIV-associated cognitive decline, an enhanced understanding of the underlying mechanisms causing cognitive impairment is required.

IV. Mechanisms of HIV-associated neurotoxicity

Cells expressing CD4 receptors and either CXCR4 or CCR5 co-receptors are susceptible to HIV infection (Dalgleish et al., 1984; Feng et al., 1996; Lapham et al., 1996; Wu et al., 1996; Kwong et al., 1998). Cells within the CNS such as microglia (Albright et al., 1999) and perivascular macrophages (Williams et al., 2001) express these receptors, but neurons do not. Thus, HIV is unable to infect neurons indicating that HIV-induced neuronal damage is indirect (Wiley et al., 1986; Gonzalez-Scarano and Martin-Garcia, 2005). As shown in Figure 1.1, HIV-infected cells can release a variety of agents that are neurotoxic including inflammatory cytokines (Genis et al., 1992), nitric oxide (Eugenin et al., 2007), glutamate (Jiang et al., 2001), as well as the viral proteins, gp120 (Schneider et al., 1986) and Tat (Chang et al., 1997).

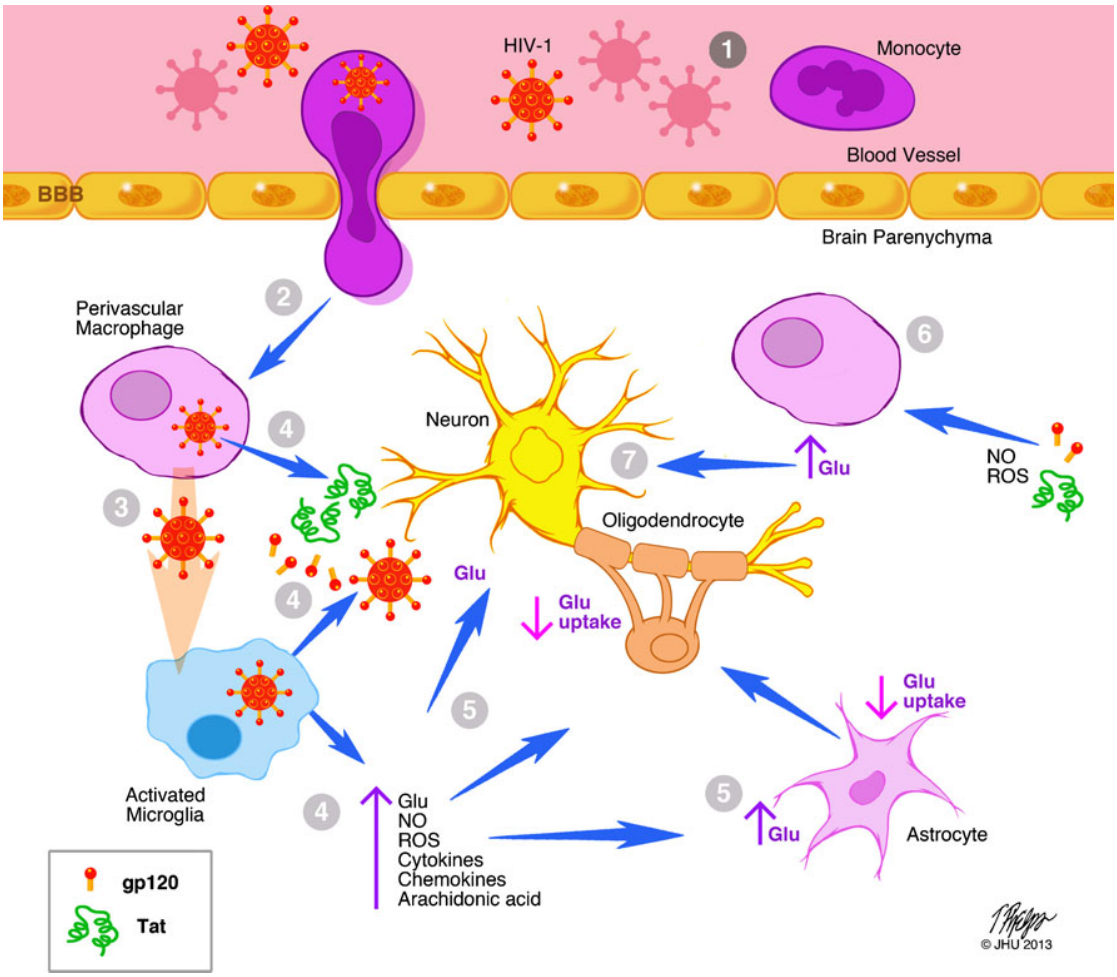

Figure 1.1: Mechanisms of glutamate excitoxicity during HIV-1 infection **(1)** Infection of circulating monocytes with HIV-1. **(2)** HIV-1 infected macrophages cross the BBB and become perivascular macrophages. **(3)** HIV-1 infected perivascular macrophages in the brain parenchyma release viral particles that infect other brain macrophages and microglial cells. **(4)** Activated macrophages and microglial cells release viral proteins gp120 and Tat, glutamate and other factors such as NO, ROS, cytokines, chemokines and arachidonic acid that can either directly or indirectly affect glutamate metabolism and/or transport. **(5)** Decrease in glutamate uptake by oligodendrocytes and astrocytes due to increased levels of these toxins released by HIV-1 infected macrophages and microglial cells. These factors also cause an increase in vesicular glutamate release by astrocytes. **(6)** Viral proteins Tat and gp120 and oxidative stress induced by ROS and NO cause an increase in the activity of glutamate-cystine antiporter in uninfected perivascular macrophages and microglia and as a consequence extracellular levels of glutamate increase. **(7)** Excessive extracellular glutamate triggers activation of glutamate receptors on neurons causing an increase in the intracellular calcium levels, cell death and neuronal degeneration (Potter et al., 2013). Reproduced with permission, © 2013 Springer

These agents create a neurotoxic environment resulting in disrupted Ca^{2+} homeostasis, synaptodendritic damage, and cell death (Kaul et al., 2001). Although cell death is observed in the brains of patients who succumbed to HIV/AIDS, the extent of cell death does not correlate closely with cognitive decline. Rather, symptoms of cognitive impairment correlate better with damage to synaptodendritic structures, including loss of dendritic spine density and dendritic beading (Ellis et al., 2007). Symptoms of cognitive impairment that result from synaptodendritic damage include memory loss, difficulty with comprehension, and reduced information processing speed (Heaton et al., 2004; Antinori et al., 2007). Additionally, HIV causes motor deficits (Arendt et al., 1990) and psychiatric disorders (Atkinson et al., 1988). Intriguingly, *in vitro* studies indicate that the synaptodendritic damage thought to give rise to cognitive impairment is preventable, and in some instances, reversible (Kim et al., 2008; Shin et al., 2012; Hargus and Thayer, 2013). Thus, it may be possible to preserve cognitive function in HIV+ patients with the appropriate therapy.

V. HIV-1 Tat: A potent neurotoxin

HIV-infected cells can release many substances that contribute to HAND (Potter et al., 2013). Although the neuropathogenesis of HAND likely involves a combination of factors, evidence suggests that the HIV protein transactivator of transcription (Tat) plays a prominent role in neurotoxicity (Shin et al., 2012) and cognitive impairment (Fitting et al., 2010; Carey et al., 2012; Bachani et al., 2013; Fitting et al., 2013).

Tat is a nonstructural viral protein that is responsible for initiating transcription of the HIV genome (Sodroski et al., 1985a; Sodroski et al., 1985b). After activation of genomic transcription, Tat binds to the trans-activation response region (Berkhout et al., 1989; Dingwall et al., 1990) and forms a complex with transcriptional machinery including RNA polymerase II, cyclin T1 and cyclin-dependent kinase 9 (CDK9) (Isel and Karn, 1999). Cyclin T1 activates CDK 9 to phosphorylate RNA polymerase II leading to transcription of the HIV-1 genome.

Tat is encoded by two exons; the first exon encodes amino acids 1-72 while the second exon encodes amino acids 73-104 (Kuppuswamy et al., 1989; Ruben et al., 1989; Romani et al., 2010). The first exon contains domains that are essential for Tat's neurotoxic properties and transactivation abilities. Domains 1 through 3, known as the activation domain, consist of the N-terminal domain, a cysteine-rich domain, and the core domain. The fourth domain aids in the nuclear localization of Tat, while the fifth domain is required for transactivation. The second exon encodes a basic, C-terminal region that is critical for cellular uptake of Tat (Ma and Nath, 1997).

Tat is shed from HIV-infected cells (Chang et al., 1997) and detected in the CNS of HIV-infected patients (Chang et al., 1997; Hudson et al., 2000). The level of anti-Tat antibodies in the CSF of HIV-infected patients is higher in patients without cognitive impairment and lower in patients with cognitive decline suggesting antibody responses against Tat may preserve cognitive function (Bachani et al., 2013). Despite significant improvement in the efficacy of cART for treating HIV infection, current regimens remain unable to halt the production of Tat once viral DNA is integrated into the host genome

(Li et al., 2009). *In vivo*, expression of Tat causes loss of dendritic spines and synaptodendritic damage resulting in learning and memory impairment (Fitting et al., 2010; Carey et al., 2012; Fitting et al., 2013). *In vitro*, Tat directly depolarizes neurons (Cheng et al., 1998), potentiates NMDA receptor (NMDAR) function (Haughey et al., 2001; Krogh et al., 2014), and disrupts intracellular Ca^{2+} ($[Ca^{2+}]_i$) homeostasis (Haughey et al., 1999). Additionally, Tat causes loss of excitatory synapses (Kim et al., 2008) and presynaptic terminals (Shin and Thayer, 2013), inhibitory synapse gain (Hargus and Thayer, 2013), and neuronal death (Eugenin et al., 2007; Shin et al., 2012). Cognitive decline in HAND correlates more closely with synaptodendritic damage, which occurs prior to neuronal cell death (Ellis et al., 2007). Intriguingly, synaptic changes observed *in vitro* that precede neuronal death are reversible (Kim et al., 2008; Shin et al., 2012; Hargus and Thayer, 2013). Importantly, almost all instances of Tat-induced neurotoxicity are prevented by pharmacologic inhibition of the NMDAR (Eugenin et al., 2007; Kim et al., 2008; Shin et al., 2012; Hargus and Thayer, 2013) indicating that Tat-induced neurotoxicity requires aberrant NMDAR-mediated Ca^{2+} influx. Thus, enhanced understanding of the mechanisms leading to NMDAR dysfunction and the consequences of abnormal receptor function are a major focus for the development of improved HAND therapies.

VI. NMDA RECEPTORS

The NMDAR is an ionotropic glutamate receptor expressed in neurons (McLennan, 1983). Activation of NMDARs requires coincident cellular depolarization

to relieve the Mg^{2+} block of the ion channel (Nowak et al., 1984) and binding of both glutamate (Jahr and Stevens, 1987) and glycine (Johnson and Ascher, 1987) to ligand binding sites. NMDAR activation causes the channel to open allowing an influx of Ca^{2+} into the neuron (MacDermott et al., 1986). The NMDAR is composed of two obligatory GluN1 subunits and two regulatory GluN2 subunits to form a tetramer (Cull-Candy et al., 2001). Four distinct GluN2 isoforms have been identified and include GluN2A, GluN2B, GluN2C, and GluN2D (Cull-Candy et al., 2001). Each tetramer has distinct properties; GluN2A- and GluN2B-containing NMDARs have high channel conductance openings, while NMDARs containing GluN2C and GluN2D have low channel conductance openings (Cull-Candy and Leszkiewicz, 2004). Additionally, deactivation kinetics are most rapid in NMDARs containing GluN2A, slowest in GluN2D-containing NMDARs, and equal between GluN2B- and GluN2C-containing NMDARs (Cull-Candy and Leszkiewicz, 2004). The hippocampus only expresses NMDARs containing GluN2A and GluN2B (Wenzel et al., 1997) that localize to synaptic and extrasynaptic regions of the neuron, respectively (Groc et al., 2006; Hardingham and Bading, 2010).

The NMDAR is an essential component in the synaptic machinery that underlies learning and memory. Overexpression or pharmacologic inhibition of NMDARs results in improved (Tang et al., 1999) or impaired (Malhotra et al., 1996; Newcomer and Krystal, 2001) cognitive function, respectively. NMDAR dysfunction is implicated in many neurodegenerative disorders including Alzheimer's (Danysz and Parsons, 2003) and Parkinson's (Hallett and Standaert, 2004) disease, amyotrophic lateral sclerosis (Spalloni et al., 2013), multiple sclerosis (Rossi et al., 2013), Huntington's disease

(Young et al., 1988), and HAND (Kaul et al., 2001; Potter et al., 2013). Although many neurodegenerative diseases are etiologically distinct, they share a common feature: NMDAR dysfunction. Tat causes NMDAR dysfunction (Haughey et al., 2001; Chandra et al., 2005; Li et al., 2008; Krogh et al., 2014) likely contributing to the symptoms of cognitive impairment in HAND patients.

VII. The role of NMDA receptors in Tat-induced neurotoxicity

Treatment with Tat affects NMDARs directly and indirectly. Tat directly activates the NMDAR (Song et al., 2003) resulting in neurotoxicity (Li et al., 2008). Additionally, Tat indirectly enhances NMDAR function via binding to and relieving the inhibitory effect of Zn^{2+} (Chandra et al., 2005) or via tyrosine kinase-mediated phosphorylation of NMDARs (Haughey et al., 2001). NMDAR-mediated Ca^{2+} influx leads to loss of excitatory synapses via ubiquitination and subsequent proteasomal degradation of the postsynaptic scaffolding protein 95 (PSD-95) by an E3 ligase-dependent mechanism (Kim et al., 2008). Distinct intracellular signaling pathways are activated depending on the NMDAR subtype mediating the Ca^{2+} influx (Hardingham et al., 2002). Pharmacologic blockade of GluN2A-containing NMDARs prevents Tat-induced synapse loss, but does not block Tat-induced cell death. Conversely, inhibition of GluN2B-containing NMDARs prevents Tat-induced cell death, but is ineffective at preventing Tat-induced synapse loss. Intriguingly, antagonism of GluN2B-containing NMDARs induces synapse recovery in the presence of Tat after synapse loss has already occurred (Shin et al., 2012). Thus, NMDAR subtypes differentially participate in adaptive

processes following exposure to Tat. Concurrent with excitatory synapse loss, NMDAR-mediated Ca^{2+} influx also increases the number of inhibitory synapses via a calmodulin-dependent protein kinase II (CAMKII)-dependent process (Hargus and Thayer, 2013). Lastly, Tat causes neuronal cell death via NMDAR-dependent production of nitric oxide (NO) (Eugenin et al., 2007). Thus, Tat-induced changes in synaptic composition and cell death require NMDAR-mediated Ca^{2+} influx.

VIII. Summary of introduction and current studies

The pandemic of HIV is far from over, but major progress in the detection, treatment, and management of this condition has been made. Anti-retroviral drugs have transformed HIV infection from a fatal disease to a manageable condition (Hogg, 2008), but the prevalence of HAND remains persistently high is likely to increasing due to prolonged lifespans of patients (Heaton et al., 2011). In order to develop new therapies or make use of existing treatments, an enhanced understanding of the mechanisms leading to HIV-associated cognitive impairment is required. Cognitive impairment stems from synaptodendritic damage (Ellis et al., 2007); a significant cause of such neurotoxicity is excessive Ca^{2+} influx through the NMDAR (Shin et al., 2012). The subject of this dissertation is the mechanism responsible for NMDAR dysfunction following exposure to the HIV-1 protein, Tat.

Tat is a potent neurotoxin that damages neurons (King et al., 2006) and causes cognitive impairment (Fitting et al., 2010; Carey et al., 2012). Tat causes loss of excitatory synapses (Kim et al., 2008), simultaneous gain of inhibitory synapses (Hargus

and Thayer, 2013), and neuronal death (Shin et al., 2012). Cell death and changes in synaptic composition are dependent on NMDAR-mediated Ca^{2+} influx. High concentrations of Tat potentiate NMDAR function following brief exposures. However, if and when concentrations of Tat similar to those measured in HAND patients affect NMDAR function was unknown.

First, it was determined that a pathophysiologically relevant concentration of Tat caused a time-dependent, biphasic change in NMDAR function. Initially, Tat potentiated NMDAR function via low-density lipoprotein receptor-related protein (LRP)-dependent activation of Src kinase. Subsequently, this potentiation adapted by gradually returning to basal levels via activation of the nitric oxide synthase (NOS), soluble guanylate cyclase (sGC), cGMP-dependent protein kinase pathway (PKG).

Next, effectors downstream of PKG responsible for the adaptation of the NMDAR function were identified. Tat activated a signaling pathway, which included the small GTPase RhoA and Rho-associated protein kinase (ROCK). Activation of RhoA/ROCK caused reorganization of the actin cytoskeleton and attenuated NMDAR function.

These studies suggest that Tat potentiates NMDAR function via LRP-dependent activation of Src kinase and adapts following activation of a signaling cascade resulting from RhoA/ROCK-mediated reorganization of the actin cytoskeleton. Adaptation of NMDAR function following exposure to Tat has not been previously described and may be a neuroprotective measure to prevent excessive Ca^{2+} influx and neurotoxicity. These studies provide molecular and temporal detail of the mechanisms that underlie Tat-

induced NMDAR dysfunction and offer insight into potential therapeutic targets for the treatment of HAND.

Chapter Two:

HIV-1 protein Tat produces biphasic changes in NMDA-evoked increases in intracellular Ca^{2+} concentration via activation of Src kinase and nitric oxide signaling pathways

Kelly A Krogh, Nicole Wydeven, Kevin Wickman and Stanley A. Thayer*

Department of Pharmacology, University of Minnesota Medical School

Minneapolis, MN

Content adapted from published article: Krogh KA, Wydeven N, Wickman K, Thayer SA (2014) HIV-1 protein Tat produces biphasic changes in NMDA-evoked increases in intracellular Ca^{2+} concentration via activation of Src kinase and nitric oxide signaling pathways. *J Neurochem*. 10.1111/jnc.12724

Contributions: KAK and SAT designed the study; KAK and NW performed experiments; KAK and NW collected and analyzed data; KAK and SAT wrote the manuscript; SAT and KW provided reagents and conceptual advice.

I. Introduction

Cognitive function is impaired in 30-55% of patients infected with human immunodeficiency virus (HIV) (Cysique et al., 2004; Tozzi et al., 2005; Heaton et al., 2011). HIV-associated neurocognitive disorders (HAND) range in severity from a subtle reduction in information processing speed to significant functional impairment (Heaton et al., 2004). Despite effectively managing viral load with combined anti-retroviral therapy (cART), the prevalence of HAND remains persistently high (Heaton et al., 2010) and may be increasing due to prolonged patient lifespans. Currently, the efficacy of drugs to treat HAND is insufficient and the options are few.

In the brain, HIV infects macrophages and microglia, but not neurons (Watkins et al., 1990). Thus, HIV-induced neurotoxicity is indirect and results from the release of neurotoxic agents such as inflammatory cytokines, nitric oxide, glutamate, and viral proteins (Genis et al., 1992; Jiang et al., 2001; Kaul et al., 2001; Nath, 2002; Eugenin et al., 2007). The transactivator of transcription (Tat) is a protein shed from HIV-infected cells (Chang et al., 1997) and detected in the sera and CNS of HIV-infected patients (Chang et al., 1997; Hudson et al., 2000). The level of anti-Tat antibodies in the CSF of HIV-infected patients without cognitive dysfunction is higher than in patients with HAND, suggesting antibody responses against Tat may be neuroprotective (Bachani et al., 2013). Despite significant improvement in the efficacy of cART for treating HIV infection, current regimens remain unable to halt the production of Tat (Li et al., 2009).

Cognitive decline in patients with HAND correlates with synaptodendritic damage (Ellis et al., 2007). Expression of Tat in transgenic rodent models causes loss of

excitatory synapses resulting in learning and memory impairment (Carey et al., 2012; Fitting et al., 2012). *In vitro*, Tat-induced synapse loss (Kim et al., 2008) and neuronal death (Eugenin et al., 2007) are initiated by NMDAR-mediated Ca^{2+} influx. Tat potentiates NMDA-evoked increases in intracellular Ca^{2+} concentration ($[Ca^{2+}]_i$) in hippocampal neurons (Haughey et al., 2001). Most studies of Tat-induced changes in NMDAR function are acute (min to h) while the neurotoxic effects of Tat occur over a prolonged time scale (h to days). Treating primary hippocampal neurons with Tat for 24 h causes loss of excitatory synapses (Kim et al., 2008) and simultaneous gain of inhibitory synapses (Hargus and Thayer, 2013) indicating that Tat evokes adaptive changes in the synaptic composition of neurons. Such neuroadaptations may be a mechanism to cope with excess excitatory input. Notably, these adaptive changes are prevented by pharmacologic inhibition of the NMDAR (Shin et al., 2012) indicating that the NMDAR is essential for synaptic neuroadaptation. How NMDA-evoked $[Ca^{2+}]_i$ responses are affected by prolonged exposure to Tat, when adaptive changes in synaptic composition occur, is the focus of this study.

Here, we examined changes in NMDA-evoked increases in $[Ca^{2+}]_i$ during 48 h exposure to Tat. We found that Tat evoked a biphasic change in NMDA-evoked $[Ca^{2+}]_i$ responses. Tat initially potentiated the NMDA-evoked increase in $[Ca^{2+}]_i$ via the low-density lipoprotein receptor-related protein (LRP) and activation of Src kinase. Tat-induced potentiation subsequently adapted by gradually returning to baseline levels. Adaptation resulted from activation of the nitric oxide synthase (NOS) / soluble guanylate cyclase (sGC) / protein kinase G (PKG) signaling pathway. This study

suggests a changing role for the NMDAR during the course of HIV neurotoxicity with implications for treatment of HAND.

II. Methods

Drugs and Reagents

Materials were obtained from the following sources: HIV-1 Tat (Clade B, full length recombinant) was from the NIH AIDS Research and Reference Reagent Program (HIV-1 Tat protein (full length, Clade B) from John Brady and DAIDS, NIAID and from Prospec Tany TechnoGene Ltd. (Rehovot, Israel); recombinant rat low-density lipoprotein receptor-related protein associated protein 1 (RAP) was from Fitzgerald Industries International (Concord, MA); Dulbecco's modified Eagle's medium (DMEM), fetal bovine serum, horse serum, fura-2-acetomethyl ester (Fura-2-AM), and glycine were from Invitrogen (Carlsbad, CA); NMDA, NG-Nitro-L-Arginine Methyl Ester (L-NAME), and 1H-(1,2,4)oxadiazolo[4,3-a]quinoxalin-1-one (ODQ) were from Sigma-Aldrich (St. Louis, MO); 4-amino-5-(4-chloro- phenyl)-7-(*t*-butyl)pyrazolo[3,4-*d*]pyrimidine (PP2) and 4-amino-7-phenylpyrazol[3,4-d]pyrimidine (PP3), 8R,9S,11S)-(-)-9-methoxy-carbamyl-8-methyl-2,3,9,10-tetrahydro-8,11-epoxy-1H,8H,11H-2,7b,11a-trizadibenzo-(a,g)-cycloocta-(c,d,e)-trinden-1-one (KT5823), and (1*R**,2*S**)-*erythro*-2-(4-Benzylpiperidino)-1-(4-hydroxyphenyl)-1-propanol hemitartrate (ifenprodil) were from Tocris (Bristol, United Kingdom); 2-(2-amino-3-methyoxyphenyl)-4 *H*-1-benzopyran-4-one (PD98059) was from Cell Signaling Technology (Danvers, MA); recombinant rat interleukin-1β was from R&D Systems (Minneapolis, MN).

DNA Constructs

Dominant-negative (DN)-Fyn with the K299M mutation and DN-Src with the K295M mutation in pRK5 were kindly provided by Dr. Filippo Giancotti (Memorial Sloan Kettering Cancer Center, New York, NY); pTagRFP-N was from Evrogen (Moscow, Russia). The catalytically inactive mutant of full-length PKG1α containing the amino terminal regulatory region fused to GFP (G1αR-GFP) in pEGFP-N1 (Clontech) was kindly provided by Darren Browning (Georgia Regents University). The G1αR fragment was removed via digestion with EcoR1 and BamH1 (New England Biolabs), and then inserted into the multiple cloning site of DsRed2-N1 (Clontech). Mammalian expression vectors containing GluN1, GluN2A, and GluN2B were kindly provided by Stephen Traynelis (Emory University).

Cell Culture

In accordance with the University of Minnesota's Institutional Animal Care and Use Committee and the NIH guide for the care and use of laboratory animals, maternal rats were euthanized by CO_2 inhalation and fetuses were removed on embryonic day 17. Rat hippocampal neurons were grown in primary culture as described previously (Li et al., 2012). Hippocampi were dissected and placed in Ca^{2+}- and Mg^{2+}-free HEPES-buffered Hanks' salt solution (HHSS), pH 7.45. HHSS contained the following (in mM): HEPES 20, NaCl 137, CaCl2 1.3, MgSO4 0.4, MgCl2 0.5, KCl 5.0, KH2PO4 0.4, Na2HPO4 0.6, NaHCO3 3.0, and glucose 5.6. Cells were dissociated by triturating through a 5 mL pipette and a flame-narrowed Pasteur pipette and then re-suspended in

DMEM without glutamine, supplemented with 10% fetal bovine serum and penicillin/streptomycin (100 U/mL and 100 mg/mL, respectively). Dissociated cells were then plated at a density of 60,000 to 80,000 cells/dish onto a 25-mm-round cover glass (#1) pre-coated with matrigel (150 μL, 0.2 mg/mL). Neurons were grown in a humidified atmosphere of 10% CO_2 at 37°C and fed on days 1 and 7 by exchange of 75% of the media with DMEM supplemented with 10% horse serum and penicillin/streptomycin. Cells used in these experiments were cultured without mitotic inhibitors resulting in a mixed glial-neuronal culture consisting of 18 ± 2% neurons, 70 ± 3% astrocytes, and 9 ± 3% microglia as indicated by immunocytochemistry (Kim et al., 2011). The cultures used for experimentation were grown for 12 to 15 days *in vitro* (DIV).

$[Ca^{2+}]_i$ imaging

Intracellular Ca^{2+} concentration ($[Ca^{2+}]_i$) was recorded as previously described (Li et al., 2013) with minor modifications. Cells were loaded by incubation with 5 μM fura-2 AM in 0.04% pluronic acid in HHSS for 30 min at 37°C followed by washing in the absence of indicator for 10 min. HIV-1 Tat and respective drugs were present during fura-2-AM loading, but were absent during the wash. Coverslips containing fura-2 loaded cells were transferred to a recording chamber, placed on the stage of an Olympus IX71 microscope (Melville, NY), and viewed through a 20X objective. Excitation wavelength was selected with a galvanometer-driven monochromator (8-nm slit width) coupled to a 75-W xenon arc lamp (Optoscan; Cairn Research). $[Ca^{2+}]_i$ was monitored using sequential excitation of fura-2 at 340 and 380 nm; image pairs were collected every 1 s.

For experimental recordings, cells were superfused at a rate of 1-2 mL/min with HHSS for 1 min followed by 30 s perfusion of Mg^{2+}-free HHSS that contained 200 μM glycine and either 10 or 100 μM NMDA. Fluorescence images (510/40 nm) were projected onto a cooled charge-coupled device camera (Cascade 512B; Roper Scientific) controlled by MetaFluor software (Molecular Devices). After background subtraction, the 340- and 380-nm image pairs were converted to $[Ca^{2+}]_i$ using the formula $[Ca^{2+}]_i = K_d\beta(R - R_{min})/(R_{max} - R)$ (Grynkiewicz et al., 1985). The dissociation constant (K_d) for fura-2 was 145 nM. β is the ratio of fluorescence intensity acquired with 380 nm excitation measured in Ca^{2+}-free buffer (1 mM EGTA) and buffer containing saturating Ca^{2+} (5 mM). R is 340 nm / 380 nm fluorescence intensity ratio. R_{min}, R_{max}, and β were determined in a series of calibration experiments on intact cells. R_{min} and R_{max} values were generated by applying 10 μM ionomycin in Ca^{2+}-free buffer (1 mM EGTA) and saturating Ca^{2+} (5 mM), respectively. Values for R_{min}, R_{max}, and β were 0.37, 9.38, and 6.46, respectively. These calibration constants were applied to all experimental recordings. To generate pseudocolor images, a binary mask was generated by applying an intensity threshold to the 380 nm image and applied to $[Ca^{2+}]_i$ images with colors assigned as indicated by the calibration bars in the figures. The neuronal cell body was selected as the region of interest for all recordings. All neurons within the imaging field were included in the analysis and no exclusions were made. For time course experiments, coverslips from the same cell culture plating were treated in parallel and each coverslip imaged only once.

Transfection

Rat hippocampal neurons were transfected between 11-12 days *in vitro* using a modification of a calcium phosphate protocol described previously (Li et al., 2012). Briefly, hippocampal cultures were incubated for 30 min in DMEM supplemented with 1 mM kynurenic acid, 10 mM $MgCl_2$, and 5 mM HEPES. A DNA/calcium phosphate precipitate containing 1 μg plasmid DNA per well was prepared, allowed to form for 30 min at 21°C then added to the culture. After 90 min of incubation, cells were washed once with DMEM supplemented with $MgCl_2$ and HEPES and then returned to conditioned media.

Biotinylation and immunoblotting

For biotinylation experiments, 7.5 x 10^6 hippocampal cells were plated in 100 x 20 mm petri dishes. Cells were treated with Tat alone or with an inhibitor of protein kinase G (KT5823) 1 h prior to the addition of Tat. Forty-eight hours later the media was removed and cells were washed three times with ice-cold PBS (pH 8.0) then incubated with 2 mM NHS-PEG_4 Biotin (Thermo Fisher Scientific Inc.) in ice-cold PBS with slow shaking at 4 °C for 30 min protected from light. Cells processed in parallel but not treated with biotin served as negative controls. Biotin was gently removed and cells were washed four times with ice-cold PBS. Cells were collected in PBS and centrifuged at 10,000 x g for 1 min. Following centrifugation, supernatants were aspirated and pellets were re-suspended in 250 μL lysis buffer consisting of PBS, 10% Triton, 20% SDS, and a mixture of protease inhibitors (10 μL PMSF, 100 μL Halt protease inhibitor). Samples

were sonicated with 3 x 1 s pulses and incubated with rocking for 30 min at 4 °C. Debris was pelleted in a microcentrifuge at 14,000 x g at 4 °C for 15 min and supernatants retained. 30 μL of sample ("Total protein") was removed, and the rest of the sample was mixed by rotation for 30 min at 4 °C with 60 μL of a 50% slurry of NeutrAvidin beads (Thermo Fisher Scientific Inc.). Beads were washed 3 times with lysis buffer and bound proteins eluted in 75 μL of 2X SDS sample buffer plus 25 μL 1 M DTT by heating at 75°C for 30 min. For immunoblotting, 3 μL 1M DTT was added to 15 μL of sample, and the mixture was incubated at 75°C for 10 min. Samples were then loaded onto 8% Bis-Tris gels and run in a Tris–glycine buffer under reducing conditions. Samples were transferred using the iBlot transfer system (Invitrogen) onto nitrocellulose membranes and probed with a rabbit anti-GluN2B polyclonal antibody (1:200 dilution, Millipore). An IRDye 800CW donkey anti-rabbit secondary antibody (LiCor Biosciences; Lincoln, NE, USA) was used at a dilution of 1:1000. Visualization and quantification of band intensity was performed using the Odyssey Imaging System (LiCor Biosciences). Integrated intensity values were recorded for all lanes and normalized to the intensity of the untreated control.

Statistical analysis

For $[Ca^{2+}]_i$ imaging studies, an individual experiment (n=1) was defined as the response from a single neuron on a single coverslip. Changes in NMDA-evoked increases in $[Ca^{2+}]_i$ are presented as mean ± SEM. Each experiment was replicated using at least 4 separate coverslips from at least 2 separate cultures. For biotinylation experiments, an

individual experiment (n=1) was defined as the change in surface-to-total GluN2B from a single 100 x 20 mm petri dish. Changes in GluN2B surface expression are presented mean ± SEM. Each experiment was replicated using at least 10 separate petri dishes from 10 separate cultures. Significance was determined by one-way ANOVA with Tukey's *post hoc* test for multiple comparisons (OriginPro v8.5).

III. Results

Tat potentiates NMDA-evoked $[Ca^{2+}]_i$ responses via LRP and a Src family kinase

Treating primary hippocampal neurons with Tat potentiated NMDA-evoked increases in $[Ca^{2+}]_i$ (Haughey et al., 2001). We replicated this finding using fura-2-based digital imaging of rat hippocampal neurons *in vitro*. As shown in Figure 2.1, increases in $[Ca^{2+}]_i$ evoked by 100 μM NMDA were potentiated following 40 min treatment with 100 nM Tat, but not by 100 nM heat-inactivated (HI, 85°C x 30 min) Tat.

Tat is internalized via the LRP (Liu et al., 2000) and Tat-induced neurotoxicity requires binding to the LRP with subsequent NMDA receptor (NMDAR)-mediated Ca^{2+} influx (Eugenin et al., 2007; Kim et al., 2008). We sought to determine whether the LRP was required for Tat-induced NMDAR potentiation by using the LRP antagonist, receptor-associated protein (RAP). RAP binds to the LRP and prevents neuronal uptake of Tat (Bu, 2001). Application of RAP (50 nM) 1 h prior to Tat application completely blocked Tat-induced potentiation (Fig. 2.1 G, H), suggesting that Tat potentiates NMDAR function via the LRP.

Tyrosine phosphorylation can potentiate NMDAR currents (Wang and Salter, 1994). Tat-induced NMDAR potentiation occurs via tyrosine kinase-dependent phosphorylation of GluN2A and GluN2B (Haughey et al, 2001), although the specific tyrosine kinase involved in NMDAR potentiation remains unknown. Src family kinases (SFKs) enhance NMDAR function (Kohr and Seeburg, 1996), therefore we used the SFK inhibitor, PP2, to determine the role of SFKs in Tat-induced potentiation of NMDARs. Pretreatment for 1 h with PP2 (10 μM), but not its inactive analog PP3 (10 μM), completely blocked the Tat-induced potentiation of NMDA–evoked responses (Fig. 2.1 G, H). Thus, Tat-induced potentiation of NMDA-evoked increases in $[Ca^{2+}]_i$ requires the activation of a SFK.

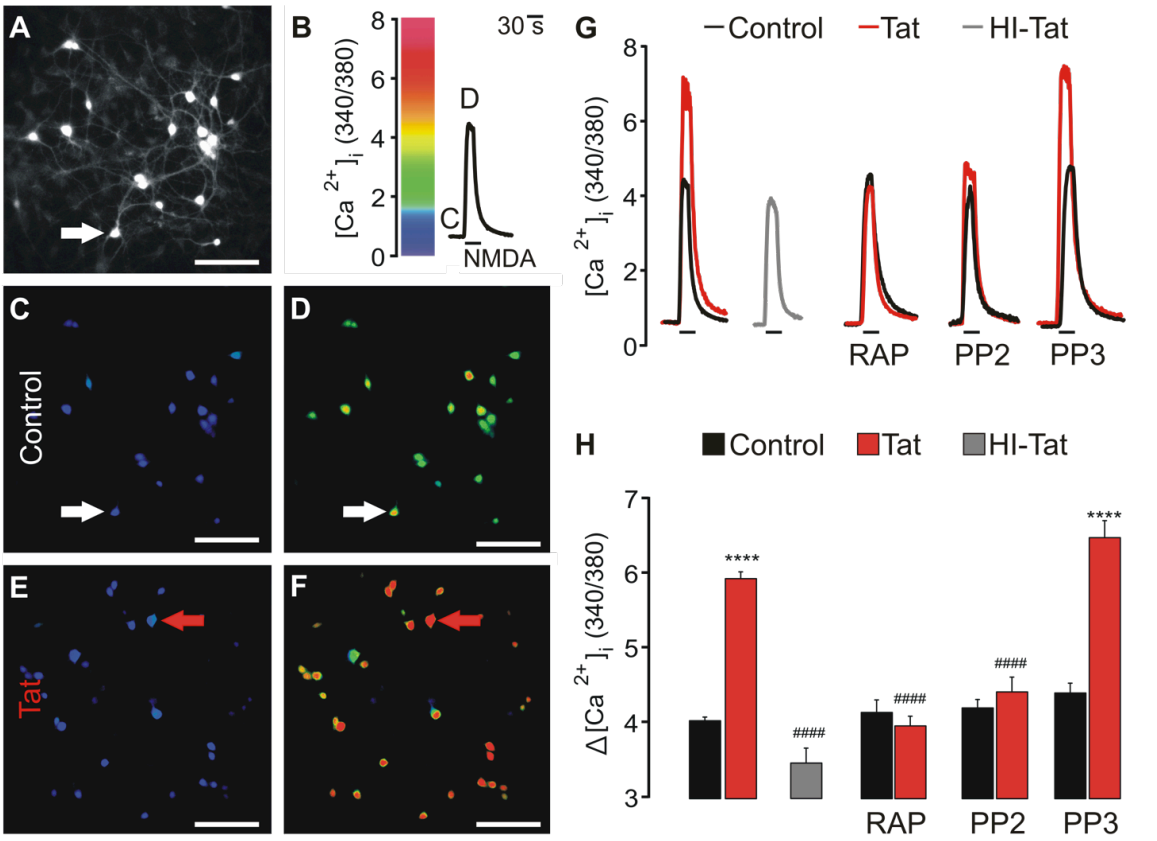

Figure 2.1: **HIV-1 Tat potentiates NMDA-evoked $[Ca^{2+}]_i$ responses via LRP and a SFK.** $[Ca^{2+}]_i$ was recorded using fura-2-based digital imaging (Methods). **A,** representative image shows fura-2 loaded neurons (scale bar = 100 μm). **B,** trace shows change in $[Ca^{2+}]_i$ expressed as 340 nm / 380 nm intensity ratio for the cell identified by the arrow in A. Cells were superfused with 100 μM NMDA (30 s) at the time indicated by the horizontal bar. **C-F**, pseudocolor images show $[Ca^{2+}]_i$ before (C, E) and during (D, F) 30 s application of 100 μM NMDA for control (C, D) and Tat treated (100 nM x 40 min; E, F) cells. Images were scaled as shown in B. Images were collected at times indicated by the letters annotating the traces in B. **G,** representative traces show NMDA-evoked $[Ca^{2+}]_i$ increases for control (▬) cells, Tat-treated cells (▬), and cells treated with heat-inactivated (HI) Tat (▬). Control (⇨) and Tat-treated (⇦) traces were from the cells indicated by the arrows in C-D and E-F, respectively. Cells were pretreated for 1 h prior to Tat application with 50nM RAP, 10 μM PP2, or 10 μM PP3 as indicated. **H,** Bar graph shows net $[Ca^{2+}]_i$ increase evoked by 100 μM NMDA in control (■) cells, cells treated with 100 nM Tat (■), or 100 nM heat-inactivated (HI) Tat (■) for 40 min. Cells were pretreated with 50nM RAP, 10 μM PP2, or 10 μM PP3 as indicated. ****p<0.0001 relative to respective control; ####p<0.0001 relative to Tat alone as determined by one-way ANOVA with 9 levels followed by Tukey's post-test for multiple comparisons.

Tat induces a biphasic change in NMDA-evoked increases in $[Ca^{2+}]_i$

Up to 40 ng/mL of Tat has been detected in the sera of HIV-infected patients (Xiao et al., 2000). Previously, we have observed Tat-induced changes in synapse number following treatment with 50 ng/mL (3.6 nM) Tat for 24 h (Kim et al., 2008; Hargus and Thayer, 2013). Thus, we hypothesized that 3.6 nM Tat would potentiate the NMDA-evoked increase in $[Ca^{2+}]_i$, but that these changes might require longer exposure to develop compared with 100 nM Tat. To test this hypothesis, we recorded NMDA-evoked $[Ca^{2+}]_i$ responses following treatment with 50 ng/mL Tat within a 48 h window (Fig. 2.2). Control and Tat-treated cultures were imaged in parallel. Exposure to Tat for 2 h potentiated NMDA-evoked increases in $[Ca^{2+}]_i$. Tat-induced potentiation of the NMDA-evoked response peaked by 8 h then adapted, returning to baseline by 24 h and dropping below control by 48 h.

Tat is susceptible to degradation by the Ca^{2+}-activated protease, calpain-1 (Passiatore et al., 2009). To examine the possibility that adaptation of NMDAR potentiation was due to the degradation of Tat, cultures received either one (0 h) or two (0 h, 12 h) applications of Tat (50 ng/mL). Following 16 h exposure to Tat, NMDAR function was potentiated in neurons treated with Tat once or twice at 39 ± 2% and 22 ± 2% larger than control, respectively. By 24 h, amplitudes of NMDA-evoked Ca^{2+} influx from single and double Tat-treated groups returned to baseline levels and were comparable to control suggesting that adaptation of the NMDA-evoked response is not due to the degradation of Tat. Taken together, these data indicate that Tat evokes a biphasic change in NMDAR function. In an attempt to determine whether enhanced Ca^{2+}

flux during the Tat-induced potentiation phase was required for subsequent adaptation, we blocked NMDAR-mediated Ca^{2+} influx with the readily reversible NMDAR antagonist AP5 during Tat exposure. However, chronic NMDAR antagonism in the absence of Tat enhanced NMDA-evoked responses, consistent with a previous report showing that chronic NMDAR blockade produced a compensatory increase in the surface expression of NMDARs (Crump et al., 2001). Thus, we were unable to determine whether potentiation was necessary for adaptation.

Application of 100 μM NMDA evoked $[Ca^{2+}]_i$ increases in Tat-treated cells that peaked near saturation of the fura-2 Ca^{2+} indicator. A concentration-response experiment was conducted to determine if Tat-induced potentiation was observed when lower NMDA concentrations were used to probe NMDAR function. Tat-induced potentiation of NMDA-evoked responses was independent of NMDA concentration and was 35 ± 2%, 14 ± 3% and 32 ± 1% larger than control for 10, 30, and 100 μM NMDA, respectively. Thus, to enable more accurate measurement of the $[Ca^{2+}]_i$ responses, we conducted the remaining experiments using 10 μM NMDA.

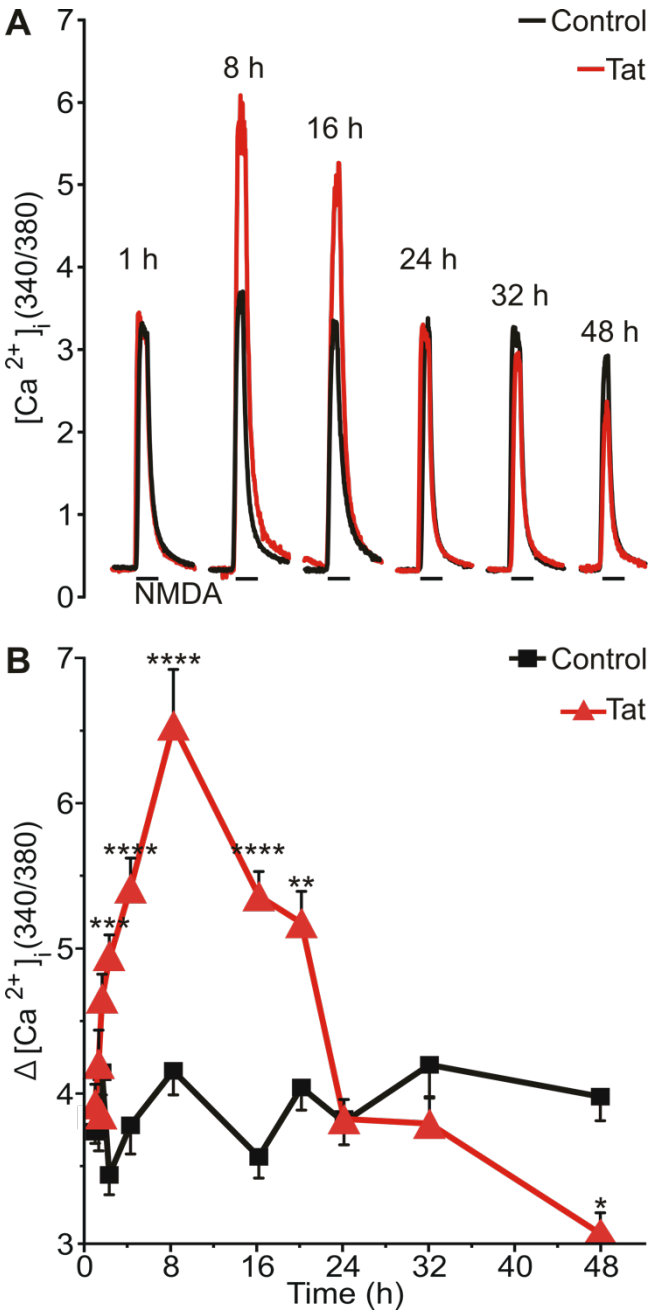

Figure 2.2: **Tat-induces a biphasic change in NMDA-evoked $[Ca^{2+}]_i$ responses**. **A,** representative traces show NMDA-evoked $[Ca^{2+}]_i$ (100 μM x 30 s) increases from control (▬) neurons or neurons treated with 50 ng/mL Tat (▬) for the times indicated above the traces. **B,** plot summarizes changes in NMDA-evoked $[Ca^{2+}]_i$ responses under control (■) conditions or after treatment with Tat (▲) for 0 to 48 h. *p<0.05, **p<0.01, ***p<0.001, ****p<0.0001 relative to control as determined by one-way ANOVA with 24 levels followed by Tukey's post-test for multiple comparisons.

Tat-induced potentiation of the NMDA-evoked increase in $[Ca^{2+}]_i$ is reversible

Tat-induced potentiation was prevented by inhibition of LRP or SFKs (Fig. 2.1). We next determined whether Tat-induced potentiation of NMDARs could be reversed by inhibition of LRP or SFKs after the potentiation was already established. Changes in NMDA-evoked increases in $[Ca^{2+}]_i$ were studied after 16, 24, 32, or 48 h exposure to Tat. Either RAP (50 nM) or PP2 (10 μM) was applied 1 h prior to Ca^{2+} imaging in the continued presence of Tat (50 ng/mL). Exposure to Tat for 16 h potentiated NMDA-evoked increases in $[Ca^{2+}]_i$ (Fig. 2.3 A, E). Potentiation was reversed by application of RAP or PP2 1 h prior to evoking the test response with NMDA (Fig. 2.3 A, E). Potentiation of NMDA-evoked responses adapted by 24 h (Fig. 2.3 B, F) and then dropped below control by 32 h (Fig. 2.3 C, G) and 48 h (Fig. 2.3 D, H). RAP and PP2 did not affect control cultures, but further reduced NMDA-evoked $[Ca^{2+}]_i$ responses in cultures treated with Tat for 24 to 48 h (Fig. 2.3 B-D, F-H). These data indicate that Tat-induced potentiation of NMDA-evoked increase in $[Ca^{2+}]_i$ requires sustained activation of LRP and SFK. Furthermore, this potentiation pathway remains activated during the adaptation process as indicated by the reduced amplitude of NMDA-evoked $[Ca^{2+}]_i$ responses in fully-adapted cultures (24-48 h treated with Tat).

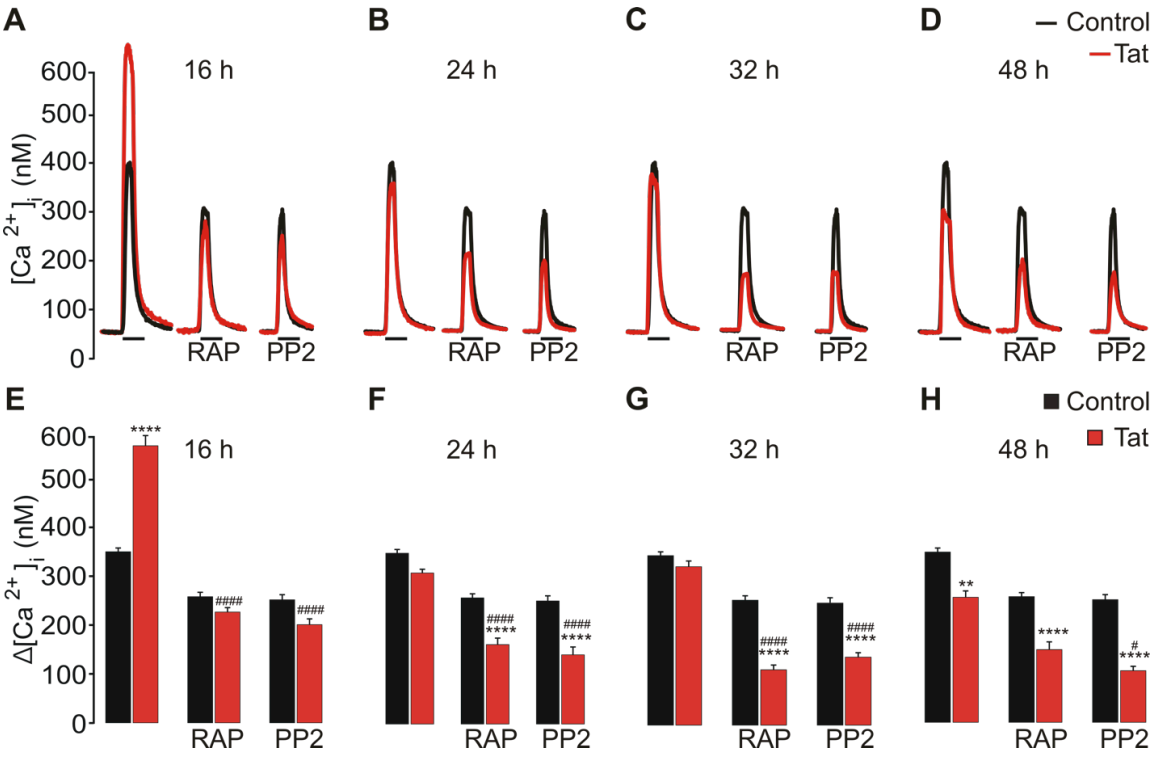

Figure 2.3: **HIV-1 Tat-induced potentiation of NMDA-evoked increases in $[Ca^{2+}]_i$ is reversible.** **A-D,** representative traces show NMDA-evoked $[Ca^{2+}]_i$ increases from control (▬) neurons or neurons treated with 50 ng/mL Tat (▬) for the times indicated above the traces. NMDA (10 μM x 30 s) was applied by superfusion at the times indicated by the horizontal bars. Cells were pretreated with 50 nM RAP or 10 μM PP2 1 h prior to superfusion with 10 μM NMDA as indicated. **E-H,** Bar graph shows net $[Ca^{2+}]_i$ increase evoked by NMDA in control (■) cells or cells treated with Tat (■). Cells were pretreated for 1 h with 50nM RAP or 10 μM PP2 as indicated. **p<0.01, ****p<0.0001 relative to respective control; #p<0.05, ####p<0.0001 relative to Tat alone as determined by separate, one-way ANOVAs with 6 levels for each treatment time followed by Tukey's post-test for multiple comparisons.

Src kinase mediates Tat-induced potentiation of NMDA-evoked increases in $[Ca^{2+}]_i$

The SFKs, Src and Fyn, have been shown to enhance NMDAR function (Kohr and Seeburg, 1996). Following exposure to Tat, Src but not Fyn, associates with NMDARs (King et al., 2010). Due to the potential off-target effects of PP2 (Bain et al., 2007) and the lack of drugs that are selective for Src versus Fyn, we next used a genetic approach to determine which SFK is responsible for potentiating the NMDA-evoked increase in $[Ca^{2+}]_i$. Primary hippocampal cultures were co-transfected with plasmids encoding a red-fluorescent protein (pTag-RFP-N) and dominant-negative (DN)-Fyn or DN-Src (Fig. 2.4 A, B). Twenty-four hours after transfection, cells were treated with Tat (50 ng/mL) for 16 h, loaded with fura-2, and then imaged. Non-expressing cells in the same imaging field served as controls. Tat potentiated NMDA-evoked $[Ca^{2+}]_i$ responses in non-expressing controls and cells expressing DN-Fyn (Fig. 2.4 C, D). However, expression of DN-Src completely blocked Tat-induced potentiation (Fig. 2.4 C, D). These data suggest that Tat-induced activation of Src kinase potentiates NMDA-evoked $[Ca^{2+}]_i$ responses.

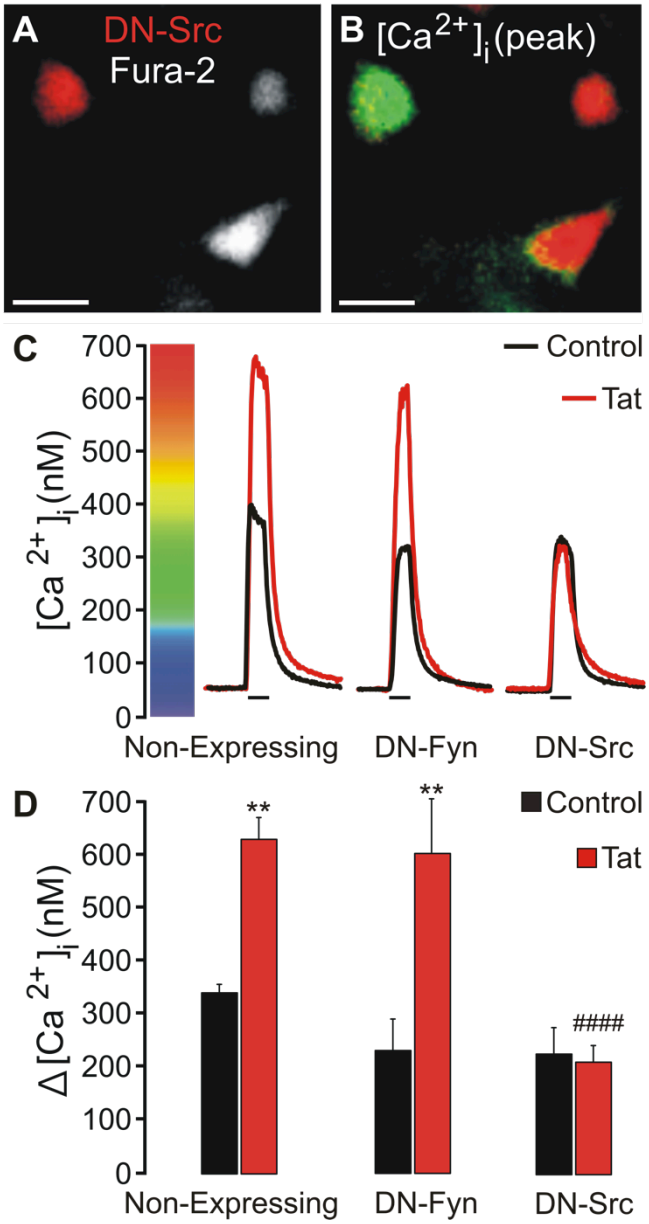

Figure 2.4: **Src kinase mediates Tat-induced NMDAR potentiation.** Cells were treated with Tat (50 ng/mL) for 16 h as indicated. **A,** representative image shows neuron expressing DN-Src and DsRed2 in a field of fura-2 loaded neurons (Scale bar = 25 μm). **B,** pseudocolor image shows peak $[Ca^{2+}]_i$ response to 10 μM NMDA (30 s) after 16 h Tat treatment. Image is scaled to bar in C. **C,** representative traces show NMDA-evoked $[Ca^{2+}]_i$ increases for control (—) and Tat-(—) treated neurons. Recordings from non-expressing cells were from the same imaging field as cells expressing DN-Fyn or DN-Src. **D,** Bar graph shows net $[Ca^{2+}]_i$ increase evoked by 10 μM NMDA (30 s) in control neurons (■) or neurons treated with 50 ng/mL Tat (■) for 16 h. **p<0.01 relative to respective control; ####p<0.0001 relative to non-expressing, Tat-treated cells as determined by one-way ANOVA with 6 levels followed by Tukey's post test for multiple comparisons.

Tat-induced potentiation of NMDA-evoked increases in $[Ca^{2+}]_i$ adapts via the NOS/sGC/PKG pathway

We next wanted to better understand the mechanism of adaptation following Tat-induced NMDAR potentiation. Because adaptation of Tat-induced NMDAR potentiation occurred in the presence of sustained Src activation, we hypothesized that adaptation resulted from a sustained increase in NMDAR-mediated Ca^{2+} influx. NMDAR-mediated Ca^{2+} influx following exposure to Tat leads to sustained production of nitric oxide (NO) (Eugenin et al., 2007). To determine whether NO production was mediating the Tat-induced adaptation in NMDAR function, we used a pharmacological approach. Cultures were pretreated with L-NAME (100 μM), an inhibitor of nitric oxide synthase (NOS), 1 h prior to and during exposure to Tat for 16, 24, 32, and 48 h. L-NAME did not affect Tat-induced NMDAR potentiation (Fig. 2.5 A, E) but did prevent adaptation of the NMDA-evoked increase in $[Ca^{2+}]_i$ for 48 h (Fig. 2.5 B-D, F-H).

NO can activate soluble guanylate cyclase (sGC) resulting in the synthesis of cyclic guanosine monophosphate (cGMP) (Arnold et al., 1977). To determine whether Tat-induced NO production was mediating the adaptation of NMDA-evoked responses by elevating cGMP, we treated cultures with ODQ (1 μM), an inhibitor of sGC, 1 h prior to and during exposure to Tat for 16, 24, 32, and 48 h. ODQ did not affect Tat-induced NMDAR potentiation (Fig. 2.5 A, E) but did prevent adaption of NMDA-evoked $[Ca^{2+}]_i$ responses for 48 h (Fig. 2.5 B-D, F-H).

Elevated cGMP activates cGMP-dependent protein kinase (PKG) (Kuo and Greengard, 1972). To determine whether Tat-induced NO production was mediating the

adaptation of NMDA-evoked $[Ca^{2+}]_i$ responses by activating PKG, we treated cultures with the PKG inhibitor, KT5823 (10 μM), 1 h prior to and during exposure to Tat for 16, 24, 32, and 48 h. KT5823 did not affect Tat-induced NMDAR potentiation (Fig. 2.5 A, E), but did prevent adaptation of NMDA-evoked increases in $[Ca^{2+}]_i$ for 48 h (Fig. 2.5 B-D, F-H).

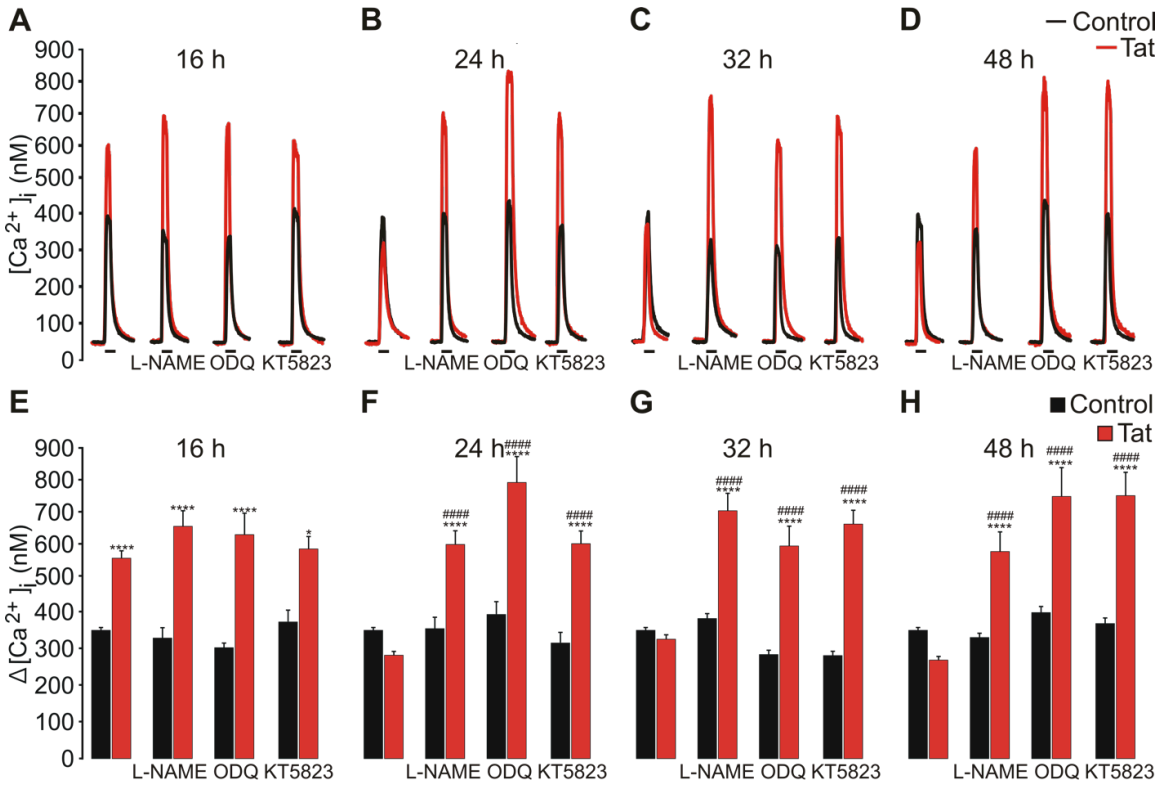

Figure 2.5: **Tat-induced potentiation of NMDAR function adapts via a NOS/sGC/PKG pathway**. **A-D,** representative traces show NMDA-evoked $[Ca^{2+}]_i$ increases from control neurons (—) or neurons treated with 50 ng/mL Tat (—) for the times indicated above the traces. NMDA (10 μM x 30 s) was applied at the times indicated by the horizontal bars. Cells were untreated or pretreated 1 h prior to addition of Tat with 100 μM L-NAME, 1 μM ODQ, or 10 μM KT5823 as indicated. **E-H,** Bar graphs show net $[Ca^{2+}]_i$ increase evoked by 10 μM NMDA (30 s) in control neurons (■) or neurons treated with 50 ng/mL Tat (■) for 16, 24, 32, or 48 h.*p<0.05; ****p<0.0001 relative to respective control; ####p<0.0001 relative to Tat alone as determined by separate, one-way ANOVAs with 8 levels for each treatment time followed by Tukey's post-test for multiple comparisons.

To confirm that adaptation was mediated by PKG we complimented these pharmacological studies using a genetic approach. The catalytically inactive mutant of PKG1α, G1αR, acts in a dominant-negative manner to inhibit PKG activity (Browning et al., 2001). This dominant-negative PKG construct (DN-PKG) was expressed in neurons; cells were then treated with Tat for 16 or 24 h, loaded with Fura-2, and then imaged. Exposure to Tat for 16 h potentiated the NMDA-evoked increase in $[Ca^{2+}]_i$ in non-expressing controls and neurons expressing DN-PKG. By 24 h, NMDA-evoked responses adapted in non-expressing cells, but expression of DN-PKG prevented adaptation (Fig. 2.6). Taken together, these data suggest that adaptation of NMDA-evoked responses following Tat-induced potentiation occurs via a NOS/cGMP/PKG pathway.

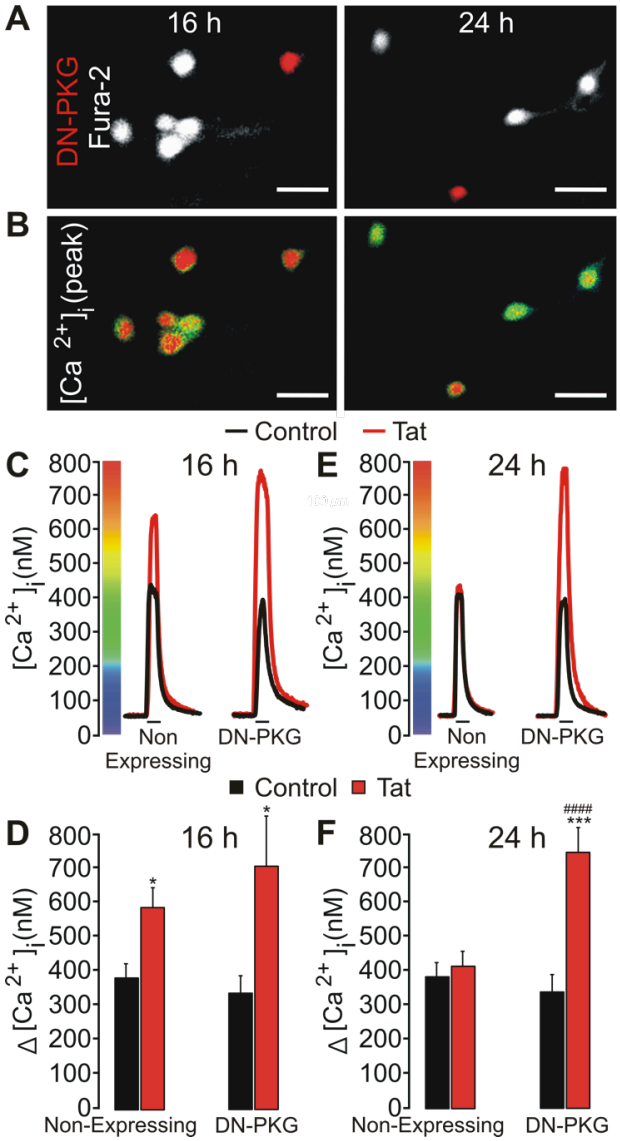

Figure 2.6: PKG mediates adaptation of NMDAR function following Tat-induced potentiation. **A,** representative images show neuronal expression of DN-PKG-DsRed2 in a field of neurons treated with Tat for 16 h or 24 h and loaded with fura-2 (scale bar = 50 μm). **B,** pseudocolor images show peak $[Ca^{2+}]_i$ response to 10 μM NMDA (30 s) following 16 h or 24 h Tat treatment. Images are scaled to bar in C and E. **C and E**, representative traces show NMDA-evoked $[Ca^{2+}]_i$ increases for control (▬) and Tat-treated (▬) cells following 16 h (C) or 24 h (E) exposure to Tat. Recordings from non-expressing cells were from the same imaging field as cells expressing DN-PKG. **D and F**, Bar graphs show net $[Ca^{2+}]_i$ increase evoked by 10 μM NMDA (30 s) in control neurons (■) or neurons treated with 50 ng/mL Tat (■) for 16 h (D) or 24 h (F). *p<0.01; ***p<0.001 relative to respective control; ####p<0.0001 relative to non-expressing, Tat-treated cells as determined by separate, one-way ANOVA with 4 levels for each treatment time followed by Tukey's post test for multiple comparisons.

PKG activates extracellular signal-regulated kinase (ERK) leading to the expression of neuroplasticity-associated proteins such as c-Fos, Egr-1, Arc, and BDNF (Gallo and Iadecola, 2011). Therefore, we tested the hypothesis that Tat-induced activation of PKG stimulates ERK signaling to affect NMDA-evoked $[Ca^{2+}]_i$ responses. The MAP kinase kinase 1 (MEK1) inhibitor PD98059 (50 μM) was applied 1 h prior to and during treatment with Tat for 16 or 24 h. PD98059 inhibits ERK1/2 phosphorylation and prevents expression of the aforementioned neuroplasticity-associated proteins (Gallo and Iadecola, 2011). Tat-induced NMDAR potentiation was comparable in the absence and presence of PD98059 at 49 ± 3% and 62 ± 8% larger than control, respectively. By 24 h, amplitudes of NMDA-evoked increases in $[Ca^{2+}]_i$ from both treatment groups returned to baseline and were comparable to control, suggesting that activation of ERK signaling is not required for Tat-induced potentiation or adaptation of NMDARs.

To determine if adaptation following NMDAR potentiation is unique to Tat, we conducted a time course experiment using interleukin-1β (IL-1β). IL-1β is a pro-inflammatory cytokine that potentiates NMDAR-mediated currents (Liu et al., 2013) and NMDA-evoked $[Ca^{2+}]_i$ increases via activation of a SFK (Viviani et al., 2003). We replicated this result and found that 5 min exposure to IL-1β (50 pg/mL) potentiated NMDA-evoked $[Ca^{2+}]_i$ responses. IL-1β-induced NMDAR potentiation persisted for longer than 24 h then NMDA-evoked $[Ca^{2+}]_i$ responses adapted, gradually reversing towards baseline by 48 h (Fig. 2.7). Pretreatment for 1 h with the soluble guanylate cyclase inhibitor ODQ had no effect on IL-1β-induced NMDAR potentiation and failed to prevent adaptation. Thus, while adaptation of potentiated NMDA-evoked Ca^{2+}

responses may be common, it appears that the mechanism of adaptation is stimulus specific.

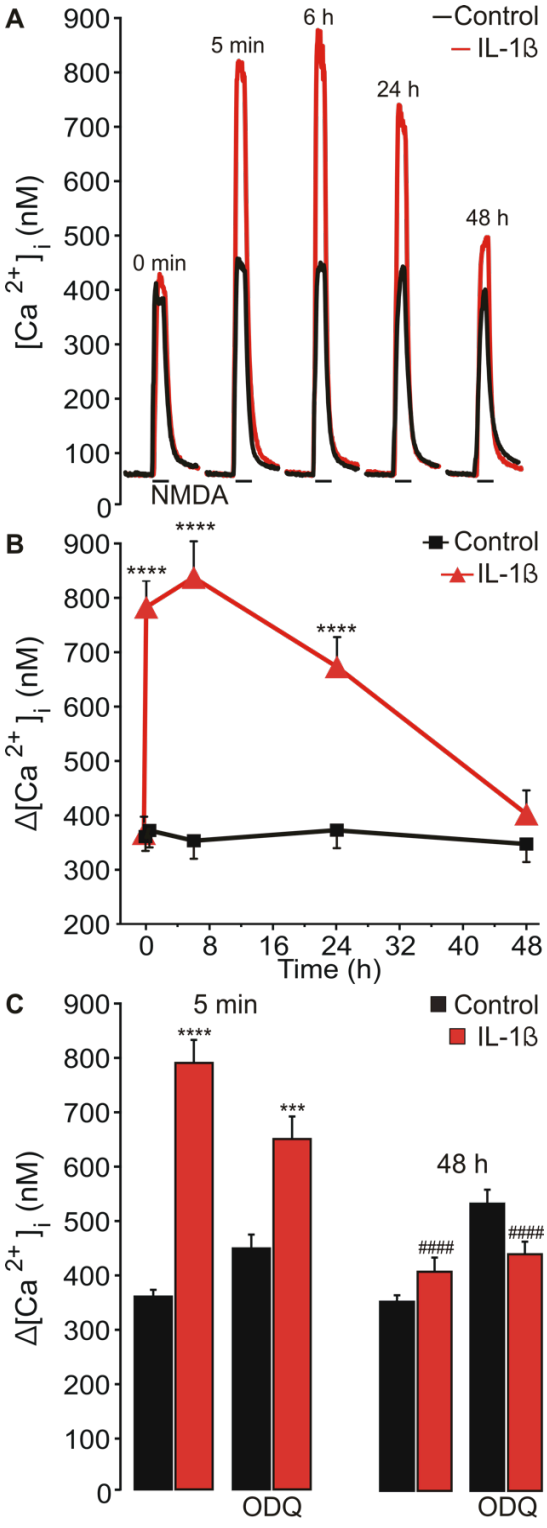

Figure 2.7: Interleukin-1β (IL-1β)-induced a biphasic change in NMDA-evoked $[Ca^{2+}]_i$ responses. **A**, representative traces show NMDA-evoked $[Ca^{2+}]_i$ (10 μM x 30 s) increases from control (—) neurons or neurons treated with 50 pg/mL IL-1β (—) for the times indicated above the traces. **B**, plot summarizes the changes in NMDA-evoked $[Ca^{2+}]_i$ responses under control (■) conditions or after treatment with IL-1β (▲) for 0 to 48 h. ****p<0.0001 relative to control as determined by one-way ANOVA with 10 levels followed by Tukey's post-test for multiple comparisons. **C**, Cells were left untreated or pretreated with ODQ (1 μM) 1 h prior to the addition of IL-1β as indicated. Bar graphs show net $[Ca^{2+}]_i$ increase evoked by 10 μM NMDA (30 s) in control neurons (■) or neurons treated with 50 pg/mL IL-1β (■) for 5 min or 48 h.***p<0.001; ****p<0.0001 relative to respective control; ####p<0.0001 relative to respective IL-1β x 5 min as determined by one-way ANOVA with 8 levels followed by Tukey's post-test for multiple comparisons.

Tat does not affect surface expression of GluN2B

We hypothesized that the reduction in the amplitude of NMDA-evoked $[Ca^{2+}]_i$ increases following 48 h exposure to Tat was due to NMDAR internalization (Nong et al., 2003). We first determined the GluN2 subtype mediating the NMDA-evoked response using a pharmacological approach (Fig. 2.8). We recorded an initial NMDA evoked control response (response #1), allowed the cell to recover for 5 min in presence of ifenprodil (10 μM), a selective GluN2B antagonist (Williams, 1993), and then evoked a second response in the continued presence of ifenprodil (response #2). The majority (74 ± 1%) of the NMDA-evoked increase in $[Ca^{2+}]_i$ was mediated by ifenprodil-sensitive GluN2B-containing NMDARs, consistent with previous reports indicating that GluN2B preferentially localizes to extrasynaptic sites (Tovar and Westbrook, 1999), including the neuronal cell body (She et al., 2012). Additionally, the response amplitude in the presence of ifenprodil was not different in untreated control cells compared to cells treated with Tat for 48 h (Fig. 2.8), suggesting that the ifenprodil-insensitive component was not participating in the Tat-induced adaptive changes. Thus, even though both GluN2A- and GluN2B-containing NMDARs are susceptible to internalization (Lavezzari et al., 2004), we focused on the surface expression of GluN2B subunits because the NMDA-evoked increase in $[Ca^{2+}]_i$ was predominantly mediated by GluN2B-containing NMDARs, the surface expression of GluN2B is more dynamic than GluN2A (Groc et al., 2006), and our region of interest focused on the neuronal cell body.

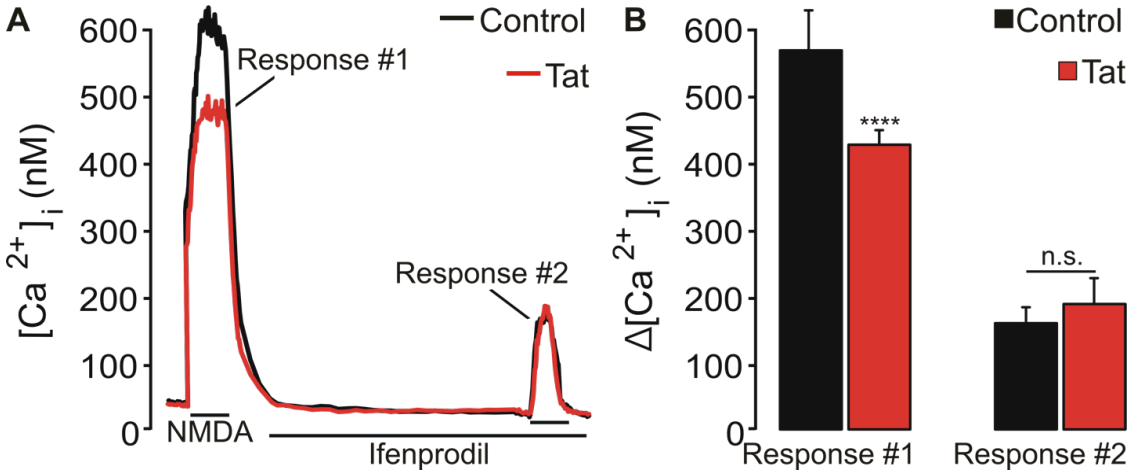

Figure 2.8: GluN2B-containing NMDARs mediate adaptation of NMDAR function. Forty-eight hour exposure to Tat does not affect the amplitude of NMDA-evoked $[Ca^{2+}]_i$ responses in the presence of the GluN2B antagonist ifenprodil. **A**, representative traces show NMDA-evoked $[Ca^{2+}]_i$ increases from control (—) cells or neurons treated with 50 ng/mL Tat (—) for 48 h. NMDA (10 μM x 30 s) was applied twice by superfusion at the times indicated by the horizontal bars. Following recovery from an NMDA-evoked control response (response #1), the selective GluN2B antagonist ifenprodil (10 μM) was superfused for 5 min. The test response (response #2) was evoked in the sustained presence of ifenprodil. **B**, Bar graph shows net $[Ca^{2+}]_i$ increase evoked by 10 μM NMDA in control (■) cells or cells treated with Tat (■) for 48 h in the absence (response #1) or presence (response #2) of the GluN2B antagonist, ifenprodil (10 μM). ****$p<0.0001$ relative to control as determined by one-way ANOVA with 4 levels followed by Tukey's post-test for multiple comparisons.

Next, we determined whether 48 h exposure to Tat affected GluN2B surface expression in primary hippocampal cultures using a biotinylation approach. To confirm the selectivity of our antibody for GluN2B, we first transfected HEK293 cells with plasmids encoding GluN1 with GluN2A or GluN2B and quantified protein expression via Western blot. The antibody selectively labeled GluN2B, but not GluN2A (data not shown). As shown in Fig. 2.9, GluN2B surface expression was unaffected by 48 h exposure to Tat (50 ng/mL). Addition of KT5823 (10 μM) 1 h prior to and during treatment with Tat for 48 h also had no effect on GluN2B surface expression. We conducted a time course experiment in which cultures were treated with Tat (50 ng/mL) for 0, 8, 24, and 48 h. GluN2B surface expression was unaffected by Tat exposure at all time points (data not shown). Furthermore, treating cultures with 100 nM Tat for 1 h did not affect surface expression of GluN2B-containing NMDARs (data not shown). To confirm that the assay was sufficiently sensitive to detect changes in NMDAR surface expression, we induced NMDAR internalization by a 5 min pretreatment with glycine followed by 5 min treatment with glycine + NMDA (Nong et al., 2003). Treatment with glycine + NMDA evoked a 62 ± 33% decrease in GluN2B surface expression while 48 h treatment with Tat (50 ng/mL) tested in parallel had no effect (data not shown). These data indicate that adaptation following Tat-induced NMDAR potentiation is not due to internalization of GluN2B.

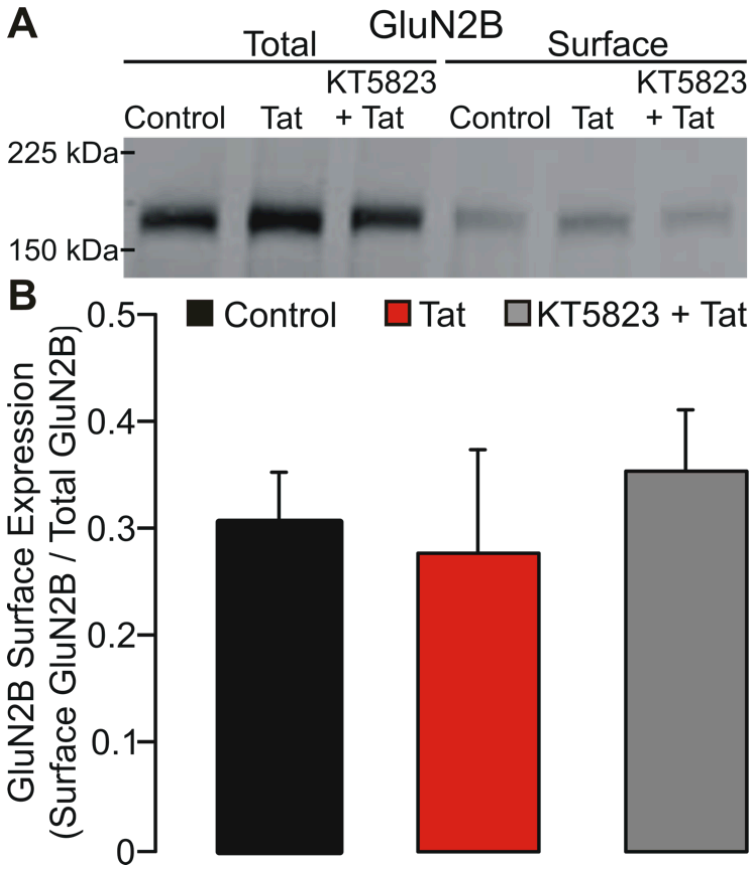

Figure 2.9: Tat does not affect surface expression of GluN2B-containing NMDARs. **A,** representative Western blot showing total and surface GluN2B. **B,** Bar graph shows GluN2B surface expression, expressed as the ratio of surface-to-total GluN2B. Cultures were left untreated (■, n=10), treated with 50 ng/mL Tat (■, n=10) for 48 h, or treated with 10 μM KT5823 (■, n=11) 1 h prior to the addition of Tat for 48 h. Data are expressed as mean +/- SEM. One-way ANOVA with 3 conditions were performed followed by Tukey's post-test for multiple comparisons.

IV. Discussion

NMDARs are implicated in many neurodegenerative disorders including HAND (Young et al., 1988; Kaul et al., 2001; Snyder et al., 2005; Potter et al., 2013; Rossi et al., 2013; Spalloni et al., 2013). The HIV-1 protein Tat is a neurotoxin involved in the neuropathogenesis of HIV (Nath, 2002; King et al., 2006). Here, we used fura-2-based Ca^{2+} imaging to investigate the effects of Tat on NMDA-evoked $[Ca^{2+}]_i$ responses in rat hippocampal neurons *in vitro*. Tat potentiated NMDA-evoked increases in $[Ca^{2+}]_i$ by LRP-dependent activation of Src kinase. Intriguingly, NMDA-evoked responses adapted following Tat-induced potentiation by activation of the NOS/sGC/PKG pathway. Adaptation of NMDA-evoked responses may be a novel neuroprotective mechanism to prevent excessive Ca^{2+} influx through NMDARs and could identify new targets for the treatment of HAND. The signaling pathways responsible for the biphasic modulation of NMDARs during exposure to Tat are summarized in Figure 2.10.

Tat has been detected in the brains of patients with HIV (Wiley et al., 1996; Del Valle et al., 2000; Hudson et al., 2000). Tat is shed by HIV-infected cells (Steinaa et al., 1994; Chang et al., 1997) and can affect NMDAR function directly and indirectly. Previous work showed that Tat directly activates the NMDAR (Song et al., 2003) resulting in neurotoxicity (Li et al., 2008). Other reports indicate that Tat indirectly enhances NMDAR function via binding to and relieving the inhibitory effect of Zn^{2+} (Chandra et al., 2005) or via tyrosine kinase-mediated phosphorylation of NMDARs (Haughey et al., 2001). We found that Tat indirectly potentiated NMDA-evoked increases in $[Ca^{2+}]_i$ as indicated by prevention of potentiation by the LRP antagonist, RAP. Tat also

induces synapse loss (Kim et al., 2008; Shin et al., 2012) and cell death (Eugenin et al., 2007) via an LRP-dependent mechanism (Liu et al., 2000). LRP1 recognizes over 30 ligands with high affinity (Herz and Strickland, 2001). Some of these agents alter NMDAR function. For example, activated α2-macroglobulin (Qiu et al., 2002) and amyloid-β (Snyder et al., 2005) inhibit NMDA-evoked currents and ApoE4 potentiates NMDAR function (Qiu et al., 2003). We used a combined pharmacological and genetic approach to show that the previously described potentiation of NMDA-evoked $[Ca^{2+}]_i$ responses by Tat (Haughey et al., 2001) was mediated by LRP-dependent activation of Src. The mechanism by which Tat activates Src following binding to LRP is unclear. Ligand binding to LRP activates SFKs (Bock and Herz, 2003); (Shi et al., 2009). Neurons from animals with an inactivating knock-in mutation in the *Lrp1* gene exhibit reduced phosphorylation of GluN2B tyrosine-1472, although this particular mutation increased both LRP1 and GluN2B surface expression (Maier et al., 2013). Thus, it's possible that Tat binding to the LRP activates a signaling cascade resulting in phosphorylation of NMDARs. Alternatively, following internalization, Tat causes fundamental changes in endolysosomal structure and function (Hui et al., 2012); thus, it's possible that Tat disrupts endolysosomal membrane integrity and escapes the endosome to activate Src. NMDAR function could be directly affected by Src-mediated phosphorylation (Salter and Kalia, 2004) or indirectly via activation of other Src substrates.

Tat-induced potentiation of the NMDA-evoked increase in $[Ca^{2+}]_i$ followed a biphasic time course. The Tat-induced NMDAR potentiation peaked at 8 h and then NMDA-evoked responses returned to baseline by 24 h eventually dropping below control

by 48 h. Down-regulation of NMDAR function over the course of hours to days has been described previously following ethanol exposure (Wu et al., 2011) and for excitatory conditions such as benzodiazepine withdrawal (Shen and Tietz, 2011). Adaptation following Tat-induced NMDAR potentiation has not been previously described, although it does correlate with adaptive changes in synapse number induced by Tat. Twenty-four hour exposure to 50 ng/ml Tat produced a 50 ± 7% loss of glutamatergic synapses and a simultaneous 38 ± 3% increase in GABAergic synapses (Kim et al., 2008; Hargus and Thayer, 2013). We suggest that Tat-induced synaptic changes and attenuation of NMDA-evoked $[Ca^{2+}]_i$ responses are part of a neuroprotective response orchestrated by the cell to reduce excess excitatory input.

Adaptation of NMDA-evoked $[Ca^{2+}]_i$ responses resulted from the activation of a NOS/sGC/PKG signaling pathway. A series of pharmacological and genetically-expressed inhibitors of this pathway prevented adaptation without affecting potentiation of NMDARs or NMDA-evoked responses in cells that were not exposed to Tat. PKG-mediated phosphorylation of the vasodilator-stimulated phosphoprotein (VASP), a protein expressed in neurons and used to assess PKG activity (Butt et al., 1994; Wang and Robinson, 1997), increased following 24 h exposure to Tat (Shin & Thayer 2014) providing further support for Tat-induced activation of an NO-PKG pathway. Thus, this pathway was only activated after exposure to Tat, possibly resulting from potentiation. Sustained Tat-induced NO production results following the formation of a macromolecular complex composed of LRP, PSD95, NMDAR, and nNOS (Eugenin et al., 2007). NO inhibits NMDA receptor function (Manzoni et al., 1992), although this

feedback inhibition is generally thought to result from the direct nitrosylation of NMDARs (Lei et al., 1992; Lipton and Stamler, 1994) rather than activation of PKG. Activation of PKG leads to suppression of NMDAR-mediated currents (Furukawa and Mattson, 1998), however the mechanism by which PKG attenuates NMDAR function is unclear.

Adaptation of potentiated NMDA-evoked $[Ca^{2+}]_i$ increases is not unique to Tat. Prolonged exposure to IL-1β also resulted in potentiated followed by attenuated responses to NMDA, although it appears that the mechanism of adaptation is stimulus specific. Adaptation of Tat-induced NMDAR potentiation does not appear to result from attenuation of Src activity. The SFK inhibitor, PP2, suppressed NMDA-evoked increases in $[Ca^{2+}]_i$ below control in fully-adapted, Tat-treated cells, although it had no effect on NMDA-evoked responses in naive cells, suggesting that Src remained active even in cells in which NMDA-evoked responses had returned to control levels. Sustained Src-mediated phosphorylation of Tyr 1472 on the C-terminal tail of GluN2B could disrupt AP-2 binding and prevent clathrin-mediated endocytosis (Lavezzari et al., 2003), which might explain the sustained NMDAR surface expression indicated by the biotinylation experiments. Biotinylation experiments indicated that adaptation was not due to internalization of GluN2B-containing NMDARs. Thus, an additional process was activated to counteract the sustained Src-mediated potentiation of the NMDA-evoked increase in $[Ca^{2+}]_i$. One possibility that could account for the reduction in NMDA-evoked responses without a concomitant decrease in GluN2B surface expression is Ca^{2+}-induced cytoskeletal changes. Depolymerization of actin protects from excitotoxicity by

reducing glutamate receptor-mediated Ca^{2+} influx (Furukawa et al., 1995). PKG is known to alter actin polymerization via Rho-associated kinase (Sunico et al., 2010) and such cytoskeletal changes reduce Ca^{2+} influx through the NMDAR (Rosenmund and Westbrook, 1993; Lei et al., 2001). Perhaps prolonged exposure to Tat alters the gating or ligand binding properties of the NMDAR by affecting the physical interaction between the actin cytoskeleton and NMDARs resulting in attenuated NMDA-evoked responses.

The biphasic change in NMDA-evoked $[Ca^{2+}]_i$ responses induced by Tat raises interesting questions about the balance between optimal NMDAR function and neuronal survival. Pharmacologic inhibition of NMDARs protects neurons from Tat-induced cell death (Shin et al., 2012); thus, the adaptation described here would seem likely to improve neuronal survival. However, Tat-induced cell death and NMDAR adaptation are both prevented by inhibition of NOS with L-NAME (Eugenin et al., 2007). Does the timing, duration, and amount of NO production distinguish protective from toxic effects? Intriguingly, NO can be neuroprotective or neurotoxic (Lipton et al., 1993). NO confers neuroprotection by several mechanisms. It directly attenuates NMDAR-mediated Ca^{2+} influx via s-nitrosylation resulting in improved neuronal survival (Choi et al., 2000; Jaffrey et al., 2001). Furthermore, NO can stimulate the sGC/cGMP/PKG pathway to produce neuroprotective proteins such as the transcription factor CREB and the kinase Akt (Contestabile and Ciani, 2004). Alternatively, the neuroprotective effects of NO may be overwhelmed by nitrosative stress following prolonged, persistent, and excessive production of NO, ultimately resulting in neurotoxicity and cell death.

Although NO production is necessary for Tat-induced cell death to occur (Eugenin et al., 2007), impaired brain function from HIV initially results from synaptodendritic injury that precedes overt neuronal death. Proper NMDAR function is essential for normal cognition. For example, overexpression of GluN2B-containing NMDARs enhances learning and memory function (Tang et al., 1999) while inhibition of NMDARs impairs these processes (Malhotra et al., 1996; Newcomer and Krystal, 2001). Does the cognitive decline observed in patients with HAND result, in part, from excessive attenuation of NMDAR function? If so, then the pathways that potentiate and attenuate NMDARs during a neurotoxic challenge may prove useful targets for the pharmacological treatment of HAND. Additionally, if the complex time course of NMDAR modulation observed during *in vitro* exposure to Tat is extrapolated to HAND, then different therapeutic approaches may be required for different stages of the disease.

In summary, we have shown that exposure to Tat evokes a biphasic modulation of NMDA-evoked $[Ca^{2+}]_i$ responses. An LRP/Src pathway initially potentiates NMDA-evoked increases in $[Ca^{2+}]_i$ and then activation of the NOS/sGC/PKG signaling pathway attenuates NMDA-evoked responses. Future experiments to determine how these pathways balance NMDAR-dependent cognitive functions with NMDAR-dependent toxicity *in vivo* may inform the targeting and timing of neuroprotective agents of potential use in treating HAND.

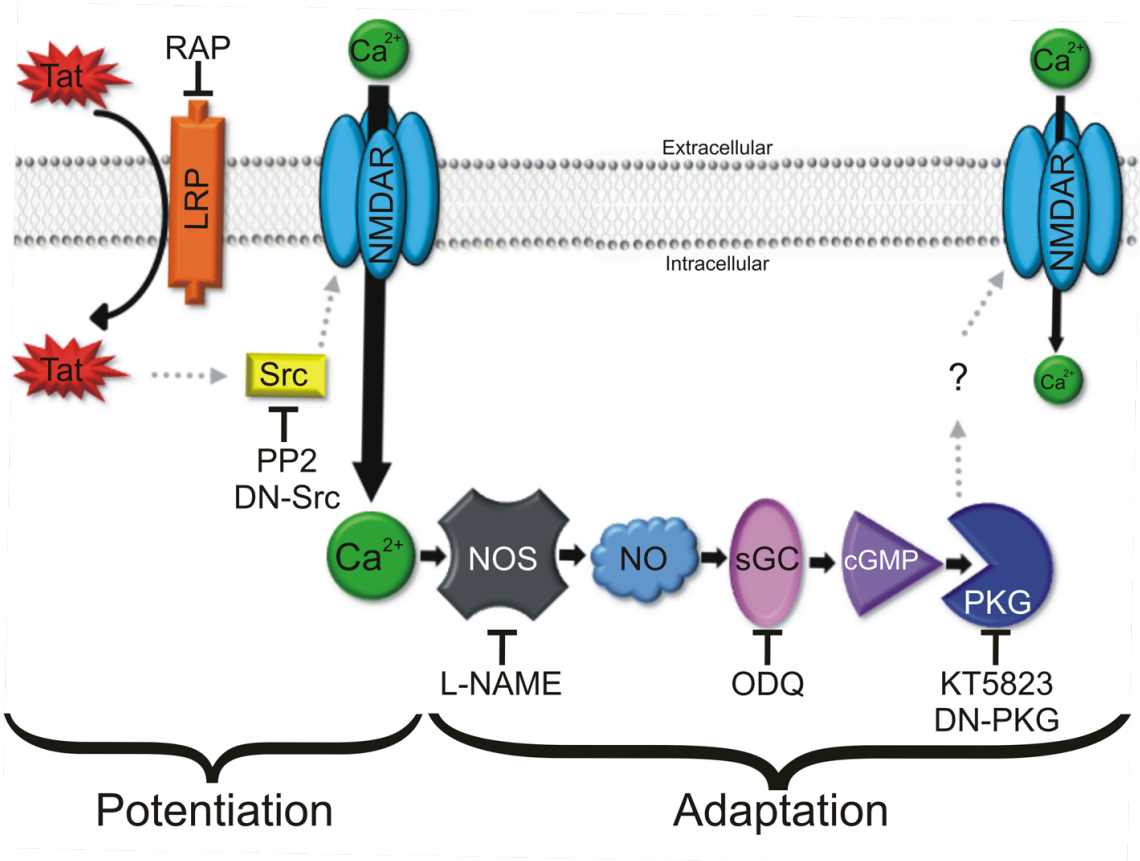

Figure 2.10: Proposed mechanism of Tat-induced NMDAR potentiation and adaptation. Tat interacts with LRP leading to the activation Src-kinase. Src kinase potentiates NMDA-evoked $[Ca^{2+}]_i$ responses. Increased Ca^{2+} flux activates NOS to produce NO. NO binds to sGC stimulating the synthesis of cGMP. cGMP then activates PKG leading to the reduction of NMDA-evoked $[Ca^{2+}]_I$ responses. Solid and dashed arrows represent direct and potentially indirect connections, respectively.

Chapter Three:

HIV-1 Tat activates a RhoA signaling pathway to reduce NMDA-evoked calcium responses in hippocampal neurons via an actin-dependent mechanism

Kelly A. Krogh, Elizabeth Lyddon, and Stanley A. Thayer

Department of Pharmacology, University of Minnesota Medical School

Minneapolis, MN

Content adapted from manuscript submitted to The Journal of Neurochemistry, July 2014.

Contributions: KAK and SAT designed the study; KAK performed experiments and collected data; KAK, EL, and SAT analyzed data; KAK and SAT wrote the manuscript; SAT provided reagents and conceptual advice.

I. Introduction

Approximately half of HIV-infected patients in the U.S. are affected by HIV-associated neurocognitive disorders (HAND) (Cysique et al., 2004; Tozzi et al., 2005; Heaton et al., 2011) and the prevalence is likely higher in areas of the world where effective pharmacotherapy is uncommon. HAND ranges in severity from asymptomatic to severely debilitating (Heaton et al., 2004; Antinori et al., 2007). Multiple reports during the past decade indicate that cognitive dysfunction remains a significant and persistent problem despite effective management of viral load with combination anti-retroviral therapy (cART) (Antinori et al., 2007; Heaton et al., 2010; Heaton et al., 2011). Current cART regimens prolong the lifespan of patients by effectively managing viral load. Unfortunately, HAND remains common among HIV-infected patients (Heaton et al., 2010) and the therapeutic approaches to combat HIV-associated cognitive impairment remain ineffective (Uthman and Abdulmalik, 2008).

Penetrance of HIV into the CNS occurs as early as 2 weeks post infection (Resnick et al., 1988; Davis et al., 1992; An et al., 1999). Once inside the CNS, HIV infects microglial cells and perivascular macrophages (Albright et al., 1999; Williams et al., 2001), which serve as reservoirs for viral replication. HAND is thought to arise, in part, from latent viral reservoirs that are not entirely accessible to cART. Because HIV does not infect neurons, neuronal injury leading to cognitive impairment results from indirect mechanisms. Namely, HIV-infected cells within the CNS release agents that are neurotoxic including inflammatory cytokines (Genis et al., 1992), nitric oxide (Eugenin et al., 2007), and glutamate (Jiang et al., 2001), as well as the viral proteins, gp120

(Schneider et al., 1986) and the transactivator of transcription (Tat) (Chang et al., 1997). While, HIV-induced neuropathogenesis likely involves a combination of these agents to create a neurotoxic environment, Tat is particularly important because current antiretroviral therapy is unable to halt the production of this potent neurotoxin once integrated into cellular DNA (Li et al., 2009).

Tat is a non-structural viral protein that is responsible for initiating transcription of the HIV genome (Sodroski et al., 1985a; Sodroski et al., 1985b). In addition to its role as a transcriptional transactivator, Tat is shed from HIV-infected cells (Chang et al., 1997) and is detected in the CNS and sera of HIV-infected patients (Del Valle et al., 2000; Hudson et al., 2000). Anti-Tat antibody titers in the cerebrospinal fluid of HIV+ patients are approximately 30% lower in cognitively impaired patients relative to unimpaired patients, suggesting that antibody responses against Tat may be neuroprotective and preserve cognitive function (Bachani et al., 2013). Cognitive decline in HAND correlates with damage to synaptodendritic structures, including axonal disruptions and pruning of dendritic spines (Ellis et al., 2007). In a transgenic mouse model, induction of Tat expression results in a loss of dendritic spines resulting in learning and memory impairment (Fitting et al., 2010; Carey et al., 2012; Fitting et al., 2013). Similarly, exposure of primary hippocampal neurons to Tat *in vitro* causes loss of excitatory synapses (Kim et al., 2008), gain of inhibitory synapses (Hargus and Thayer, 2013), and causes loss of presynaptic terminals (Shin and Thayer, 2013). Importantly, almost all instances of Tat-induced neurotoxicity are prevented by pharmacologic inhibition of the NMDA receptor (NMDAR) (Eugenin et al., 2007; Kim et al., 2008; Shin

et al., 2012; Hargus and Thayer, 2013) indicating that Tat-induced neurotoxicity requires NMDAR-mediated Ca^{2+} influx.

Tat potentiates NMDA-evoked responses (Haughey et al., 2001; Chandra et al., 2005) which then adapt by gradually returning to and eventually dropping below basal responses (Krogh et al., 2014). Reduction of NMDAR function and a decrease in the ratio of excitatory-to-inhibitory synapses may be neuroprotective responses orchestrated by the cell to prevent excessive Ca^{2+} influx and excitotoxicity. Thus, these adaptive changes may improve neuronal survival at the cost of impaired network function. The signaling pathway responsible for adaptation of NMDA-evoked $[Ca^{2+}]_i$ responses following prolonged exposure to Tat is therefore the focus of this study.

Here we examined NMDAR function during 24 h exposure to Tat. Previously, we found that Tat evoked a biphasic change in NMDAR function (Krogh et al., 2014). As illustrated in figure 3.1, Tat potentiated NMDA-evoked increases in intracellular Ca^{2+} concentration ($[Ca^{2+}]_i$) via the low-density lipoprotein receptor-related protein (LRP) and activation of Src tyrosine kinase. Subsequently, NMDA-evoked responses adapted by gradually returning to basal levels after 24 h exposure to Tat and eventually dropping below baseline responses by 48 h. Adaptation resulted from activation of a nitric oxide synthase (NOS), soluble guanylate cyclase (sGC), cGMP-dependent protein kinase (PKG) signaling pathway (Krogh et al., 2014). However, effectors downstream of PKG responsible for attenuating the NMDA-evoked response have not been identified. Here we show that Tat activates a signaling pathway that includes the small GTPase RhoA and Rho-associated protein kinase (ROCK). Activation of RhoA/ROCK results in

reorganization of the actin cytoskeleton leading to attenuated NMDA-evoked increases in $[Ca^{2+}]_i$. Abnormal activation of RhoA/ROCK has been observed in various models of CNS disorders including Alzheimer's disease, stroke, and multiple sclerosis. Thus, RhoA/ROCK are promising drug targets for the treatment of various neurological conditions; however, little is known about this signaling pathway in HAND. This study suggests that following Tat-induced potentiation, NMDA-evoked responses are reduced following RhoA/ROCK-mediated reorganization of the actin cytoskeleton.

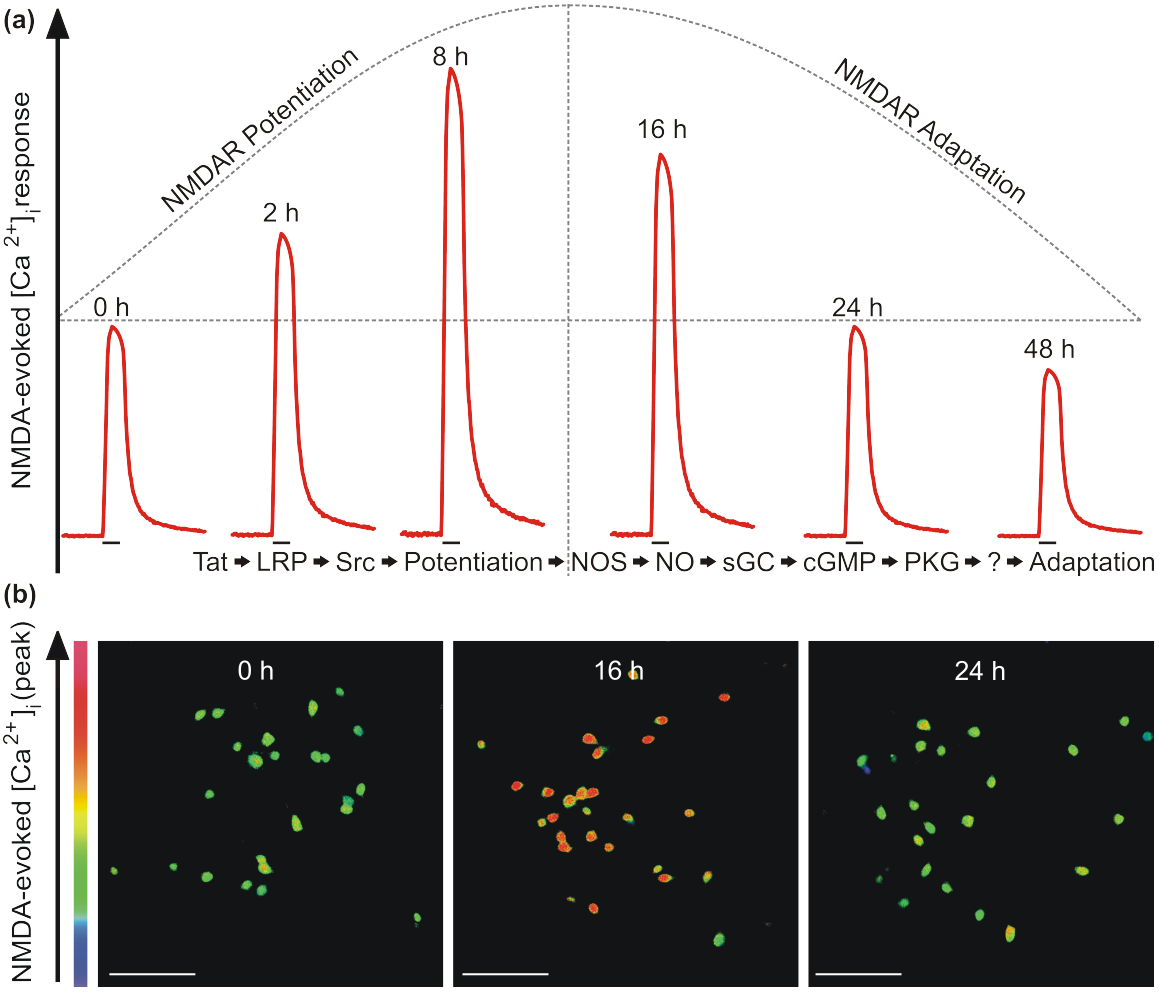

Figure 3.1: HIV-1 Tat causes a biphasic change in NMDA-evoked increases in $[Ca^{2+}]_i$

a, Stylized traces (▬) depict time-dependent, biphasic changes in NMDA-evoked increases $[Ca^{2+}]_i$ following exposure to HIV-1 Tat for the time indicated above the trace. The previously reported (Krogh et al., 2014) sequence of events listed below the traces indicates that Tat-induced activation of an LRP/Src kinase pathway resulted in NMDAR potentiation. Subsequently, NMDARs adapted following activation of the NOS/sGC/PKG signaling pathway. Identifying downstream effector(s) of PKG is the goal of this study. **b,** Representative pseudocolor images (scale bar = 100 μm) show peak response to NMDA (10μM, 30 s) in primary hippocampal neurons treated with Tat for the time indicated in the image panel. Images were scaled from 0 to 700 nM as indicated by the color bar on the y-axis.

II. Materials and Experimental Methods

Drugs and Reagents

Materials were obtained from the following sources: HIV-1 Tat (Clade B, 1-86 amino acids) was acquired from the NIH AIDS Research and Reference Reagent Program (HIV-1 Tat protein from Dr. John Brady and DAIDS, NIAID) and from Prospec Tany TechnoGene Ltd. (Rehovot, Israel); Dulbecco's modified Eagle's medium (DMEM), fetal bovine serum, horse serum, fura-2-acetomethyl ester (Fura-2-AM), and glycine were obtained from Invitrogen (Carlsbad, CA). Phalloidin-Oleate, Y27632 (*Trans*-4-[(1*R*)-1-Aminoethyl]-*N*-4pyridinylcyclohexanecarboxamide dihydrochloride), and Cytochalasin D (zygosporium mansonii) were acquired from EMD Millipore (Billerica, MA); Rho Inhibitor I (exoenzyme C3 transferase) was obtained from Cytoskeleton, Inc. (Denver, CO); H1152 ((*S*)-(+)-2-Methyl-1-[(4-methyl-5-isoquinolinyl)sulfonyl]-hexahydro-1*H*-1,4-diazepine dihydrochloride), latrunculin A (4-[(1*R*,4*Z*,8*E*,10*Z*,12*S*,15*R*,17*R*)-17-Hydroxy-5,12-dimethyl-3-oxo-2,16-dioxabicyclo[13.3.1]nonadeca-4,8,10-trien-17-yl)-2-thiazolidinone), and jasplakinolide (Cyclo[(3*R*)-3-(4-hydroxyphenyl)-β-alanyl-(2*S*,4*E*,6*R*,8*S*)-8-hydroxy-2,4,6-trimethyl-4-nonenoyl-L-alanyl-2-bromo-*N*-methyl-D-tryptophyl]) were acquired from Tocris (Bristol, UK); ML-7 (1-(5-Iodonaphthalene-1-sulfonyl)-1H-hexahydro-1,4-diazepine hydrochloride) and NMDA were obtained from Sigma-Aldrich (St. Louis, MO).

DNA Constructs

Dominant Negative (DN)-RhoA (plasmid 15901) and constitutively active (CA)-RhoA (plasmid 15900) were obtained from Addgene (Cambridge, MA). pTagRFP-N was acquired from Evrogen (Moscow, Russia). pEGFP-Actin was obtained from Clontech (Mountain View, CA).

Cell Culture

In accordance with the University of Minnesota's Institutional Animal Care and Use Committee and the NIH guide for the care and use of laboratory animals, maternal rats were euthanized by CO_2 inhalation and fetuses were removed on embryonic day 17. Rat hippocampal neurons were grown in primary culture as described previously (Waataja et al. 2008). Hippocampi were dissected and placed in Ca^{2+}- and Mg^{2+}-free HEPES-buffered Hanks' salt solution (HHSS), pH 7.45. HHSS contained the following (in mM): HEPES 20, NaCl 137, CaCl2 1.3, MgSO4 0.4, MgCl2 0.5, KCl 5.0, KH2PO4 0.4, Na2HPO4 0.6, NaHCO3 3.0, and glucose 5.6. Cells were dissociated by triturating through a 5 mL pipette and a flame-narrowed Pasteur pipette and then re-suspended in DMEM without glutamine, supplemented with 10% fetal bovine serum and penicillin/streptomycin (100 U/mL and 100 mg/mL, respectively). Dissociated cells were then plated at a density of 50,000 to 60,000 cells/dish onto a 25-mm-round cover glass (#1) pre-coated with matrigel (150 µL, 0.2 mg/mL). Neurons were grown in a humidified atmosphere of 10% CO2 (pH 7.4) at 37°C, and fed on days 1 and 7 by exchange of 75% of the media with DMEM supplemented with 10% horse serum and

penicillin/streptomycin. Cells used in these experiments were cultured without mitotic inhibitors resulting in a mixed glial-neuronal culture consisting of 18 ± 2% neurons, 70 ± 3% astrocytes, and 9 ± 3% microglia as indicated by immunocytochemistry (Kim et al. 2011). The cultures used for experiments were 12 to 15 days *in vitro* (DIV).

$[Ca^{2+}]_i$ imaging

Intracellular Ca^{2+} concentration ($[Ca^{2+}]_i$) was recorded as previously described (Li et al., 2013) with minor modifications. Cells were loaded with indicator by incubation with 5 μM fura-2 AM in 0.04% pluronic acid in HHSS for 30 min at 37°C followed by washing in the absence of indicator for 10 min. HIV-1 Tat and respective drugs were present during fura-2-AM loading, but were absent during the wash. Coverslips containing fura-2-AM loaded cells were transferred to a recording chamber, placed on the stage of an Olympus IX71 microscope (Melville, NY), and viewed through a 20X objective. Excitation wavelength was selected with a galvanometer-driven monochromator (8-nm slit width) coupled to a 75-W xenon arc lamp (Optoscan; Cairn Research). $[Ca^{2+}]_i$ was monitored using sequential excitation of fura-2 at 340 and 380 nm; image pairs were collected every 1 s. For experimental recordings, cells were superfused at a rate of 1-2 mL/min with HHSS for 1 min followed by 30 s perfusion of Mg^{2+}-Free HHSS that contained 200 μM glycine and 10 μM NMDA. Fluorescence images (510/40 nm) were projected onto a cooled charge-coupled device camera (Cascade 512B; Roper Scientific) controlled by MetaFluor software (Molecular Devices). After background subtraction, the 340- and 380-nm image pairs were converted to $[Ca^{2+}]_i$ using the formula

$[Ca^{2+}]_i = K_d\beta(R - R_{min})/(R_{max} - R)$ (Grynkiewicz et al. 1985). The dissociation constant (K_d) for fura-2 is 145 nM and R is the 340 nm / 380 nm fluorescence intensity ratio. R_{min}, R_{max}, and β were determined in a series of calibration experiments on intact cells. R_{min} and R_{max} values were generated by applying 10 μM ionomycin in Ca^{2+}-free HHSS supplemented with 1 mM EGTA and saturating (5 mM) Ca^{2+}, respectively. β is the ratio of fluorescence intensity acquired with 380 nm excitation measured in Ca^{2+}-free buffer and buffer containing saturating (5 mM) Ca^{2+}. Values for R_{min}, R_{max}, and β were 0.37, 9.38, and 6.46, respectively. These calibration constants were applied to all experimental recordings. For time course experiments, coverslips from the same cell culture plating were treated in parallel and each coverslip imaged only once. To generate pseudocolor images, a binary mask was created by applying an intensity threshold to the 380 nm image and then applied to $[Ca^{2+}]_i$ images with colors assigned as indicated by the calibration bars in the figures (Fig. 3.1 b). The neuronal cell body was selected as the region of interest for all recordings. All neuronal cells types within imaging fields were included in the analysis and no exclusions were made.

Transfection

Rat hippocampal neurons were transfected between 11-12 days *in vitro* using a modification of a calcium phosphate protocol described previously (Li et al., 2012). Briefly, hippocampal cultures were incubated for 30 min in DMEM supplemented with 1 mM kynurenic acid, 10 mM $MgCl_2$, and 5 mM HEPES. A DNA/calcium phosphate precipitate containing 1 μg plasmid DNA per well was prepared, allowed to form for 30

min at 21°C then added to the culture. Following a 90 min incubation, cells were washed once with DMEM supplemented with $MgCl_2$ and HEPES and then returned to conditioned media.

Confocal microscopy of EGFP-Actin

Glass-bottom petri dishes containing neurons transfected with EGFP-Actin and Tag-RFP were sealed with Parafilm, transferred to the stage of an inverted confocal microscope (Olympus Fluoview 300, Melville, NY) and viewed through a 60X oil-immersion objective (NA=1.4). EGFP-Actin was excited at 488 nm with an argon ion laser and emission collected at 530 nm (10 nm band pass). Tag-RFP was excited at 543 nm with a green HeNe laser and emission collected at >605 nm. 1 μm optical sections spanning 8 μm in the z-dimension were collected and these optical sections were combined through the z-axis into a compressed z-stack. To enable repeated imaging of the same cell, the location of the cell was recorded using micrometers attached to the stage of the microscope. The cell culture dish was returned to the CO_2 incubator between image collections. Images were processed using MetaMorph 7.7 image processing software. Compressed z-stacks were created from the Tag-RFP and EGFP-Actin image stacks and then overlaid.

Statistical analysis

For $[Ca^{2+}]_i$ imaging studies, an individual experiment (n=1) was defined as the change in NMDA-evoked $[Ca^{2+}]_i$ response from a single neuron on a single coverslip.

Changes in NMDA-evoked $[Ca^{2+}]_i$ are presented as mean ± SEM. Each experiment was replicated using at least 4 separate coverslips from at least 2 separate cultures. Significant differences were determined by one-way ANOVA with Tukey's *post hoc* test for multiple comparisons (OriginPro v8.5).

III. Results

HIV Tat-induced potentiation of NMDAR function adapts via activation of RhoA

Our previous study showed that treating rat hippocampal neurons in culture with the HIV Tat protein initially potentiated NMDA-evoked Ca^{2+} responses, which then adapted back to baseline during continued exposure to Tat (Krogh et al., 2014). Adaptation of NMDAR function occurred after activation of a NOS/sGC/PKG signaling cascade, however effectors downstream of PKG had not yet been identified (Fig. 3.1). Because cytoskeletal changes regulate NMDAR function (Rosenmund and Westbrook, 1993; Furukawa et al., 1995) and RhoA is a downstream effector of PKG (Sauzeau et al., 2003; Rolli-Derkinderen et al., 2005; Sunico et al., 2010) that affects the actin cytoskeleton, we examined the possibility that adaptation of NMDARs required RhoA. We hypothesized that RhoA activation was necessary for the reduction in NMDA-evoked $[Ca^{2+}]_i$ responses after Tat-induced potentiation. To test this hypothesis, we used pharmacological and genetic approaches. NMDAR function was assessed in rat hippocampal neurons (DIV12-15) using fura-2-based digital imaging to record $[Ca^{2+}]_i$ increases evoked by superfusing NMDA (10 μM) and glycine (200 μM) in Mg^{2+}-free HHSS onto the cells for 30 s. Cultures were pretreated with a cell-permeable inhibitor of RhoA, exoenzyme C3

transferase (ExoC3, 2.5 μg/mL), 1 h prior to and during exposure to Tat for 16 or 24 h. ExoC3 did not affect Tat-induced NMDAR potentiation, but did prevent adaptation of the NMDA-evoked increase in $[Ca^{2+}]_i$ by 24 h (Fig. 3.2 a, b).

Next, we wanted to confirm the role of RhoA in reducing NMDA-evoked $[Ca^{2+}]_i$ responses by co-expressing plasmids encoding either dominant negative (DN)-RhoA (T19N) or constitutively active (CA)-RhoA (Q63L) with a red-fluorescent protein (RFP) and imaging these cells in parallel. Neurons expressing the constructs of interest were compared to non-expressing neurons in the same imaging field for an internal comparison. Cells were treated with Tat for 16 or 24 h, loaded with fura-2, and then imaged (Fig. 3.2 c, d). In non-expressing control (untreated) cells, NMDA-evoked $[Ca^{2+}]_i$ responses were similar to responses in neurons expressing DN-RhoA. However, expression of CA-RhoA inhibited NMDA-evoked responses by approximately 50%. Exposure to Tat for 16 h potentiated NMDAR function in non-expressing cells and in neurons expressing DN-RhoA. However, cells expressing CA-RhoA were markedly inhibited relative to non-expressing and DN-RhoA-expressing neurons with the same treatment time. After 24 h exposure to Tat, NMDAR function adapted in non-expressing cells, but cells expressing DN-RhoA remained potentiated. Neurons expressing DN-RhoA (Fig. 3.2 f) were morphologically distinct and exhibited increased dendritic branching relative to neurons expressing RFP only (Fig. 3.2 e), while expression of CA-RhoA (Fig. 3.2 g) caused dendritic simplification consistent with previous reports (Da Silva *et al.* 2003, Chen & Firestein 2007). These data indicate that adaptation of NMDAR function following Tat-induced potentiation requires activation RhoA.

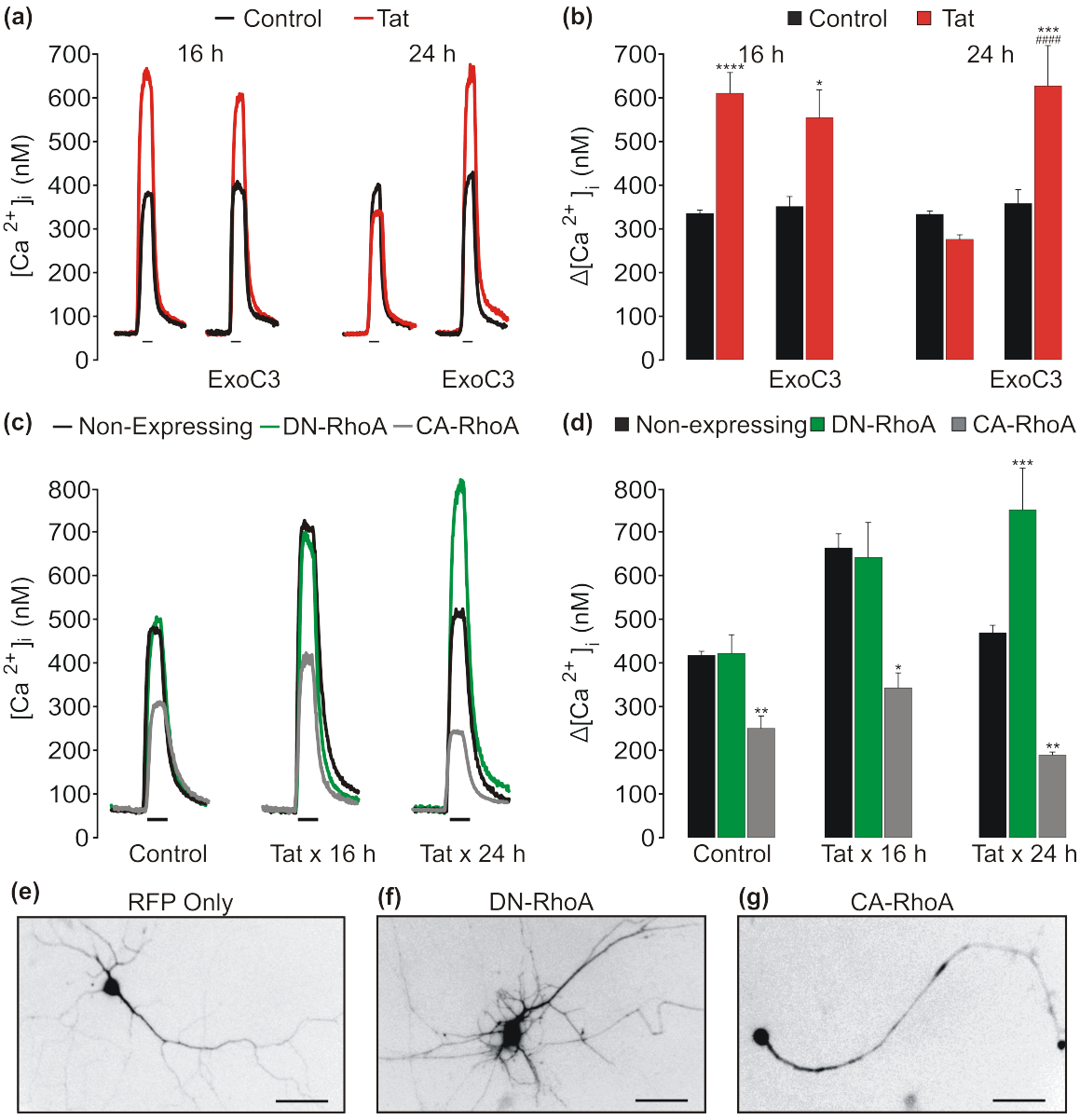
(a)
Control
Tat
16 h
24 h
700
600
500
400
300
200
100
0
[Ca 2+]i (nM)
ExoC3
ExoC3
(b)
Control
Tat
16 h
24 h
****
*
***
####
Δ[Ca 2+]i (nM)
ExoC3
ExoC3
(c)
Non-Expressing
DN-RhoA
CA-RhoA
800
700
600
500
400
300
200
100
0
[Ca 2+]i (nM)
Control
Tat x 16 h
Tat x 24 h
(d)
Non-expressing
DN-RhoA
CA-RhoA
***
*
**
**
Δ[Ca 2+]i (nM)
Control
Tat x 16 h
Tat x 24 h
(e)
RFP Only
(f)
DN-RhoA
(g)
CA-RhoA

Figure 3.2: Adaptation of NMDAR function after Tat-induced potentiation requires RhoA

a, Representative traces show NMDA-evoked $[Ca^{2+}]_i$ increases from control (▬) neurons or neurons treated with 50 ng/mLTat (▬) for 16 h or 24 h. Cells were pretreated with 2.5 μg/mL Exoenzyme C3 Transferase (ExoC3) 1 h prior to the addition of Tat. NMDA (10 μM, 30 s) was applied by superfusion at the times indicated by the horizontal bars. **b,** Bar graph shows net $[Ca^{2+}]_i$ increase evoked by 10 μM NMDA in control (■) cells or cells treated with Tat (■) for 16 h or 24 h. *p<0.05; ***p<0.001; ****p<0.0001 relative to respective control; ####p<0.0001 relative to 24 h Tat-treated neurons as determined by separate, one-way ANOVAs with 4 levels per treatment time followed by Tukey's post-test for multiple comparisons. **c,** representative traces show NMDA-evoked $[Ca^{2+}]_i$ increases from non-expressing (▬) neurons or neurons expressing DN-RhoA (▬) or CA-RhoA (▬) that were left untreated (control) or treated with Tat for 16 h or 24 h. **d,** Bar graph shows net $[Ca^{2+}]_i$ increase evoked by 10 μM NMDA in non-expressing (■) neurons or neurons expressing DN-RhoA (■) or CA-RhoA (■). Neurons were left untreated (control) or treated with Tat for 16 h or 24 h as indicated. Representative images of neurons expressing RFP only **(e)** or RFP and DN-RhoA **(f)** or CA-RhoA **(g)** (scale bar = 50 μm). Images were inverted to enhance contrast between the neuron and background. *p<0.05; **p<0.01; ***p<0.001 relative to non-expressing neurons within respective treatment group as determined by separate, one-way ANOVAs with 3 levels per treatment time followed by Tukey's post-test for multiple comparisons.

Tat-induced potentiation of NMDAR function adapts via activation of ROCK

The principal downstream effector of RhoA is ROCK (Matsui et al., 1996) and activation of ROCK results in rundown of NMDA-evoked currents via an actin-dependent mechanism (Beazely et al., 2008). Therefore, we hypothesized that ROCK activation was necessary for adaptation of NMDAR function after Tat-induced potentiation. To test this hypothesis, cultures were pretreated with an inhibitor of ROCK 1 h prior to and during Tat treatment for 16 or 24 h (Fig. 3.3). Inhibition of ROCK with Y27632 (10 μM) or H1152 (10 μM) did not affect Tat-induced NMDAR potentiation after 16 h treatment. However, the ROCK inhibitors prevented adaptation of NMDA-evoked $[Ca^{2+}]_i$ after exposure to Tat for 24 h. These data suggest that adaptation of NMDAR function following Tat-induced potentiation requires activation ROCK.

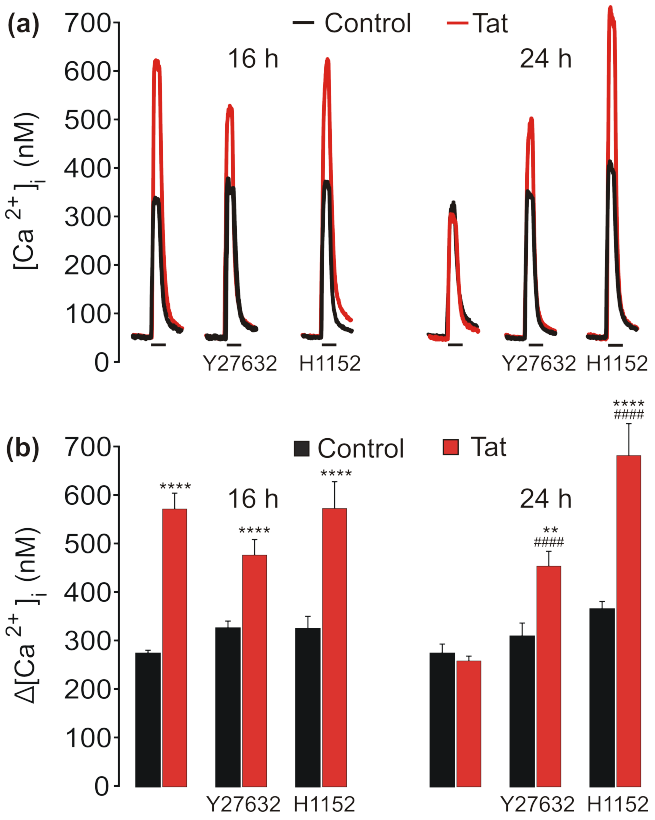

Figure 3.3: Adaptation of NMDAR function after Tat-induced potentiation requires ROCK

a, Representative traces show NMDA-evoked $[Ca^{2+}]_i$ increases from control (▬) neurons or neurons treated with 50 ng/mLTat (▬) for 16 h or 24 h. Cells were pretreated with 10 μM Y27632 or 10μM H1152 for 1 h prior to the addition of Tat. NMDA (10 μM, 30 s) was applied by superfusion at the times indicated by the horizontal bars. **b,** Bar graph shows net $[Ca^{2+}]_i$ increase evoked by 10 μM NMDA in control (■) cells or neurons treated with Tat (■) for 16 h or 24 h. **p<0.01, ****p<0.0001 relative to respective control; ####p<0.0001 relative to 24 h Tat-treated neurons as determined by separate, one-way ANOVAs with 6 levels per treatment time followed by Tukey's post-test for multiple comparisons.

Actin reorganization reduces NMDAR function

RhoA/ROCK signaling activates several targets that affect the actin cytoskeleton including LIM-kinase and cofilin (Maekawa et al., 1999), profilin (Da Silva et al., 2003), as well as myosin light chain phosphatase and myosin light chain kinase (MLCK) (Totsukawa et al., 2000). MLCK regulates NMDAR activity by increasing actomyosin contractility (Lei et al., 2001), thus we hypothesized that MLCK activation is necessary for the reduction in NMDA-evoked responses after Tat-induced potentiation. To test this hypothesis, cultures were pretreated with an inhibitor of MLCK, ML-7 (10 μM), for 1 h prior to and during Tat treatment for 16 or 24 h. ML-7 did not affect Tat-induced NMDAR potentiation by 16 h and, unexpectedly, did not block adaptation of NMDAR function by 24 h (Fig 3.4. a, b). Consistent with previous reports (Lei et al., 2001), ML-7 inhibited NMDA-evoked responses by approximately 40% and 25% following 16 h and 24 h treatment, respectively. Additionally, neurons exposed to ML-7 had vacuole-like structures present within the neuronal cell body similar to previous reports (Sulzer et al., 2008). These data do not support the hypothesized role for MLCK and suggest that adaptation of NMDAR function occurs via another effector downstream from ROCK.

We next examined the role of the actin cytoskeleton in Tat induced regulation of NMDAR function. Cultures were pretreated with cytochalasin D (1 μM), which binds to the barbed end of F-actin to prevent the addition of G-actin monomers (Cingolani and Goda, 2008), for 1 hour prior to and during treatment with Tat. Cytochalasin D did not affect Tat-induced NMDAR potentiation by 16 h, but did prevent the reduction of NMDA-evoked $[Ca^{2+}]_i$ responses observed after 24 h treatment with Tat (Fig. 3.4 c, d).

Additionally, cultures were pretreated with phalloidin (1 μM), which binds to and stabilizes F-actin polymers (Cingolani and Goda, 2008), for 1 hour prior to and during treatment with Tat. Phalloidin did not affect Tat-induced NMDAR potentiation by 16 h, but did block adaptation of NMDA-evoked $[Ca^{2+}]_i$ responses after 24 h treatment with Tat (Fig. 3.4 e, f). These data suggest that Tat-induced reorganization of the actin cytoskeleton reduces NMDA-evoked $[Ca^{2+}]_i$ responses.

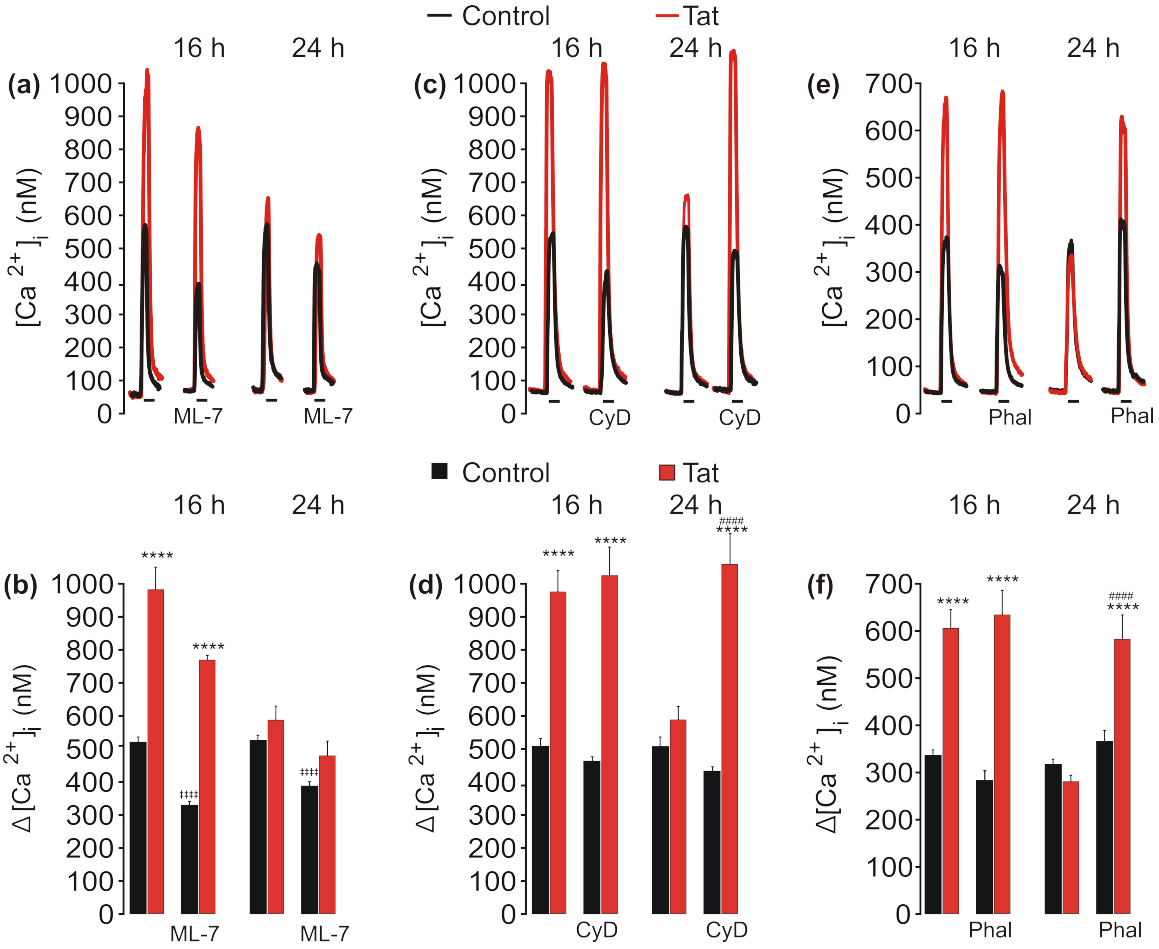

Figure 3.4: Adaptation of NMDAR function requires remodeling of the actin cytoskeleton

a, c, e, Representative traces show NMDA-evoked $[Ca^{2+}]_i$ increases from control (▬) neurons or neurons treated with 50 ng/mLTat (▬) for 16 h or 24 h. Cells were pretreated with ML-7 (10 μM), Cytochalasin D (CyD, 1 μM), or Phalloidin (Phal, 1 μM) for 1 h prior to the addition of Tat. NMDA (10 μM, 30 s) was applied by superfusion at the times indicated by the horizontal bars. **b, d, f,** bar graphs show net $[Ca^{2+}]_i$ increase evoked by 10 μM NMDA in control (■) cells or cells treated with Tat (■) for 16 h or 24 h. Cells were pretreated with ML-7, CyD, or Phal as indicated. ****$p<0.0001$ relative to respective control; ‡‡‡‡$p<0.0001$ relative to untreated control within timepoint; ####$p<0.0001$ relative to 24 h Tat-treated neurons as determined by separate, one-way ANOVAs with 4 levels per treatment time followed by Tukey's post-test for multiple comparisons.

Because phalloidin and cytochalasin D have opposing effects on the actin cytoskeleton, but similarly prevented adaptation, we further examined the effects of actin polymerization and depolymerization on the neuronal distribution of actin and NMDA-evoked responses. To examine the effects of these agents on the actin cytoskeleton, neurons were cotransfected with plasmids encoding EGFP-Actin and Tag-RFP; cultures were then treated for 1 h with jasplakinolide (10 μM), which promotes F-actin polymerization, or latrunculin A (5 μM), which sequesters G-actin to promote F-actin depolymerization (Cingolani and Goda, 2008). Treatment for 1 h with jasplakinolide induced robust somatic and dendritic redistribution of the actin cytoskeleton and caused retraction of dendritic spines (Fig. 3.5 a). Latrunculin A dispersed the actin cytoskeleton, revealed fibers in the neuronal cell body, and caused a dramatic loss of dendritic spines (Fig. 3.5 b). To determine if changes in the actin cytoskeleton affect NMDAR function, cultures were treated for 1 h to 24 h with jasplakinolide (10 μM) or latrunculin A (5 μM). Treatment with jasplakinolide attenuated NMDA-evoked $[Ca^{2+}]_i$ responses as early as 1 h. (Fig. 3.5 c, d). Treatment with latrunculin A also reduced NMDA-evoked $[Ca^{2+}]_i$ responses, but required 24 h for significant functional impairment to develop (Fig. 3.5 c, d). Such rapid and persistent changes to the actin cytoskeleton caused by Jasplakinolide and Latrunculin A are consistent with previous reports (Okamoto et al., 2004) and indicate that bidirectional reorganization of actin reduces NMDAR function.

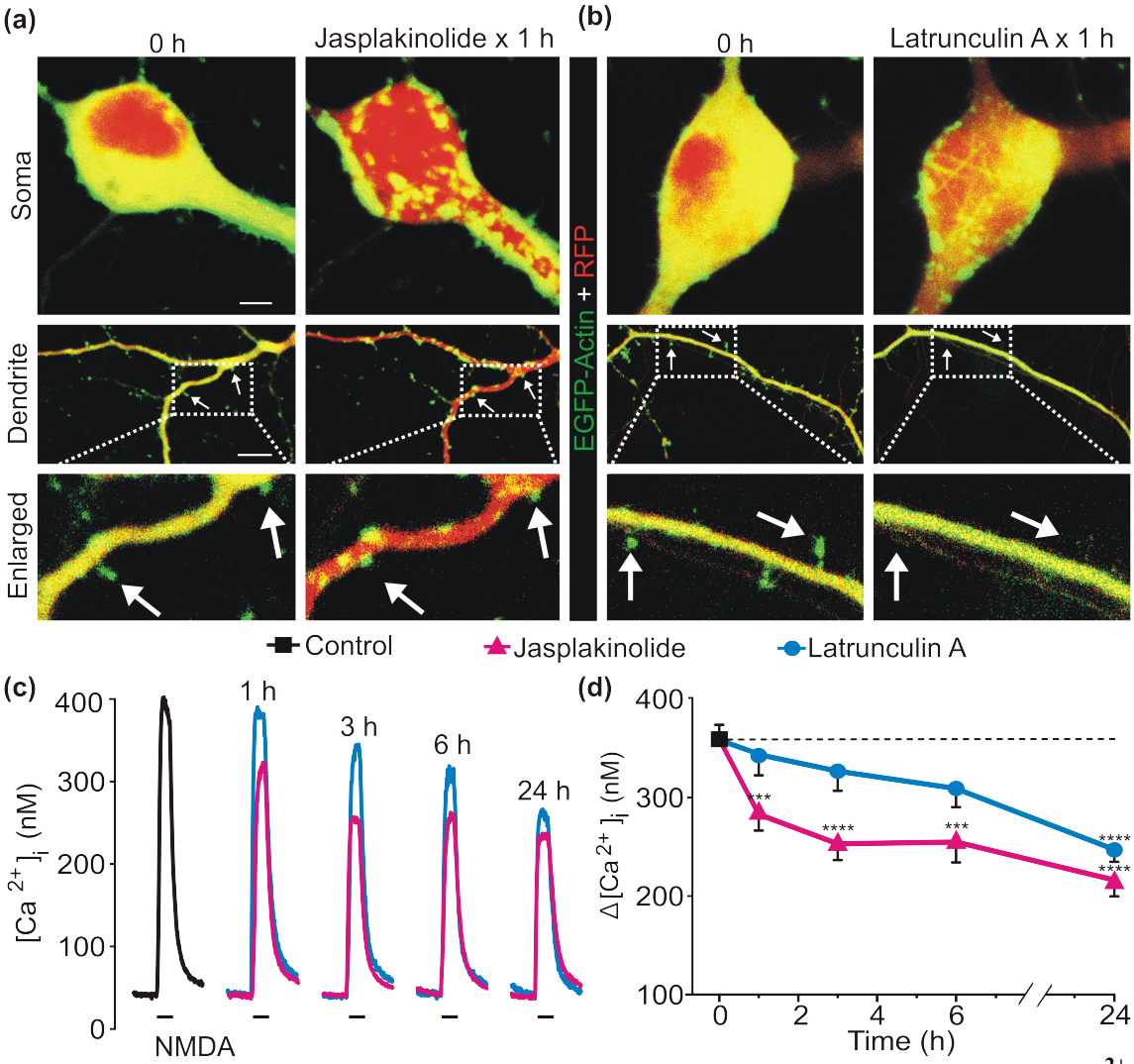

Figure 3.5: Reorganization of the actin cytoskeleton reduces NMDA-evoked $[Ca^{2+}]_i$ responses

a, b, Representative confocal images (Scale bar = 10 μm) of neurons expressing EGFP-Actin and Tag-RFP before (0 h) and after 1 h treatment with 10μM Jasplakinolide **(a)** or 5 μM Latrunculin A **(b).** Compressed z-stacks of red (Tag-RFP) and green (EGFP-Actin) were superimposed. **c,** representative traces show NMDA-evoked $[Ca^{2+}]_i$ increases from control (▬) neurons or neurons treated with 10 μM jasplakinolide (▬) or 5 μM latrunculin A (▬) for the times indicated above the traces. NMDA (10 μM, 30 s) was applied by superfusion at the times indicated by the horizontal bars below the traces. **d,** plot summarizes time-dependent changes in NMDA-evoked $[Ca^{2+}]_i$ increases from control (▬) neurons and neurons treated with 10 μM jasplakinolide (▲) or 5 μM latrunculin A (●).***p<0.001, ****p<0.0001 relative to control as determined by separate, one-way ANOVAs with 5 levels per treatment followed by Tukey's post-test for multiple comparisons.

IV. Discussion

NMDAR dysfunction contributes to the neurotoxicity that underlies many neurodegenerative disorders including HAND (Young et al., 1988; Danysz and Parsons, 2003; Hallett and Standaert, 2004; Rossi et al., 2013; Spalloni et al., 2013). Although the neuropathogenesis of HAND likely involves a combination of factors, evidence suggests that the HIV protein Tat plays a prominent role by altering the activity of NMDARs (Haughey et al., 2001; Song et al., 2003; Chandra et al., 2005; Krogh et al., 2014) and impairing cognitive function (Fitting et al., 2010; Carey et al., 2012; Bachani et al., 2013). Here we used digital Ca^{2+} imaging to study the pathways that modulate NMDA-evoked $[Ca^{2+}]_i$ responses during prolonged exposure to Tat. Previous work described a biphasic change in NMDA-evoked increases in $[Ca^{2+}]_i$ during prolonged exposure to Tat. Initially, Tat potentiated NMDAR function via LRP-dependent activation of Src kinase; NMDAR function subsequently adapted after activation of the NOS/sGC/PKG pathway (Krogh et al., 2014). The goal of this study was to identify effectors downstream of PKG responsible for adaptation of NMDA-evoked responses following Tat-induced NMDAR potentiation. We determined that a RhoA/ROCK-dependent remodeling of the actin cytoskeleton was an obligatory step in NMDAR adaptation (Fig. 3.6). Adaptation of NMDAR function may be a neuroprotective mechanism to prevent excessive NMDAR-mediated Ca^{2+} influx.

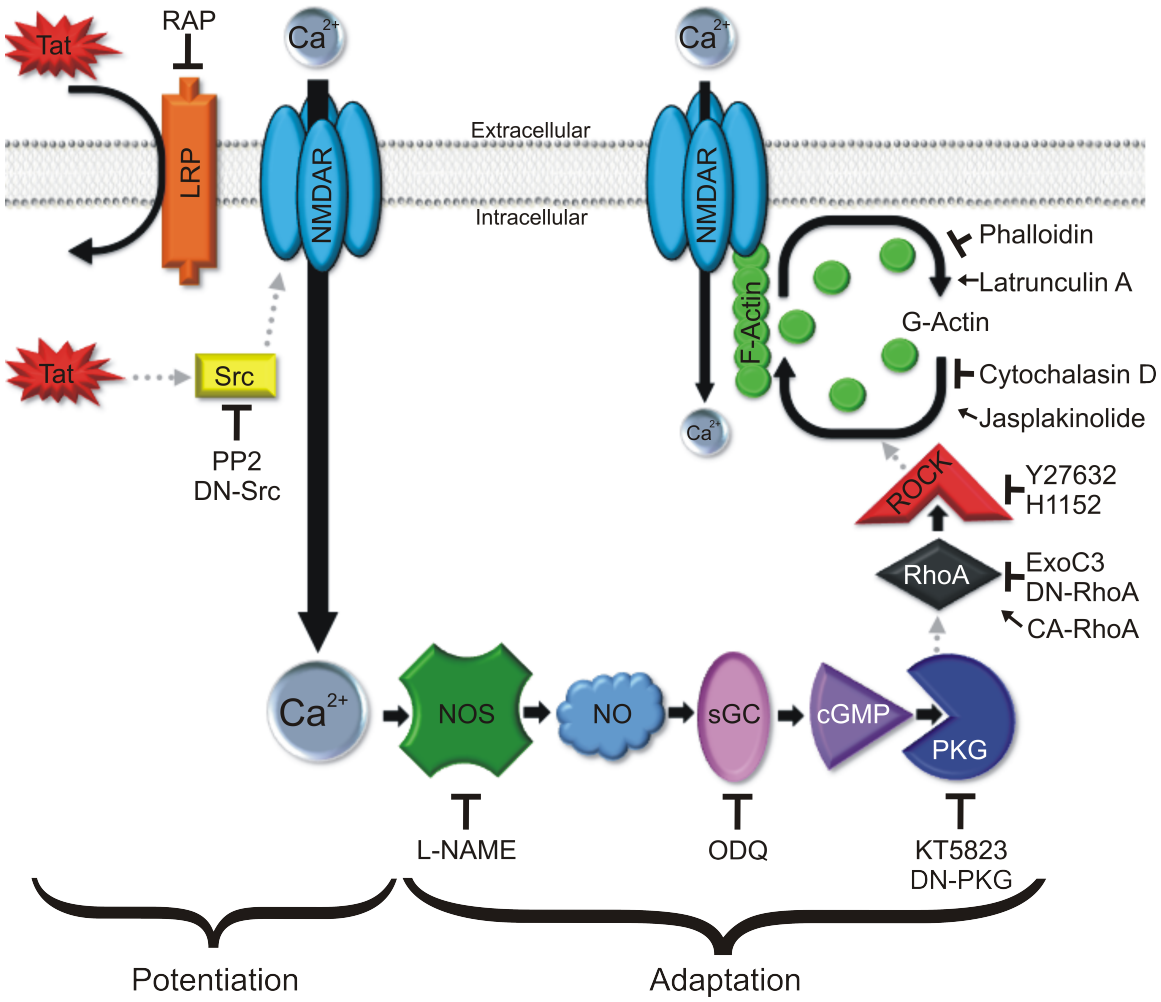

Figure 3.6: Proposed mechanism of Tat-induced biphasic change in NMDAR function.
HIV-1 Tat interacts with LRP leading to Src-dependent potentiation of the NMDAR and activation of the NOS/sGC/PKG signaling pathway. PKG activates a RhoA/ROCK signaling pathway leading to remodeling of the actin cytoskeleton and subsequent reduction of NMDAR function.

The small GTPase RhoA is a well-known regulator of the actin cytoskeleton (Kaibuchi et al., 1999). The expression and function of RhoA is regulated by NO-mediated activation of PKG in vascular smooth muscle cells (Sauzeau et al., 2003; Rolli-Derkinderen et al., 2005) consistent with our hypothesis that Tat activates a NOS/sGC/PKG signaling cascade upstream from RhoA. Tat activates RhoA in endothelial cells (Urbinati et al., 2005; Yuen et al., 2010; Zhong et al., 2010; Xu et al., 2012), however much less is known about the effects of Tat on RhoA in neurons. Our data show that adaptation of NMDAR function following Tat-induced potentiation required activation of RhoA. Pharmacologic or genetic inhibition of RhoA prevented adaptation of NMDAR function following Tat-induced potentiation. Furthermore, constitutive activation of RhoA attenuated NMDA-evoked responses by approximately 50% relative to non-expressing neurons in the same imaging field, consistent with our hypothesis that RhoA activation reduces NMDAR function. Thus, Tat-induced activation of RhoA attenuates NMDAR function. Because inhibition of RhoA had no effect on NMDA-evoked responses until the cell had been treated with Tat for over 8 h, we speculate that the adaptive response is a mechanism to compensate for the excess Ca^{2+} influx resulting from potentiation of NMDARs.

Activation and inhibition of RhoA profoundly affected neuronal morphology. Consistent with previous reports (Da Silva et al., 2003; Chen and Firestein, 2007), neurons expressing DN-RhoA exhibited increased dendritic branching while cells expressing CA-RhoA displayed simplified dendritic structures with minimal branching and no noticeable dendritic spines. Interestingly, activation of RhoA causes synapse loss

in vitro (Sunico et al., 2010) and loss of dendritic spines resulting in cognitive impairment *in vivo* (Pozueta et al., 2013). Similarly, treatment with Tat causes synapse loss *in vitro* (Kim et al., 2008; Shin et al., 2012) and loss of dendritic spines resulting in cognitive impairment *in vivo* (Fitting et al., 2010; Carey et al., 2012). Whether RhoA activation is required for Tat-induced synaptodendritic changes *in vivo* remains unknown.

ROCK is the primary downstream target of RhoA and is a serine/threonine kinase that modifies the cytoskeleton to regulate cell migration and proliferation (Matsui et al., 1996; Amano et al., 2010). Tat increases expression of ROCK in endothelial cells of the blood brain barrier (Zhong et al., 2012) and activation of ROCK in neurons induces rundown of NMDAR currents via an actin-dependent mechanism (Beazely et al., 2008). Based on these studies, we hypothesized that Tat-induced activation of ROCK would attenuate NMDA-evoked responses. Consistent with our hypothesis, we show that inhibition of ROCK prevented adaptation of NMDAR function following Tat-induced potentiation. These data indicate that Tat-induced activation of ROCK reduces NMDAR function. Abnormal activation of ROCK is observed in many models of neuronal disorders including Alzheimer's disease, spinal-cord injury, neuropathic pain, and excitotoxicity (Mueller et al., 2005). However, little is known about the role of ROCK in HAND.

RhoA activates ROCK to regulate the actin cytoskeleton by acting on multiple targets including MLCK (Maekawa et al., 1999). We found that adaptation of NMDA-evoked responses did not require MLCK. Inhibition of MLCK with ML-7 significantly inhibited NMDAR function. These results are consistent with previous reports indicating that

MLCK regulates NMDAR activity by contraction of actomyosin (Lei et al., 2001), however the effector between ROCK and the actin cytoskeleton remains unknown.

Activation of ROCK increases F-actin formation (Da Silva et al., 2003). The status of F-actin polymerization affects NMDAR function. Indeed, depolymerization of the actin cytoskeleton reduces NMDAR-mediated currents (Rosenmund and Westbrook, 1993) while polymerization of actin enhances glutamate receptor function (Furukawa et al., 1995). As anticipated, we found that F-actin depolymerization with latrunculin A reduced NMDAR function. Unexpectedly, increased F-actin polymerization with jasplakinolide also decreased NMDAR function. Both jasplakinolide (Bubb et al., 1994) and CA-RhoA (Ishizaki et al., 1997) increase the formation of F-actin and both cause approximately 50% reduction in NMDAR function, suggesting that increased actin polymerization reduces NMDAR function. Although the mechanism leading to impaired NMDAR function remains unclear, there is precedent for modulation of NMDAR function through tension exerted on the NMDAR via its physical connection with the actin cytoskeleton (Lei et al., 2001). Perhaps the robust somatic and dendritic redistribution of actin shown in Figure 3.5 disrupts the connections between the NMDAR and the actin cytoskeleton resulting in reduced NMDAR function.

Adaptation of NMDAR function following Tat-induced potentiation was blocked by cytochalasin D and phalloidin, agents which inhibit polymerization and depolymerization, respectively (Cingolani and Goda, 2008). These results suggest that adaptation occurs in response to remodeling of the actin cytoskeleton, an effect that requires both depolymerization and polymerization of actin. Tat is known to affect the

cytoskeleton; it depolymerizes actin in endothelial cells (Wu et al., 2004) and produces a loss of F-actin puncta in hippocampal neurons *in vitro* (Bertrand et al., 2014). Our data indicate that Tat activates a RhoA/ROCK pathway leading to remodeling of the actin cytoskeleton resulting in reduced NMDA-evoked responses.

Adaptation of Tat-induced NMDAR potentiation might improve neuronal survival. However, increasing evidence suggests that over compensation following neuronal insult can lead to excessive inhibitory tone (Hargus and Thayer, 2013; Wu et al., 2014) and impaired connectivity due to lost excitatory synapses (Kim et al., 2008). Reduced NMDAR function during prolonged exposure to HIV neurotoxins may contribute to cognitive impairment analogous to the impairment seen in transgenic animals with reduced NMDAR expression (Tsien et al., 1996; Shimizu et al., 2000) or humans given NMDAR antagonists (Krystal et al., 1994; Malhotra et al., 1996). Thus, inhibiting ROCK might prevent cognitive decline. Indeed, RhoA/ROCK are promising targets for treating various neurological disorders. ROCK inhibition lowers brain levels of amyloid-β in a transgenic mouse model of Alzheimer's disease (Zhou et al., 2003) and improves cognitive function in aged rats (Huentelman et al., 2009). Inhibition of ROCK also improves neurological function and reduces infarct size in models of ischemic stroke (Toshima et al., 2000; Satoh et al., 2001) and accelerates functional recovery from spinal cord injuries (Hara et al., 2000; Dergham et al., 2002; Fournier et al., 2003; Sung et al., 2003; Tanaka et al., 2004). Thus, ROCK is a valuable drug target with neuroprotective and neuroregenerative potential. The ROCK inhibitor, fasudil, is a well-tolerated vasodilator that has been used clinically in Japan since 1995 for the treatment of

subarachnoid hemorrhage (Shibuya et al., 1992) and improves physical performance in patients with angina pectoris (Shimokawa et al., 2002). Importantly, fasudil is neuroprotective in models of Alzheimer's disease (Song et al., 2013), amyotrophic lateral sclerosis (Takata et al., 2013), and Parkinson's disease (Tonges et al., 2012). Whether fasudil or other ROCK inhibitors are effective against HAND remains to be determined.

In summary, we show that adaptation of NMDAR function following Tat-induced potentiation results from RhoA/ROCK-dependent remodeling of the actin cytoskeleton. These finding suggest that different signaling pathways mediate the neurotoxicity induced by HIV Tat over the course of prolonged exposure. As such, drugs that modulate ROCK signaling may warrant exploration as neuroprotective agents for the treatment of HAND.

Chapter Four:

Concluding Remarks

I. Summary of current studies

The studies described in this dissertation add novel temporal and molecular detail regarding the mechanisms affecting NMDAR function following exposure to the HIV-1 protein, Tat. Tat-induced NMDAR potentiation is reported in multiple investigations, however many of the observations involve acute (min to h) effects of very high concentrations (up to 1500 ng/mL) of Tat that greatly exceed the concentration of Tat (up to 40 ng/mL) detected in the sera of HIV-infected patients (Xiao et al., 2000). In Chapter Two, it was demonstrated that 50 ng/mL Tat caused a biphasic change in NMDAR function over 48 hours. Tat initially potentiated NMDAR function following LRP-dependent activation of Src kinase, which subsequently adapted by gradually returning to basal levels after activation of a NOS/sGC/PKG signaling pathway. In Chapter Three, effectors downstream of PKG responsible for reducing NMDAR function were identified. Tat activated a RhoA/ROCK signaling pathway resulting in actin remodeling and reduced NMDAR function. Adaptation of NMDAR function may be a novel neuroprotective mechanism to prevent Ca^{2+}-induced neurotoxicity.

II. Advantages and limitations of Ca^{2+} imaging

Calcium imaging is a useful tool for the functional study many cell types including neurons. Ca^{2+}-sensitive dyes allow accurate measurement of $[Ca^{2+}]_i$ in live cells via imaging. Fura-2 is one of the most widely used ratiometric, Ca^{2+}-sensitive dyes and has been a staple of Ca^{2+} imaging since 1985 (Grynkiewicz et al., 1985) receiving more than 11,000 citations thus far. The use of ratiometric dyes is advantageous because the

measurement of $[Ca^{2+}]_i$ is minimally affected by unequal probe loading, varying cell thickness, or dye leakage. Additionally, these Ca^{2+} indicators are bright at low intracellular concentrations thereby minimizing $[Ca^{2+}]_i$ buffering potential and are less susceptible to photobleaching compared with non-ratiometric indicators. Furthermore, this approach is non-invasive, does not disturb the cytoplasm, and leaves the cell membrane intact. Lastly, it is difficult to study 'sick' cells using other techniques, such as patch-clamping, but is easily achieved using Ca^{2+} imaging. These probes are available with wide-ranging affinities for Ca^{2+} and are attached to diverse chemical moieties for broad applicability. Ultimately, the properties of fura-2 and similar ratiometric Ca^{2+}-sensitive dyes result in enhanced experimental reproducibility.

Despite the widespread popularity and broad applicability, Ca^{2+} imaging has several limitations. The use of chemical Ca^{2+} probes limits the duration of imaging. During extended imaging sessions, the Ca^{2+} probe is increasingly susceptible to compartmentalization and extrusion from the cell, which may negatively affect experimental recordings. Fortunately, several high molecular weight probes are available to prevent removal of the dye from the cell, but introduction of such large molecules into the cell requires microinjection or electroporation; challenging techniques to master. Another limitation is targeting the chemical Ca^{2+} indicator to organelles of interest or controlling the cellular localization. Genetically encoded Ca^{2+} indicators (GECIs) combat this limitation and allow expression and localization of fluorescent Ca^{2+}-sensitive proteins to regions of interests. One such GECI, known as GCaMP, can be localized to the plasma membrane, post-synaptic densities, presynaptic terminals, or expressed

throughout the entire cell. Lastly, Ca^{2+} imaging does not precisely reflect the rate in intracellular Ca^{2+} signaling. Intracellular events can happen much faster than the Ca^{2+} probe is able to report, resulting in less-than-accurate quantification of Ca^{2+} signaling kinetics.

Fortunately, the assay used for the studies outlined in this dissertation minimized many of the pitfalls of fura-2-based Ca^{2+} imaging by keeping imaging sessions brief and by studying the change in NMDA-evoked increases in $[Ca^{2+}]_i$ in the neuronal cell body. In doing so, experimental reproducibility was maximized. However, this approach suffers from being unable to measure changes in $[Ca^{2+}]_i$ at the synapse. Additionally, it remains unknown if these *in vitro* observations correlate with changes observed *in vivo*. Finally, it remains to be determined if changes in NMDAR function correlate with cognitive impairment. Although, if reduced NMDAR function following prolonged exposure to HIV neurotoxins is observed *in vivo,* then cognitive impairment similar to the impairment observed in humans given NMDAR antagonists (Krystal et al., 1994; Malhotra et al., 1996) is a reasonable expectation.

III. Future directions

The most exciting discovery from the studies in this dissertation is that the NMDA receptor undergoes a biphasic change in function. Potentiation of NMDAR function has been described in many reports since the 1980's, however adaptation following NMDAR potentiation has not been previously described. The mechanisms regulating NMDAR adaptation may be just as important to the progression of disease as NMDAR

potentiation. Thus, a better understanding of the mechanisms regulating NMDAR adaptation may provide insight into the pathophysiology of certain diseases.

Moving forward it will be important to determine if the biphasic change in NMDAR function measured in the neuronal cell body also occurs at the synapse. Cognitive impairment in patients with HAND correlates with synaptodendritic changes. Thus, a logical next step will be to determine if Tat causes biphasic changes in synaptic NMDAR function. NMDAR subtypes GluN2A and GluN2B localize to synaptic and extrasynaptic regions, respectively and activate distinct intracellular signaling pathways (Hardingham and Bading, 2010). Although the studies outlined in this dissertation indicate that GluN2A is not involved in NMDAR adaptation following exposure to Tat, synaptic measurements may reveal exciting differences.

A logical next step in determining the relevance of the current studies and in identifying therapeutic targets for HAND is to determine if Tat-induced activation of signaling pathways *in vitro* translates in an *in vivo* model. Currently, the Thayer lab is working with a transgenic mouse model with inducible Tat expression. This transgenic mouse model is reported to have cognitive shortcomings, but the precise mechanism leading to such impairment is unknown. Perhaps, Tat-induced activation of the signaling pathway outlined in this dissertation is involved, and pharmacologic blockade of the proposed therapeutic targets can prevent Tat-induced cognitive decline.

IV. Therapeutic potential of targeting the NMDA receptor

More than 35 million of people suffer from neurodegenerative diseases worldwide (Mayeux, 2003; Prince et al., 2013). The prevalence and economic cost for many of these diseases are estimated to triple by the year 2050 (Prince et al., 2013). Unfortunately, effective treatment options for neurodegeneration are rare. Consequently, millions of patients are in desperate need for effective, next-generation pharmacotherapeutics.

Alzheimer's disease, Parkinson's disease, Huntington's disease, amyotrophic lateral sclerosis, multiple sclerosis, and HAND are etiologically distinct, but share a common pathway leading to neuronal injury: NMDA receptor dysfunction. This dissertation describes how the HIV-1 protein Tat causes a biphasic change in NMDAR function. An enhanced understanding of the mechanisms leading to NMDAR dysfunction may help to guide the development of targeted therapeutics for the treatment of HAND and other neurodegenerative diseases.

There is enormous potential for the treatment of neurodegenerative diseases by targeting the NMDA receptor. As such, scientists have eagerly pursued agents that selectively target the NMDAR for therapeutic benefit since the 1980s. It was not until recently that this fervor began to yield a small number of clinically approved drugs. Such a slow pace of development is indicative of the level of difficulty regarding the creation of safe and effective compounds that target the NMDAR. Excessive antagonism of the NMDAR results in hallucinations and sedation thereby precluding the use of most NMDAR antagonists in patients, while insufficient blockade lacks therapeutic benefit. Thus, the ideal NMDAR antagonist should allow normal neurotransmission to occur

while inhibiting excessive NMDAR activation. Memantine is a drug that possesses these qualities and is FDA-approved for temporary symptomatic relief in patients suffering from Alzheimer's disease. Memantine is an uncompetitive NMDAR antagonist with inhibitory action that is contingent upon prior activation of the receptor. Thus, memantine only inhibits the NMDAR when it is overactivated. Intriguingly, memantine is useful against Tat-induced neurotoxicity; it prevents Tat-induced cell death and promotes the recovery of excitatory synapses after Tat-induced synapse loss has occurred (Shin et al., 2012). Unfortunately, a clinical trial concluded that memantine had no effect on cognitive performance in HAND patients (Schifitto et al., 2007b; Zhao et al., 2010). Furthermore, memantine only provides symptomatic relief from Alzheimer's disease for up to 6 months and fails to prevent disease progression. Ideally, compounds generated in the future will be well tolerated, provide symptomatic relief, and prevent disease progression.

Adaptation of NMDAR function following prolonged exposure to HIV neurotoxins may be a compensatory measure that allows neurons to adapt to a neurotoxic environment resulting in improved neuronal survival. However, overcompensation following neuronal insult can lead to impaired NMDAR function (Krogh et al., 2014). Reduced NMDAR function impairs cognitive performance in humans (Krystal et al., 1994; Malhotra et al., 1996). Thus, drugs outlined in this dissertation that prevented the reduction of NMDAR function may be valuable agents for the prevention of HIV-associated cognitive decline. ROCK has been shown to be a promising target for the treatment of various neurological disorders (Mueller et al., 2005). Inhibition of ROCK with a drug used in this dissertation, Y27632, reduces levels amyloid-β in transgenic and

cell culture-based models of Alzheimer's disease (Zhou et al., 2003). Inhibition of ROCK also improves learning and memory in aged rats (Huentelman et al., 2009), and improves neurological deficits following acute cerebral ischemia (Toshima et al.; Satoh et al.). Additionally, ROCK inhibition is neuroprotective against excitotoxicity (Kitaoka et al., 2004) and prevents neuropathic pain (Inoue et al., 2004). Lastly, inhibition of ROCK accelerates the functional recovery of spinal-cord injury in rodent models (Hara et al., 2000; Dergham et al., 2002; Fournier et al., 2003; Sung et al., 2003; Tanaka et al., 2004). Thus, ROCK inhibitors have great potential as neuroprotective agents. The ROCK inhibitor fasudil is a well-tolerated and clinically approved drug indicated for the treatment of subarachnoid hemorrhage (Shibuya and Douglas, 1992). Intriguingly, fasudil protects against neurodegeneration in models of ALS (Takata et al., 2013), Parkinson's disease (Tonges et al., 2012), and Alzheimer's disease (Song et al., 2013). Despite such promising reports, it remains unknown if the neuroprotective capabilities of fasudil will be applicable against HIV-associated neurotoxicity. However, targeting ROCK may be an indirect way to influence NMDAR function while bypassing the unwanted side effects that arise from directly targeting the NMDAR. While the NMDAR is an important target to prevent HIV-associated neurotoxicity, it is likely that combined approaches may yield the most favorable results. For instance, administration of cART with enhanced penetrance into the CNS combined with adjunctive therapy that indirectly targets the NMDAR may be an effective approach to reduce the symptoms of HAND while minimizing unwanted side effects. Targeting the NMDAR will continue to be

challenging, but if done successfully has the potential to help millions of patients suffering from neurodegenerative diseases including HAND.

In conclusion, the number of patients with neurodegenerative disorders and the cost of treatment are projected to skyrocket within the next 35 years and effective treatment options are scarce. NMDAR dysfunction contributes to the progression of many neurodegenerative diseases including HAND. In order to develop next-generation pharmacotherapeutics, an enhanced understanding of the pathways leading to NMDAR-mediated neurotoxicity is required. The studies outlined in this dissertation provide molecular and temporal detail of NMDAR dysfunction following exposure to the HIV-1 protein, Tat. Thus, the pathways described in this dissertation may provide insight into the development of new therapies for the treatment of HAND and other neurodegenerative diseases.

Chapter Five:

Bibliography

Adekeye OA, Heiman HJ, Onyeabor OS, Hyacinth HI (2012) The new invincibles: HIV screening among older adults in the U.S. PLoS One 7:e43618.

Albright AV, Shieh JT, Itoh T, Lee B, Pleasure D, O'Connor MJ, Doms RW, Gonzalez-Scarano F (1999) Microglia express CCR5, CXCR4, and CCR3, but of these, CCR5 is the principal coreceptor for human immunodeficiency virus type 1 dementia isolates. J Virol 73:205-213.

Amano M, Nakayama M, Kaibuchi K (2010) Rho-kinase/ROCK: A key regulator of the cytoskeleton and cell polarity. Cytoskeleton 67:545-554.

An SF, Groves M, Gray F, Scaravilli F (1999) Early entry and widespread cellular involvement of HIV-1 DNA in brains of HIV-1 positive asymptomatic individuals. J Neuropathol Exp Neurol 58:1156-1162.

Antinori A et al. (2007) Updated research nosology for HIV-associated neurocognitive disorders. Neurology 69:1789-1799.

Arendt G, Hefter H, Elsing C, Strohmeyer G, Freund HJ (1990) Motor dysfunction in HIV-infected patients without clinically detectable central-nervous deficit. J Neurol 237:362-368.

Arnold WP, Mittal CK, Katsuki S, Murad F (1977) Nitric oxide activates guanylate cyclase and increases guanosine 3':5'-cyclic monophosphate levels in various tissue preparations. Proc Natl Acad Sci U S A 74:3203-3207.

Atkinson JH, Jr., Grant I, Kennedy CJ, Richman DD, Spector SA, McCutchan JA (1988) Prevalence of psychiatric disorders among men infected with human immunodeficiency virus. A controlled study. Arch Gen Psychiatry 45:859-864.

Bachani M, Sacktor N, McArthur JC, Nath A, Rumbaugh J (2013) Detection of anti-tat antibodies in CSF of individuals with HIV-associated neurocognitive disorders. Journal of neurovirology 19:82-88.

Bain J, Plater L, Elliott M, Shpiro N, Hastie CJ, McLauchlan H, Klevernic I, Arthur JS, Alessi DR, Cohen P (2007) The selectivity of protein kinase inhibitors: a further update. Biochem J 408:297-315.

Banks WA, Robinson SM, Wolf KM, Bess JW, Jr., Arthur LO (2004) Binding, internalization, and membrane incorporation of human immunodeficiency virus-1 at the blood-brain barrier is differentially regulated. Neuroscience 128:143-153.

Barin F, McLane MF, Allan JS, Lee TH, Groopman JE, Essex M (1985) Virus envelope protein of HTLV-III represents major target antigen for antibodies in AIDS patients. Science 228:1094-1096.

Barre-Sinoussi F, Chermann JC, Rey F, Nugeyre MT, Chamaret S, Gruest J, Dauguet C, Axler-Blin C, Vezinet-Brun F, Rouzioux C, Rozenbaum W, Montagnier L (1983) Isolation of a T-lymphotropic retrovirus from a patient at risk for acquired immune deficiency syndrome (AIDS). Science 220:868-871.

Beazely MA, Weerapura M, MacDonald JF (2008) Abelson tyrosine kinase links PDGFbeta receptor activation to cytoskeletal regulation of NMDA receptors in CA1 hippocampal neurons. Mol Brain 1:20.

Berger EA, Doms RW, Fenyo EM, Korber BTM, Littman DR, Moore JP, Sattentau QJ, Schuitemaker H, Sodroski J, Weiss RA (1998) A New Classification For Hiv-1. Nature 391:240.

Berkhout B, Silverman RH, Jeang KT (1989) Tat trans-activates the human immunodeficiency virus through a nascent RNA target. Cell 59:273-282.

Bertrand SJ, Mactutus CF, Aksenova MV, Espensen-Sturges TD, Booze RM (2014) Synaptodendritic recovery following HIV Tat exposure: neurorestoration by phytoestrogens. J Neurochem 128:140-151.

Bock HH, Herz J (2003) Reelin activates SRC family tyrosine kinases in neurons. Curr Biol 13:18-26.

Bomsel M (1997) Transcytosis of infectious human immunodeficiency virus across a tight human epithelial cell line barrier. Nat Med 3:42-47.

Browning DD, Mc Shane M, Marty C, Ye RD (2001) Functional analysis of type 1alpha cGMP-dependent protein kinase using green fluorescent fusion proteins. J Biol Chem 276:13039-13048.

Bu G (2001) The roles of receptor-associated protein (RAP) as a molecular chaperone for members of the LDL receptor family. International review of cytology 209:79-116.

Bubb MR, Senderowicz AM, Sausville EA, Duncan KL, Korn ED (1994) Jasplakinolide, a cytotoxic natural product, induces actin polymerization and competitively inhibits the binding of phalloidin to F-actin. J Biol Chem 269:14869-14871.

Bukrinsky MI, Sharova N, Dempsey MP, Stanwick TL, Bukrinskaya AG, Haggerty S, Stevenson M (1992) Active nuclear import of human immunodeficiency virus type 1 preintegration complexes. Proc Natl Acad Sci U S A 89:6580-6584.

Butt E, Abel K, Krieger M, Palm D, Hoppe V, Hoppe J, Walter U (1994) cAMP- and cGMP-dependent protein kinase phosphorylation sites of the focal adhesion vasodilator-stimulated phosphoprotein (VASP) in vitro and in intact human platelets. J Biol Chem 269:14509-14517.

Carey AN, Sypek EI, Singh HD, Kaufman MJ, McLaughlin JP (2012) Expression of HIV-Tat protein is associated with learning and memory deficits in the mouse. Behav Brain Res 229:48-56.

Chan DC, Fass D, Berger JM, Kim PS (1997) Core structure of gp41 from the HIV envelope glycoprotein. Cell 89:263-273.

Chandra A, Gerber T, Chandra P (1986) Biochemical heterogeneity of reverse transcriptase purified from the AIDS virus, HTLV-III. FEBS Lett 197:84-88.

Chandra T, Maier W, Konig HG, Hirzel K, Kogel D, Schuler T, Chandra A, Demirhan I, Laube B (2005) Molecular interactions of the type 1 human immunodeficiency virus transregulatory protein Tat with N-methyl-d-aspartate receptor subunits. Neuroscience 134:145-153.

Chang HC, Samaniego F, Nair BC, Buonaguro L, Ensoli B (1997) HIV-1 Tat protein exits from cells via a leaderless secretory pathway and binds to extracellular matrix-associated heparan sulfate proteoglycans through its basic region. AIDS 11:1421-1431.

Chen H, Firestein BL (2007) RhoA regulates dendrite branching in hippocampal neurons by decreasing cypin protein levels. J Neurosci 27:8378-8386.

Cheng J, Nath A, Knudsen B, Hochman S, Geiger JD, Ma M, Magnuson DS (1998) Neuronal excitatory properties of human immunodeficiency virus type 1 Tat protein. Neuroscience 82:97-106.

Choi YB, Tenneti L, Le DA, Ortiz J, Bai G, Chen HSV, Lipton SA (2000) Molecular basis of NMDA receptor-coupled ion channel modulation by S-nitrosylation. Nature Neuroscience 3:15-21.

Chu C, Selwyn PA (2011) Complications of HIV infection: a systems-based approach. Am Fam Physician 83:395-406.

Cingolani LA, Goda Y (2008) Actin in action: the interplay between the actin cytoskeleton and synaptic efficacy. Nat Rev Neurosci 9:344-356.

Clifford DB, Ances BM (2013) HIV-associated neurocognitive disorder. The Lancet infectious diseases 13:976-986.

Cohen MS, Gay CL, Busch MP, Hecht FM (2010) The detection of acute HIV infection. J Infect Dis 202 Suppl 2:S270-277.

Contestabile A, Ciani E (2004) Role of nitric oxide in the regulation of neuronal proliferation, survival and differentiation. Neurochem Int 45:903-914.

Crump FT, Dillman KS, Craig AM (2001) cAMP-dependent protein kinase mediates activity-regulated synaptic targeting of NMDA receptors. J Neurosci 21:5079-5088.

Cull-Candy S, Brickley S, Farrant M (2001) NMDA receptor subunits: diversity, development and disease. Curr Opin Neurobiol 11:327-335.

Cull-Candy SG, Leszkiewicz DN (2004) Role of distinct NMDA receptor subtypes at central synapses. Sci STKE 2004:re16.

Cysique LA, Maruff P, Brew BJ (2004) Prevalence and pattern of neuropsychological impairment in human immunodeficiency virus–infected/acquired immunodeficiency syndrome (HIV/AIDS) patients across pre- and post-highly active antiretroviral therapy eras: A combined study of two cohorts. Journal of neurovirology 10:350-357.

Cysique LA, Vaida F, Letendre S, Gibson S, Cherner M, Woods SP, McCutchan JA, Heaton RK, Ellis RJ (2009) Dynamics of cognitive change in impaired HIV-positive patients initiating antiretroviral therapy. Neurology 73:342-348.

Da Silva JS, Medina M, Zuliani C, Di Nardo A, Witke W, Dotti CG (2003) RhoA/ROCK regulation of neuritogenesis via profilin IIa-mediated control of actin stability. J Cell Biol 162:1267-1279.

Dalgleish AG, Beverley PC, Clapham PR, Crawford DH, Greaves MF, Weiss RA (1984) The CD4 (T4) antigen is an essential component of the receptor for the AIDS retrovirus. Nature 312:763-767.

Danysz W, Parsons CG (2003) The NMDA receptor antagonist memantine as a symptomatological and neuroprotective treatment for Alzheimer's disease: preclinical evidence. International journal of geriatric psychiatry 18:S23-32.

Davis LE, Hjelle BL, Miller VE, Palmer DL, Llewellyn AL, Merlin TL, Young SA, Mills RG, Wachsman W, Wiley CA (1992) Early viral brain invasion in iatrogenic human immunodeficiency virus infection. Neurology 42:1736-1739.

Del Valle L, Croul S, Morgello S, Amini S, Rappaport J, Khalili K (2000) Detection of HIV-1 Tat and JCV capsid protein, VP1, in AIDS brain with progressive multifocal leukoencephalopathy. Journal of neurovirology 6:221-228.

Dergham P, Ellezam B, Essagian C, Avedissian H, Lubell WD, McKerracher L (2002) Rho signaling pathway targeted to promote spinal cord repair. J Neurosci 22:6570-6577.

Dingwall C, Ernberg I, Gait MJ, Green SM, Heaphy S, Karn J, Lowe AD, Singh M, Skinner MA (1990) HIV-1 tat protein stimulates transcription by binding to a U-rich bulge in the stem of the TAR RNA structure. EMBO J 9:4145-4153.

Dorfman T, Bukovsky A, Ohagen A, Hoglund S, Gottlinger HG (1994) Functional domains of the capsid protein of human immunodeficiency virus type 1. J Virol 68:8180-8187.

Ellis R, Langford D, Masliah E (2007) HIV and antiretroviral therapy in the brain: neuronal injury and repair. Nat Rev Neurosci 8:33-44.

Eugenin EA, King JE, Nath A, Calderon TM, Zukin RS, Bennett MV, Berman JW (2007) HIV-tat induces formation of an LRP-PSD-95- NMDAR-nNOS complex that promotes apoptosis in neurons and astrocytes. Proc Natl Acad Sci U S A 104:3438-3443.

Evans SR, Yeh TM, Sacktor N, Clifford DB, Simpson D, Miller EN, Ellis RJ, Valcour V, Marra CM, Millar L, Schifitto G, Group ACT, the Neurologic ARC (2007) Selegiline transdermal system (STS) for HIV-associated cognitive impairment: open-label report of ACTG 5090. HIV clinical trials 8:437-446.

Feinberg MB, Jarrett RF, Aldovini A, Gallo RC, Wong-Staal F (1986) HTLV-III expression and production involve complex regulation at the levels of splicing and translation of viral RNA. Cell 46:807-817.

Feng Y, Broder CC, Kennedy PE, Berger EA (1996) Hiv-1 entry cofactor - functional cdna cloning of a seven-transmembrane, g protein-coupled receptor. Science 272:872-877.

Fitting S, Xu R, Bull C, Buch S, El-Hage N, Nath A, Knapp PE, Hauser KF (2010) Interactive Comorbidity between Opioid Drug Abuse and HIV-1 Tat: Chronic Exposure Augments Spine Loss and Sublethal Dendritic Pathology in Striatal Neurons. Am J Pathol 177:1397-1410.

Fitting S, Ignatowska-Jankowska BM, Bull C, Skoff RP, Lichtman AH, Wise LE, Fox MA, Su J, Medina AE, Krahe TE, Knapp PE, Guido W, Hauser KF (2012) Synaptic dysfunction in the hippocampus accompanies learning and memory deficits in human immunodeficiency virus type-1 tat transgenic mice. Biol Psychiatry 73:443-453.

Fitting S, Ignatowska-Jankowska BM, Bull C, Skoff RP, Lichtman AH, Wise LE, Fox MA, Su J, Medina AE, Krahe TE, Knapp PE, Guido W, Hauser KF (2013) Synaptic dysfunction in the hippocampus accompanies learning and memory deficits in human immunodeficiency virus type-1 Tat transgenic mice. Biol Psychiatry 73:443-453.

Fournier AE, Takizawa BT, Strittmatter SM (2003) Rho kinase inhibition enhances axonal regeneration in the injured CNS. J Neurosci 23:1416-1423.

Furukawa K, Mattson MP (1998) Secreted amyloid precursor protein alpha selectively suppresses N-methyl-D-aspartate currents in hippocampal neurons: involvement of cyclic GMP. Neuroscience 83:429-438.

Furukawa K, Smithswintosky VL, Mattson MP (1995) Evidence that actin depolymerization protects hippocampal neurons against excitotoxicity by stabilizing [ca2+](i). Experimental Neurology 133:153-163.

Furuta RA, Wild CT, Weng Y, Weiss CD (1998) Capture of an early fusion-active conformation of HIV-1 gp41. Nat Struct Biol 5:276-279.

Gallo EF, Iadecola C (2011) Neuronal nitric oxide contributes to neuroplasticity-associated protein expression through cGMP, protein kinase G, and extracellular signal-regulated kinase. J Neurosci 31:6947-6955.

Gallo RC, Salahuddin SZ, Popovic M, Shearer GM, Kaplan M, Haynes BF, Palker TJ, Redfield R, Oleske J, Safai B, et al. (1984) Frequent detection and isolation of cytopathic retroviruses (HTLV-III) from patients with AIDS and at risk for AIDS. Science 224:500-503.

Gelderblom H, Hausmann E, Ozel M, Pauli G, Koch M (1987) Fine structure of human immunodeficiency virus (HIV) and immunolocalization of structural proteins. Virology 156:171-176.

Genis P, Jett M, Bernton EW, Boyle T, Gelbard HA, Dzenko K, Keane RW, Resnick L, Mizrachi Y, Volsky DJ, Epstein LG, Gendelman HE (1992) Cytokines and arachidonic metabolites produced during human immunodeficiency virus (HIV)-infected macrophage interactions: implications for the neuropathogenesis of HIV disease. J Exp Med 176:1703-1718.

Gonzalez-Scarano F, Martin-Garcia J (2005) The neuropathogenesis of AIDS. Nat Rev Immunol 5:69-81.

Gonzalez-Scarano F, Waxham MN, Ross AM, Hoxie JA (1987) Sequence similarities between human immunodeficiency virus gp41 and paramyxovirus fusion proteins. AIDS Res Hum Retroviruses 3:245-252.

Greene WC, Peterlin BM (2002) Charting HIV's remarkable voyage through the cell: Basic science as a passport to future therapy. Nat Med 8:673-680.

Groc L, Heine M, Cousins SL, Stephenson FA, Lounis B, Cognet L, Choquet D (2006) NMDA receptor surface mobility depends on NR2A-2B subunits. Proc Natl Acad Sci U S A 103:18769-18774.

Grynkiewicz G, Poenie M, Tsien RY (1985) A new generation of Ca^{2+} indicators with greatly improved fluorescence properties. Journal of Biological Chemistry 260:3440-3450.

Hallett PJ, Standaert DG (2004) Rationale for and use of NMDA receptor antagonists in Parkinson's disease. Pharmacol Ther 102:155-174.

Hara M, Takayasu M, Watanabe K, Noda A, Takagi T, Suzuki Y, Yoshida J (2000) Protein kinase inhibition by fasudil hydrochloride promotes neurological recovery after spinal cord injury in rats. J Neurosurg 93:94-101.

Hardingham GE, Bading H (2010) Synaptic versus extrasynaptic NMDA receptor signalling: implications for neurodegenerative disorders. Nat Rev Neurosci.

Hardingham GE, Fukunaga Y, Bading H (2002) Extrasynaptic NMDARs oppose synaptic NMDARs by triggering CREB shut-off and cell death pathways. Nat Neurosci 5:405-414.

Hargus NJ, Thayer SA (2013) Human Immunodeficiency Virus-1 Tat Protein Increases the Number of Inhibitory Synapses between Hippocampal Neurons in Culture. J Neurosci 33:17908-17920.

Haughey NJ, Holden CP, Nath A, Geiger JD (1999) Involvement of inositol 1,4,5-trisphosphate-regulated stores of intracellular calcium in calcium dysregulation and neuron cell death caused by HIV-1 protein Tat. Journal of Neurochemistry 73:1363-1374.

Haughey NJ, Nath A, Mattson MP, Slevin JT, Geiger JD (2001) HIV-1 Tat through phosphorylation of NMDA receptors potentiates glutamate excitotoxicity. Journal of Neurochemistry 78:457-467.

Heaton RK, Marcotte TD, Mindt MR, Sadek J, Moore DJ, Bentley H, McCutchan JA, Reicks C, Grant I (2004) The impact of HIV-associated neuropsychological impairment on everyday functioning. J Int Neuropsychol Soc 10:317-331.

Heaton RK et al. (2010) HIV-associated neurocognitive disorders persist in the era of potent antiretroviral therapy: CHARTER Study. Neurology 75:2087-2096.

Heaton RK et al. (2011) HIV-associated neurocognitive disorders before and during the era of combination antiretroviral therapy: differences in rates, nature, and predictors. Journal of neurovirology 17:3-16.

Herz J, Strickland DK (2001) LRP: a multifunctional scavenger and signaling receptor. J Clin Invest 108:779-784.

Hirsch VM, Olmsted RA, Murphey-Corb M, Purcell RH, Johnson PR (1989) An African primate lentivirus (SIVsm) closely related to HIV-2. Nature 339:389-392.

Hogg R (2008) Life expectancy of individuals on combination antiretroviral therapy in high-income countries: a collaborative analysis of 14 cohort studies. Lancet 372:293-299.

Hudson L, Liu J, Nath A, Jones M, Raghavan R, Narayan O, Male D, Everall I (2000) Detection of the human immunodeficiency virus regulatory protein tat in CNS tissues. Journal of neurovirology 6:145-155.

Huentelman MJ, Stephan DA, Talboom J, Corneveaux JJ, Reiman DM, Gerber JD, Barnes CA, Alexander GE, Reiman EM, Bimonte-Nelson HA (2009) Peripheral delivery of a ROCK inhibitor improves learning and working memory. Behavioral neuroscience 123:218-223.

Huet T, Cheynier R, Meyerhans A, Roelants G, Wain-Hobson S (1990) Genetic organization of a chimpanzee lentivirus related to HIV-1. Nature 345:356-359.

Hui L, Chen X, Haughey NJ, Geiger JD (2012) Role of endolysosomes in HIV-1 Tat-induced neurotoxicity. ASN Neuro 4:243-252.

Inoue M, Rashid MH, Fujita R, Contos JJ, Chun J, Ueda H (2004) Initiation of neuropathic pain requires lysophosphatidic acid receptor signaling. Nat Med 10:712-718.

Isel C, Karn J (1999) Direct evidence that HIV-1 Tat stimulates RNA polymerase II carboxyl-terminal domain hyperphosphorylation during transcriptional elongation. J Mol Biol 290:929-941.

Ishizaki T, Naito M, Fujisawa K, Maekawa M, Watanabe N, Saito Y, Narumiya S (1997) p160ROCK, a Rho-associated coiled-coil forming protein kinase, works downstream of Rho and induces focal adhesions. FEBS Lett 404:118-124.

Jaffrey SR, Erdjument-Bromage H, Ferris CD, Tempst P, Snyder SH (2001) Protein S-nitrosylation: a physiological signal for neuronal nitric oxide. Nature Cell Biology 3:193-197.

Jahr CE, Stevens CF (1987) Glutamate activates multiple single channel conductances in hippocampal neurons. Nature 325:522-525.

Jiang ZG, Piggee C, Heyes MP, Murphy C, Quearry B, Bauer M, Zheng J, Gendelman HE, Markey SP (2001) Glutamate is a mediator of neurotoxicity in secretions of

activated HIV-1-infected macrophages. Journal of Neuroimmunology 117:97-107.

Johnson JW, Ascher P (1987) Glycine potentiates the NMDA response in cultured mouse brain neurons. Nature 325:529-531.

Kahn JO, Walker BD (1998) Acute Human Immunodeficiency Virus Type 1 Infection. N Engl J Med 336:33-39.

Kaibuchi K, Kuroda S, Amano M (1999) Regulation of the cytoskeleton and cell adhesion by the Rho family GTPases in mammalian cells. Annu Rev Biochem 68:459-486.

Kaplan JE, Hanson D, Dworkin MS, Frederick T, Bertolli J, Lindegren ML, Holmberg S, Jones JL (2000) Epidemiology of Human Immunodeficiency Virus–Associated Opportunistic Infections in the United States in the Era of Highly Active Antiretroviral Therapy. Clinical Infectious Diseases 30:S5-14.

Kaul M, Garden GA, Lipton SA (2001) Pathways to neuronal injury and apoptosis in HIV-associated dementia. Nature 410:988-994.

Kim HJ, Martemyanov KA, Thayer SA (2008) Human immunodeficiency virus protein Tat induces synapse loss via a reversible process that is distinct from cell death. J Neurosci 28:12604-12613.

Kim HJ, Shin AH, Thayer SA (2011) Activation of Cannabinoid Type 2 Receptors Inhibits HIV-1 Envelope Glycoprotein gp120-Induced Synapse Loss. Mol Pharmacol 80:357-366.

King JE, Eugenin EA, Buckner CM, Berman JW (2006) HIV tat and neurotoxicity. Microbes Infect 8:1347-1357.

King JE, Eugenin EA, Hazleton JE, Morgello S, Berman JW (2010) Mechanisms of HIV-tat-induced phosphorylation of N-methyl-D-aspartate receptor subunit 2A in human primary neurons: implications for neuroAIDS pathogenesis. Am J Pathol 176:2819-2830.

Kitaoka Y, Kitaoka Y, Kumai T, Lam TT, Kuribayashi K, Isenoumi K, Munemasa Y, Motoki M, Kobayashi S, Ueno S (2004) Involvement of RhoA and possible neuroprotective effect of fasudil, a Rho kinase inhibitor, in NMDA-induced neurotoxicity in the rat retina. Brain Res 1018:111-118.

Kohr G, Seeburg PH (1996) Subtype-specific regulation of recombinant NMDA receptor-channels by protein tyrosine kinases of the src family. J Physiol 492 (Pt 2):445-452.

Krogh KA, Wydeven N, Wickman K, Thayer SA (2014) HIV-1 protein Tat produces biphasic changes in NMDA-evoked increases in intracellular Ca concentration via activation of Src kinase and nitric oxide signaling pathways. J Neurochem.

Krystal JH, Karper LP, Seibyl JP, Freeman GK, Delaney R, Bremner JD, Heninger GR, Bowers MB, Jr., Charney DS (1994) Subanesthetic effects of the noncompetitive NMDA antagonist, ketamine, in humans. Psychotomimetic, perceptual, cognitive, and neuroendocrine responses. Arch Gen Psychiatry 51:199-214.

Kuo JF, Greengard P (1972) An assay method for cyclic AMP and cyclic GMP based upon their abilities to activate cyclic AMP-dependent and cyclic GMP-dependent protein kinases. Advances in cyclic nucleotide research 2:41-50.

Kuppuswamy M, Subramanian T, Srinivasan A, Chinnadurai G (1989) Multiple functional domains of Tat, the trans-activator of HIV-1, defined by mutational analysis. Nucleic Acids Res 17:3551-3561.

Kwong PD, Wyatt R, Robinson J, Sweet RW, Sodroski J, Hendrickson WA (1998) Structure of an HIV gp120 envelope glycoprotein in complex with the CD4 receptor and a neutralizing human antibody [see comments]. Nature 393:648-659.

Lambotte O, Deiva K, Tardieu M (2003) HIV-1 persistence, viral reservoir, and the central nervous system in the HAART era. Brain Pathol 13:95-103.

Lapham CK, Ouyang J, Chandrasekhar B, Nguyen NY, Dimitrov DS, Golding H (1996) Evidence for cell-surface association between fusin and the CD4-gp120 complex in human cell lines. Science 274:602-605.

Lavezzari G, McCallum J, Lee R, Roche KW (2003) Differential binding of the AP-2 adaptor complex and PSD-95 to the C-terminus of the NMDA receptor subunit NR2B regulates surface expression. Neuropharmacology 45:729-737.

Lavezzari G, McCallum J, Dewey CM, Roche KW (2004) Subunit-specific regulation of NMDA receptor endocytosis. J Neurosci 24:6383-6391.

Lei S, Czerwinska E, Czerwinski W, Walsh MP, MacDonald JF (2001) Regulation of NMDA receptor activity by F-actin and myosin light chain kinase. J Neurosci 21:8464-8472.

Lei SZ, Pan ZH, Aggarwal SK, Chen HS, Hartman J, Sucher NJ, Lipton SA (1992) Effect of nitric oxide production on the redox modulatory site of the NMDA receptor-channel complex. Neuron 8:1087-1099.

Letendre SL, Woods SP, Ellis RJ, Atkinson JH, Masliah E, van den Brande G, Durelle J, Grant I, Everall I (2006) Lithium improves HIV-associated neurocognitive impairment. Aids 20:1885-1888.

Li W, Li G, Steiner J, Nath A (2009) Role of Tat Protein in HIV Neuropathogenesis. Neurotox Res 16:205-220.

Li W, Huang Y, Reid R, Steiner J, Malpica-Llanos T, Darden TA, Shankar SK, Mahadevan A, Satishchandra P, Nath A (2008) NMDA receptor activation by HIV-Tat protein is clade dependent. J Neurosci 28:12190-12198.

Li Y, Krogh KA, Thayer SA (2012) Epileptic stimulus increases Homer 1a expression to modulate endocannabinoid signaling in cultured hippocampal neurons. Neuropharmacol 63:1140-1149.

Li Y, Popko J, Krogh KA, Thayer SA (2013) Epileptiform stimulus increases Homer 1a expression to modulate synapse number and activity in hippocampal cultures. J Neurophysiol.

Lipton SA, Stamler JS (1994) Actions of redox-related congeners of nitric oxide at the NMDA receptor. Neuropharmacology 33:1229-1233.

Lipton SA, Choi YB, Pan ZH, Lei SZ, Chen HS, Sucher NJ, Loscalzo J, Singel DJ, Stamler JS (1993) A redox-based mechanism for the neuroprotective and neurodestructive effects of nitric oxide and related nitroso-compounds. Nature 364:626-632.

Liu T, Jiang CY, Fujita T, Luo SW, Kumamoto E (2013) Enhancement by interleukin-1beta of AMPA and NMDA receptor-mediated currents in adult rat spinal superficial dorsal horn neurons. Mol Pain 9:16.

Liu Y, Jones M, Hingtgen CM, Bu G, Laribee N, Tanzi RE, Moir RD, Nath A, He JJ (2000) Uptake of HIV-1 tat protein mediated by low-density lipoprotein receptor-related protein disrupts the neuronal metabolic balance of the receptor ligands. Nat Med 6:1380-1387.

Ma M, Nath A (1997) Molecular determinants for cellular uptake of Tat protein of human immunodeficiency virus type 1 in brain cells. J Virol 71:2495-2499.

MacDermott AB, Mayer ML, Westbrook GL, Smith SJ, Barker JL (1986) NMDA-receptor activation increases cytoplasmic calcium concentration in cultured spinal cord neurones. Nature 321:519-522.

Maekawa M, Ishizaki T, Boku S, Watanabe N, Fujita A, Iwamatsu A, Obinata T, Ohashi K, Mizuno K, Narumiya S (1999) Signaling from Rho to the actin cytoskeleton through protein kinases ROCK and LIM-kinase. Science 285:895-898.

Maier W, Bednorz M, Meister S, Roebroek A, Weggen S, Schmitt U, Pietrzik CU (2013) LRP1 is critical for the surface distribution and internalization of the NR2B NMDA receptor subtype. Mol Neurodegener 8:25.

Malhotra AK, Pinals DA, Weingartner H, Sirocco K, Missar CD, Pickar D, Breier A (1996) NMDA receptor function and human cognition: the effects of ketamine in healthy volunteers. Neuropsychopharmacology 14:301-307.

Manzoni O, Prezeau L, Marin P, Deshager S, Bockaert J, Fagni L (1992) Nitric oxide-induced blockade of NMDA receptors. Neuron 8:653-662.

Marlink R, Kanki P, Thior I, Travers K, Eisen G, Siby T, Traore I, Hsieh CC, Dia MC, Gueye EH, et al (1994) Reduced rate of disease development after HIV-2 infection as compared to HIV-1. Science 265:1587-1590.

Matsui T, Amano M, Yamamoto T, Chihara K, Nakafuku M, Ito M, Nakano T, Okawa K, Iwamatsu A, Kaibuchi K (1996) Rho-associated kinase, a novel serine/threonine kinase, as a putative target for small GTP binding protein Rho. EMBO J 15:2208-2216.

Mayeux R (2003) Epidemiology of neurodegeneration. Annu Rev Neurosci 26:81-104.

McCutchan FE (2006) Global epidemiology of HIV. Journal of medical virology 78 Suppl 1:S7-S12.

McLennan H (1983) Receptors for the excitatory amino acids in the mammalian central nervous system. Prog Neurobiol 20:251-271.

Mueller BK, Mack H, Teusch N (2005) Rho kinase, a promising drug target for neurological disorders. Nat Rev Drug Discov 4:387-398.

Nath A (1999) Pathobiology of human immunodeficiency virus dementia. Semin Neurol 19:113-127.

Nath A (2002) Human immunodeficiency virus (HIV) proteins in neuropathogenesis of HIV dementia. J Infect Dis 186 Suppl 2:S193-198.

Navia BA, Dafni U, Simpson D, Tucker T, Singer E, McArthur JC, Yiannoutsos C, Zaborski L, Lipton SA (1998) A phase I/II trial of nimodipine for HIV-related neurologic complications. Neurology 51:221-228.

Newcomer JW, Krystal JH (2001) NMDA receptor regulation of memory and behavior in humans. Hippocampus 11:529-542.

Nong Y, Huang YQ, Ju W, Kalia LV, Ahmadian G, Wang YT, Salter MW (2003) Glycine binding primes NMDA receptor internalization. Nature 422:302-307.

Nowak L, Bregestovski P, Ascher P, Herbet A, Prochiantz A (1984) Magnesium gates glutamate-activated channels in mouse central neurones. Nature 307:462-465.

Okamoto K, Nagai T, Miyawaki A, Hayashi Y (2004) Rapid and persistent modulation of actin dynamics regulates postsynaptic reorganization underlying bidirectional plasticity. Nat Neurosci 7:1104-1112.

Passiatore G, Rom S, Eletto D, Peruzzi F (2009) HIV-1 Tat C-terminus is cleaved by calpain 1: implication for Tat-mediated neurotoxicity. Biochim Biophys Acta 1793:378-387.

Peluso R, Haase A, Stowring L, Edwards M, Ventura P (1985) A Trojan Horse mechanism for the spread of visna virus in monocytes. Virology 147:231-236.

Popovic M, Sarngadharan MG, Read E, Gallo RC (1984) Detection, isolation, and continuous production of cytopathic retroviruses (HTLV-III) from patients with AIDS and pre-AIDS. Science 224:497-500.

Potter MC, Figuera-Losada M, Rojas C, Slusher BS (2013) Targeting the Glutamatergic System for the Treatment of HIV-Associated Neurocognitive Disorders. J Neuroimmune Pharmacol 8:594-607.

Pozueta J, Lefort R, Ribe EM, Troy CM, Arancio O, Shelanski M (2013) Caspase-2 is required for dendritic spine and behavioural alterations in J20 APP transgenic mice. Nat Commun 4:1939.

Preston BD, Poiesz BJ, Loeb LA (1988) Fidelity of HIV-1 reverse transcriptase. Science 242:1168-1171.

Prince M, Guerchet M, Prina M (2013) Alzheimer's Disease International: The Global Impact of Dementia 2013-2050. In. London, England.

Qiu Z, Strickland DK, Hyman BT, Rebeck GW (2002) alpha 2-Macroglobulin exposure reduces calcium responses to N-methyl-D- aspartate via low density lipoprotein receptor-related protein in cultured hippocampal neurons. J Biol Chem 277:14458-14466.

Qiu Z, Crutcher KA, Hyman BT, Rebeck GW (2003) ApoE isoforms affect neuronal N-methyl-D-aspartate calcium responses and toxicity via receptor-mediated processes. Neuroscience 122:291-303.

Rao VR, Sas AR, Eugenin EA, Siddappa NB, Bimonte-Nelson H, Berman JW, Ranga U, Tyor WR, Prasad VR (2008) HIV-1 Clade-Specific Differences in the Induction of Neuropathogenesis. J Neurosci 28:10010-10016.

Resnick L, Berger JR, Shapshak P, Tourtellotte WW (1988) Early penetration of the blood-brain-barrier by HIV. Neurology 38:9-14.

Roberts JD, Bebenek K, Kunkel TA (1988) The accuracy of reverse transcriptase from HIV-1. Science 242:1171-1173.

Rolli-Derkinderen M, Sauzeau V, Boyer L, Lemichez E, Baron C, Henrion D, Loirand G, Pacaud P (2005) Phosphorylation of serine 188 protects RhoA from ubiquitin/proteasome-mediated degradation in vascular smooth muscle cells. Circ Res 96:1152-1160.

Romani B, Engelbrecht S, Glashoff RH (2010) Functions of Tat: the versatile protein of human immunodeficiency virus type 1. The Journal of general virology 91:1-12.

Root MJ, Kay MS, Kim PS (2001) Protein design of an HIV-1 entry inhibitor. Science 291:884-888.

Rosenmund C, Westbrook GL (1993) Calcium-induced actin depolymerization reduces NMDA channel activity. Neuron 10:805-814.

Rossi S, Studer V, Moscatelli A, Motta C, Coghe G, Fenu G, Caillier S, Buttari F, Mori F, Barbieri F, Castelli M, De Chiara V, Monteleone F, Mancino R, Bernardi G, Baranzini SE, Marrosu MG, Oksenberg JR, Centonze D (2013) Opposite roles of NMDA receptors in relapsing and primary progressive multiple sclerosis. PLoS One 8:e67357.

Ruben S, Perkins A, Purcell R, Joung K, Sia R, Burghoff R, Haseltine WA, Rosen CA (1989) Structural and functional characterization of human immunodeficiency virus tat protein. J Virol 63:1-8.

Sacktor N, Schifitto G, McDermott MP, Marder K, McArthur JC, Kieburtz K (2000) Transdermal selegiline in HIV-associated cognitive impairment: pilot, placebo-controlled study. Neurology 54:233-235.

Salter MW, Kalia LV (2004) Src kinases: a hub for NMDA receptor regulation. Nat Rev Neurosci 5:317-328.

Sarngadharan MG, Popovic M, Bruch L, Schupbach J, Gallo RC (1984) Antibodies reactive with human T-lymphotropic retroviruses (HTLV-III) in the serum of patients with AIDS. Science 224:506-508.

Satoh S, Utsunomiya T, Tsurui K, Kobayashi T, Ikegaki I, Sasaki Y, Asano T (2001) Pharmacological profile of hydroxy fasudil as a selective rho kinase inhibitor on ischemic brain damage. Life Sci 69:1441-1453.

Sauzeau V, Rolli-Derkinderen M, Marionneau C, Loirand G, Pacaud P (2003) RhoA expression is controlled by nitric oxide through cGMP-dependent protein kinase activation. J Biol Chem 278:9472-9480.

Schifitto G, Peterson DR, Zhong J, Ni H, Cruttenden K, Gaugh M, Gendelman HE, Boska M, Gelbard H (2006) Valproic acid adjunctive therapy for HIV-associated cognitive impairment: a first report. Neurology 66:919-921.

Schifitto G, Zhong J, Gill D, Peterson DR, Gaugh MD, Zhu T, Tivarus M, Cruttenden K, Maggirwar SB, Gendelman HE, Dewhurst S, Gelbard HA (2009) Lithium therapy for human immunodeficiency virus type 1-associated neurocognitive impairment. Journal of neurovirology:1-11.

Schifitto G, Zhang J, Evans SR, Sacktor N, Simpson D, Millar LL, Hung VL, Miller EN, Smith E, Ellis RJ, Valcour V, Singer E, Marra CM, Kolson D, Weihe J, Remmel R, Katzenstein D, Clifford DB (2007a) A multicenter trial of selegiline transdermal system for HIV-associated cognitive impairment. Neurology 69:1314-1321.

Schifitto G, Navia BA, Yiannoutsos CT, Marra CM, Chang L, Ernst T, Jarvik JG, Miller EN, Singer EJ, Ellis RJ, Kolson DL, Simpson D, Nath A, Berger J, Shriver SL,

Millar LL, Colquhoun D, Lenkinski R, Gonzalez RG, Lipton SA (2007b) Memantine and HIV-associated cognitive impairment: a neuropsychological and proton magnetic resonance spectroscopy study. Aids 21:1877-1886.

Schneider J, Kent SB (1988) Enzymatic activity of a synthetic 99 residue protein corresponding to the putative HIV-1 protease. Cell 54:363-368.

Schneider J, Kaaden O, Copeland TD, Oroszlan S, Hunsmann G (1986) Shedding and interspecies type sero-reactivity of the envelope glycopolypeptide gp120 of the human immunodeficiency virus. Journal of General Virology 67:2533-2538.

Schupbach J, Popovic M, Gilden RV, Gonda MA, Sarngadharan MG, Gallo RC (1984) Serological analysis of a subgroup of human T-lymphotropic retroviruses (HTLV-III) associated with AIDS. Science 224:503-505.

Sepkowitz KA (2002) Opportunistic infections in patients with and patients without Acquired Immunodeficiency Syndrome. Clin Infect Dis 34:1098-1107.

She K, Ferreira JS, Carvalho AL, Craig AM (2012) Glutamate binding to the GluN2B subunit controls surface trafficking of N-methyl-D-aspartate (NMDA) receptors. J Biol Chem 287:27432-27445.

Shen G, Tietz EI (2011) Down-regulation of synaptic GluN2B subunit-containing N-methyl-D-aspartate receptors: a physiological brake on CA1 neuron alpha-amino-3-hydroxy-5-methyl-4-isoxazolepropionic acid hyperexcitability during benzodiazepine withdrawal. J Pharmacol Exp Ther 336:265-273.

Shi Y, Mantuano E, Inoue G, Campana WM, Gonias SL (2009) Ligand binding to LRP1 transactivates Trk receptors by a Src family kinase-dependent pathway. Sci Signal 2:ra18.

Shibuya I, Douglas W (1992) Calcium channels in rat melanotrophs are permeable to manganese, cobalt, cadmium, and lanthanum, but not to nickel: evidence provided by fluorescence changes in fura-2-loaded cells. Endocrinology 131:1936-1941.

Shibuya M, Suzuki Y, Sugita K, Saito I, Sasaki T, Takakura K, Nagata I, Kikuchi H, Takemae T, Hidaka H, et al. (1992) Effect of AT877 on cerebral vasospasm after aneurysmal subarachnoid hemorrhage. Results of a prospective placebo-controlled double-blind trial. J Neurosurg 76:571-577.

Shimizu E, Tang YP, Rampon C, Tsien JZ (2000) NMDA receptor-dependent synaptic reinforcement as a crucial process for memory consolidation. Science 290:1170-1174.

Shimokawa H, Hiramori K, Iinuma H, Hosoda S, Kishida H, Osada H, Katagiri T, Yamauchi K, Yui Y, Minamino T, Nakashima M, Kato K (2002) Anti-anginal effect of fasudil, a Rho-kinase inhibitor, in patients with stable effort angina: a multicenter study. J Cardiovasc Pharmacol 40:751-761.

Shin AH, Thayer SA (2013) Human immunodeficiency virus-1 protein Tat induces excitotoxic loss of presynaptic terminals in hippocampal cultures. Molecular and Cellular Neuroscience 54:22-29.

Shin AH, Kim HJ, Thayer SA (2012) Subtype selective NMDA receptor antagonists induce recovery of synapses lost following exposure to HIV-1 Tat. Br J Pharmacol 166:1002-1017.

Snyder EM, Nong Y, Almeida CG, Paul S, Moran T, Choi EY, Nairn AC, Salter MW, Lombroso PJ, Gouras GK, Greengard P (2005) Regulation of NMDA receptor trafficking by amyloid-beta. Nat Neurosci 8:1051-1058.

Sodroski J, Patarca R, Rosen C, Wong-Staal F, Haseltine W (1985a) Location of the trans-activating region on the genome of human T-cell lymphotropic virus type III. Science 229:74-77.

Sodroski J, Rosen C, Wong-Staal F, Salahuddin SZ, Popovic M, Arya S, Gallo RC, Haseltine WA (1985b) Trans-acting transcriptional regulation of human T-cell leukemia virus type III long terminal repeat. Science 227:171-173.

Song L, Nath A, Geiger JD, Moore A, Hochman S (2003) Human Immunodeficiency Virus Type 1 Tat Protein Directly Activates Neuronal N -methyl- D -aspartate Receptors at an Allosteric Zinc-Sensitive Site. Journal of neurovirology 9:399 - 403.

Song Y, Chen X, Wang LY, Gao W, Zhu MJ (2013) Rho kinase inhibitor fasudil protects against beta-amyloid-induced hippocampal neurodegeneration in rats. CNS Neurosci Ther 19:603-610.

Spalloni A, Nutini M, Longone P (2013) Role of the N-methyl-d-aspartate receptors complex in amyotrophic lateral sclerosis. Biochim Biophys Acta 1832:312-322.

Steinaa L, Sorensen AM, Nielsen JO, Hansen JE (1994) Antibody to HIV-1 Tat protein inhibits the replication of virus in culture. Arch Virol 139:263-271.

Stevenson M, Stanwick TL, Dempsey MP, Lamonica CA (1990) HIV-1 replication is controlled at the level of T cell activation and proviral integration. EMBO J 9:1551-1560.

Sulzer D, Mosharov E, Talloczy Z, Zucca FA, Simon JD, Zecca L (2008) Neuronal pigmented autophagic vacuoles: lipofuscin, neuromelanin, and ceroid as macroautophagic responses during aging and disease. J Neurochem 106:24-36.

Sung JK, Miao L, Calvert JW, Huang L, Louis Harkey H, Zhang JH (2003) A possible role of RhoA/Rho-kinase in experimental spinal cord injury in rat. Brain Res 959:29-38.

Sunico CR, Gonzalez-Forero D, Dominguez G, Garcia-Verdugo JM, Moreno-Lopez B (2010) Nitric Oxide Induces Pathological Synapse Loss by a Protein Kinase G-, Rho Kinase-Dependent Mechanism Preceded by Myosin Light Chain Phosphorylation. J Neurosci 30:973-984.

Takata M, Tanaka H, Kimura M, Nagahara Y, Tanaka K, Kawasaki K, Seto M, Tsuruma K, Shimazawa M, Hara H (2013) Fasudil, a rho kinase inhibitor, limits motor neuron loss in experimental models of amyotrophic lateral sclerosis. Br J Pharmacol 170:341-351.

Tanaka H, Yamashita T, Yachi K, Fujiwara T, Yoshikawa H, Tohyama M (2004) Cytoplasmic p21(Cip1/WAF1) enhances axonal regeneration and functional recovery after spinal cord injury in rats. Neuroscience 127:155-164.

Tang YP, Shimizu E, Dube GR, Rampon C, Kerchner GA, Zhuo M, Liu G, Tsien JZ (1999) Genetic enhancement of learning and memory in mice. Nature 401:63-69.

Tonges L, Frank T, Tatenhorst L, Saal KA, Koch JC, Szego EM, Bahr M, Weishaupt JH, Lingor P (2012) Inhibition of rho kinase enhances survival of dopaminergic neurons and attenuates axonal loss in a mouse model of Parkinson's disease. Brain 135:3355-3370.

Toshima Y, Satoh S, Ikegaki I, Asano T (2000) A new model of cerebral microthrombosis in rats and the neuroprotective effect of a Rho-kinase inhibitor. Stroke 31:2245-2250.

Totsukawa G, Yamakita Y, Yamashiro S, Hartshorne DJ, Sasaki Y, Matsumura F (2000) Distinct roles of ROCK (Rho-kinase) and MLCK in spatial regulation of MLC

phosphorylation for assembly of stress fibers and focal adhesions in 3T3 fibroblasts. J Cell Biol 150:797-806.

Tovar KR, Westbrook GL (1999) The incorporation of NMDA receptors with a distinct subunit composition at nascent hippocampal synapses in vitro. J Neurosci 19:4180-4188.

Tozzi V, Balestra P, Lorenzini P, Bellagamba R, Galgani S, Corpolongo A, Vlassi C, Larussa D, Zaccarelli M, Noto P, Visco-Comandini U, Giulianelli M, Ippolito G, Antinori A, Narciso P (2005) Prevalence and risk factors for human immunodeficiency virus–associated neurocognitive impairment, 1996 to 2002: Results from an urban observational cohort. Journal of neurovirology 11:265-273

Tsien JZ, Huerta PT, Tonegawa S (1996) The Essential Role of Hippocampal Ca1 Nmda Receptor-Dependent Synaptic Plasticity in Spatial Memory. Cell 87:1327-1338.

U.S. Dept. of Health and Human Services (2014a) Panel on Antiretroviral Guidelines for Adults and Adolescents. Guidelines for the use of antiretroviral agents in HIV-1-infected adults and adolescents. In. Washington, D.C. : U.S. Dept. of Health and Human Services. http://aidsinfo.nih.gov/contentfiles/lvguidelines/adultandadolescentgl.pdf

U.S. Dept. of Health and Human Services (2014b) Just Diagnosed with HIV AIDS : HIV in Your Body : Stages of HIV Infection. In. Washington, D. C. : U.S. Dept. of Health and Human Services. http://aids.gov/hiv-aids-basics/just-diagnosed-with-hiv-aids/hiv-in-your-body/stages-of-hiv/

U.S. Dept. of Health and Human Services (2014c) HIV/AIDS 101: How do you get HIV or AIDS? In. Washington, D.C.: U.S. Dept. of Health and Human Services. http://aids.gov/hiv-aids-basics/hiv-aids-101/how-you-get-hiv-aids/

UNAIDS JUNPoHA- (2013) Global report: UNAIDS report on the global AIDS epidemic 2013. In: WHO Library.

Urbinati C, Bugatti A, Giacca M, Schlaepfer D, Presta M, Rusnati M (2005) alpha(v)beta3-integrin-dependent activation of focal adhesion kinase mediates NF-kappaB activation and motogenic activity by HIV-1 Tat in endothelial cells. J Cell Sci 118:3949-3958.

Uthman OA, Abdulmalik JO (2008) Adjunctive therapies for AIDS dementia complex. Cochrane database of systematic reviews (Online):CD006496.

Valcour V, Sithinamsuwan P, Letendre S, Ances B (2011) Pathogenesis of HIV in the central nervous system. Current HIV/AIDS reports 8:54-61.

Valcour V, Shikuma C, Shiramizu B, Watters M, Poff P, Selnes O, Holck P, Grove J, Sacktor N (2004) Higher frequency of dementia in older HIV-1 individuals: the Hawaii Aging with HIV-1 Cohort. Neurology 63:822-827.

Veronese FD, DeVico AL, Copeland TD, Oroszlan S, Gallo RC, Sarngadharan MG (1985) Characterization of gp41 as the transmembrane protein coded by the HTLV-III/LAV envelope gene. Science 229:1402-1405.

Viviani B, Bartesaghi S, Gardoni F, Vezzani A, Behrens MM, Bartfai T, Binaglia M, Corsini E, Di Luca M, Galli CL, Marinovich M (2003) Interleukin-1b Enhances NMDA Receptor-Mediated Intracellular Calcium Increase through Activation of the Src Family of Kinases. J Neurosci 23:8692-8700.

Votteler JaS, U. (2008) The Desk Encyclopedia of General Virology. Human Immunodeficiency Viruses: Molecular Biology. Erlangen, Germany: Elsevier Ltd.

Walensky RP, Paltiel AD, Losina E, Mercincavage LM, Schackman BR, Sax PE, Weinstein MC, Freedberg KA (2006) The survival benefits of AIDS treatment in the United States. J Infect Dis 194:11-19.

Wang X, Robinson PJ (1997) Cyclic GMP-dependent protein kinase and cellular signaling in the nervous system. J Neurochem 68:443-456.

Wang YT, Salter MW (1994) Regulation of NMDA receptors by tyrosine kinases and phosphatases. Nature 369:233-235.

Watkins BA, Dorn HH, Kelly WB, Armstrong RC, Potts BJ, Michaels R, Kufta CV, Dubois-Dalcq M (1990) Specific tropism of HIV-1 for microglial cells in primary human brain cultures. Science 249:549-553.

Wenzel A, Fritschy JM, Mohler H, Benke D (1997) NMDA receptor heterogeneity during postnatal development of the rat brain: differential expression of the NR2A, NR2B, and NR2C subunit proteins. J Neurochem 68:469-478.

WHO Global Health Observatory (2014) Global Health Observatory. In. Geneva, Switzerland: World Health Organization. http://www.who.int/gho/hiv/en/

Wiley CA, Baldwin M, Achim CL (1996) Expression of regulatory and structural mRNA in the central nervous system. AIDS 10:943-947.

Wiley CA, Schrier RD, Nelson JA, Lampert PW, Oldstone MB (1986) Cellular localization of human immunodeficiency virus infection within the brains of acquired immune deficiency syndrome patients. Proc Natl Acad Sci U S A 83:7089-7093.

Williams K (1993) Ifenprodil Discriminates Subtypes of the N-Methyl-D-aspartate Receptor - Selectivity and Mechanisms at Recombinant Heteromeric Receptors. Mol Pharmacol 44:851-859.

Williams KC, Corey S, Westmoreland SV, Pauley D, Knight H, deBakker C, Alvarez X, Lackner AA (2001) Perivascular macrophages are the primary cell type productively infected by simian immunodeficiency virus in the brains of

macaques: implications for the neuropathogenesis of AIDS. J Exp Med 193:905-915.

Wills JW, Craven RC (1991) Form, function, and use of retroviral gag proteins. AIDS 5:639-654.

Wu LJ, Gerard NP, Wyatt R, Choe H, Parolin C, Ruffing N, Borsetti A, Cardoso AA, Desjardin E, Newman W, Gerard C, Sodroski J (1996) Cd4-Induced Interaction of Primary Hiv-1 Gp120 Glycoproteins With the Chemokine Receptor Ccr-5. Nature 384:179-183.

Wu PJ, Coultrap SJ, Browning MD, Proctor WR (2011) Functional adaptation of the N-methyl-D-aspartate receptor to inhibition by ethanol is modulated by striatal-enriched protein tyrosine phosphatase and p38 mitogen-activated protein kinase. Mol Pharm 80:529-537.

Wu RF, Gu Y, Xu YC, Mitola S, Bussolino F, Terada LS (2004) Human immunodeficiency virus type 1 Tat regulates endothelial cell actin cytoskeletal dynamics through PAK1 activation and oxidant production. J Virol 78:779-789.

Wu Z, Guo Z, Gearing M, Chen G (2014) Tonic inhibition in dentate gyrus impairs long-term potentiation and memory in an Alzhiemer's disease model. Nat Commun 5:4159.

Xiao H, Neuveut C, Lee H, Benkirane M, Rich EA, Murphy PM, Jeang K-T (2000) Selective CXCR4 antagonism by Tat: implications for in vivo expansion of coreceptor use by HIV-1. Proc Natl Acad Sci U S A 97:11466-11471.

Xu R, Feng X, Xie X, Zhang J, Wu D, Xu L (2012) HIV-1 Tat protein increases the permeability of brain endothelial cells by both inhibiting occludin expression and cleaving occludin via matrix metalloproteinase-9. Brain Res 1436:13-19.

Young AB, Greenamyre JT, Hollingsworth A, Albin R, D'Amato C, Shoulson I, Penney JB (1988) NMDA receptor losses in putamen from patients with huntington's disease. Science 241:981-983.

Yuen EY, Zhong P, Yan Z (2010) Homeostatic regulation of glutamatergic transmission by dopamine D4 receptors. Proc Natl Acad Sci U S A.

Zhao Y, Navia BA, Marra CM, Singer EJ, Chang L, Berger J, Ellis RJ, Kolson DL, Simpson D, Miller EN, Lipton SA, Evans SR, Schifitto G (2010) Memantine for AIDS dementia complex: open-label report of ACTG 301. HIV clinical trials 11:59-67.

Zhong Y, Hennig B, Toborek M (2010) Intact lipid rafts regulate HIV-1 Tat protein-induced activation of the Rho signaling and upregulation of P-glycoprotein in brain endothelial cells. J Cereb Blood Flow Metab 30:522-533.

Zhong Y, Zhang B, Eum SY, Toborek M (2012) HIV-1 Tat triggers nuclear localization of ZO-1 via Rho signaling and cAMP response element-binding protein activation. J Neurosci 32:143-150.

Zhou Y, Su Y, Li B, Liu F, Ryder JW, Wu X, Gonzalez-DeWhitt PA, Gelfanova V, Hale JE, May PC, Paul SM, Ni B (2003) Nonsteroidal Anti-Inflammatory Drugs Can Lower Amyloidogenic A{beta}42 by Inhibiting Rho. Science 302:1215-1217.